Genetic Analysis of Pituitary Thyrotrope Development

by

Alexandre Daly

A dissertation submitted in partial fulfillment
of the requirements for the degree of
Doctor of Philosophy
(Genetics and Genomics)
in the University of Michigan
2020

Doctoral Committee:

Professor Sally Camper, Chair
Professor Doug Engel
Associate Professor Sundeep Kalantry
Associate Professor Stephen Parker
Assistant Professor Jacob Kitzman

Alexandre Daly

azdaly@umich.edu

ORCID iD: 0000-0002-1924-0755

Dedication

I dedicate this thesis to Chelsey, without whom I could not have gotten through graduate school and my parents, without whom I would not have gotten to graduate school.

I also dedicate this to Sally Camper. I could not conceive of a better mentor. You have supported me and given me years of time to become a better scientist and person.

Acknowledgements

This work represents an enormous combined effort from many people. First and fore most Sally Camper. I still remember very clearly the conversation in which she said she could not believe that Rosa26-SV40 mice did not already exist. Now, several years later, they do, and they work better than we had hoped. All of the work here represents the execution of Sally's ideas. She is truly a scientific giant on whose shoulders I have been lucky enough to stand.

One of the things that makes Sally such an effective mentor is her ability to build a lab of people who selflessly serve others and want to see each other succeed. Michelle Brinkmeier has been critical to my development, and the general publication rate of the Camper lab. Even during this time of COVID, not a week goes by without my asking her several questions. Similarly, Amanda Mortensen is constantly taking on tasks for other people in the lab. It has been a pleasure to work alongside her to characterize the Rosa26-SV40 mice. Leonard Cheung and Hironori Bando are two of the greatest teammates I could think of. Leonard was generous enough to incorporate me into his single-cell work, which has proven to be pivotal in understanding thyrotrope function. Hironori has been vital in developing the PIT-P1 and PIT1-T1 cell lines. Without him, the story would likely not have as satisfying an ending. Lindsey Dudley is a talented undergraduate student who has been very helpful this past year in the maintenance and characterization of the Rosa26-SV40 mice. Peter Gergics, Kevin Toolan, Qing Fang, Maria Ines Perez-Millan, Akima George, and Sebastian Vishnopolska all gave advice, support and guidance through my time in the Camper lab.

I had many collaborators throughout this time that provided key feedback, data, revisions, and reagents that have been critical to my success. While too long to list, I want to acknowledge Drs. Stephen Liebhaber and Michael Peel who sent unpublished RNA-seq data of two cell lines (Pit1-Triple and Pit1-Zero) which we ultimately used to find thyrotrope-specific elements. Dr. Jacques Drouin generously gave us embedded mouse heads of *Ascl1-null* mice, allowing us to quickly test the hypothesis that ASCL1 has an effect on pituitary function. Dr. Michael Imperiale gave us an antibody to detect SV40, which we use extensively. Dr. Patrice Mollard has been a constant point of contact, sharing unpublished ideas and data about thyrotrope function. Dr. Pamela Mellon offered invaluable guidance on how best to immortalize cell lines from the tumors that were developed from the Rosa26-SV40 mice.

The graduate students at the University of Michigan have also been critical in offering help and guidance. First and fore most Owen Funk who is helping develop RNA-seq libraries for the PIT-P1 and PIT-T1 cells. Also, Sierra Nishazaki, Ricardo Albanus, Peter Orchard, and Arushi Varshney have always been so responsive to questions, particularly those pertaining to software packages. It would have been impossible to do any of this without such a helpful cohort.

The cores at the University of Michigan have been invaluable. I have used the Advanced Genomics Core, previously the DNA sequencing core extensively. They QCed and sequenced all of the high-throughput sequencing libraries in the following work. The Transgenic Animal Model Core (TAMC) has also been key to this work. The TAMC generated several new mouse lines for this work, including the Rosa26-SV40 mice, the PROP1-SV40 BAC mouse (not discussed here), and the transient transgenic mice used to determine the function of regulatory elements in thyrotropes. Much of the following work would not have been possible without TAMC.

None of this work would have been possible without the funding sources. Most notably the NIH's National Institutes of Child Health and Development (NICHD), the organization from

which Sally receives most of her funding. Also, the two training programs, the Genetics Training Program led by John Moran and Tony Antonellis and the Genome Science Training Program led by Michael Boehnke have contributed greatly to my development as a geneticist and data scientist and have allowed me to conduct the research.

Finally, I thank you, my committee. Ever since my first committee meeting four years ago, I have looked forward to my committee meetings. Having my work reviewed by five prolific scientists who all ensure that I progress and want the best for my work and my career has been an enormous blessing. You have all been so supportive and have contributed greatly to this moment by writing letters of recommendation, reading over manuscripts, and spending hours in Buhl 5920, helping me to find what element is driving *Tshb* expression. Thank you.

Table of Contents

List of Tables

List of Figures

Abstract

The pituitary gland produces polypeptide hormones that regulate many functions including growth, lactation, reproduction, metabolism, and the stress response. Pituitary thyrotrope cells produce the heterodimeric glycoprotein hormone thyrotropin, which is critical for stimulating thyroid gland development and production of thyroid hormone. Less is known about the drivers of thyrotrope cell fate than the other specialized cells in this organ. The transcription factor POU1F1 is critical for generation of thyrotropes, somatotropes and lactotropes, and GATA2 is critical for both thyrotropes and gonadotropes. Additional factors are likely involved in driving thyrotrope fate. SV40-immortalized cell lines have been invaluable for studying the regulation of pituitary hormone production. Here I use two established immortalized cell lines to identify epigenomic and gene expression changes that are associated with adoption of the thyrotrope fate. GHF-T1 cells represent a POU1F1-expressing progenitor which does not produce hormones, and TαT1 cells represent a thyrotrope-like line that expresses POU1F1, GATA2 and thyrotropin (TSH). I also developed a novel, genetically engineered mouse line that expresses SV40 in response to cre recombinase, and I used this line to develop novel pituitary cell lines. These cell lines can be used for transcriptome and epigenome studies to understand the development and function of the pituitary gland.

I identified the transcription factors and epigenomic changes in chromatin that are associated with thyrotrope differentiation. I generated and integrated genome-wide information about DNA accessibility, histone modifications, POU1F1 binding and RNA expression data to

identify regulatory elements and candidate transcriptional regulators. I identified POU1F1 binding sites that are unique to each cell line. POU1F1 binding sites are commonly associated with bZIP factor motifs in GHF-T1 cells and Helix-Turn-Helix or basic Helix-Loop-Helix motifs in TαT1 cells, suggesting classes of transcription factors that may recruit POU1F1 to unique sites. I validated enhancer function of novel elements we mapped near *Cga*, *Pitx1*, *Gata2*, and *Tshb* by transfection in TαT1 cells. Finally, I confirmed that an enhancer element near *Tshb* can drive expression in thyrotropes of transgenic mice and demonstrated that GATA2 enhances *Tshb* expression via this element. These data extend the ENCODE analysis to an organ that is critical for growth and metabolism. This information could be valuable for understanding pituitary development and disease pathogenesis.

Targeted oncogenesis is the process of driving tumor formation by engineering transgenic mice that express an oncogene under the control of a cell-type specific promoter. Using CRISPR/Cas9 we inserted a cassette with coding sequences for SV40 T antigens and IRES-GFP into the *Rosa26* locus, downstream from a stop sequence flanked by loxP sites: *Rosa26*$^{LSL\text{-}SV40\text{-}GFP}$. These mice were mated with previously established *Prop1-cre* and *Tshb-cre* transgenic lines. The majority of *Rosa26*$^{LSL\text{-}SV40\text{-}GFP/+}$; *Prop1-cre* and all *Rosa26*$^{LSL\text{-}SV40\text{-}GFP/+}$; *Tshb-cre* mice developed dwarfism and large tumors by 4 weeks. *Prop1-cre*-mediated activation of SV40 expression affected cell specification, reducing thyrotrope differentiation and increasing gonadotrope cell fate selection. GFP-positive cells from flow-sorted *Rosa26*$^{LSL\text{-}SV40\text{-}GFP/+}$; *Prop1-cre* and *Rosa26*$^{LSL\text{-}SV40\text{-}GFP/+}$; *Tshb-cre* mice express PROP1 and TSH, respectively. Tumors from both of these mouse lines were adapted to growth in cell culture. I established a progenitor-like cell line (PIT-P1) that expresses *Sox2* and *Pitx1*, and a thyrotrope-like cell line (PIT-T1) that expresses *Cga* and *Pou1f1*. These studies demonstrate the utility of the novel, *Rosa26*$^{LSL\text{-}SV40\text{-}GFP}$ mouse line for targeted oncogenesis and development of cell lines.

Chapter 1: Introduction

Introduction

The pituitary gland is located at the base of the brain, and it is a small organ, approximately the size of a pea in humans. It is often referred to as the master gland because it is a key regulator of multiple organ systems, controlling growth, fertility, the stress response, and homeostasis. The pituitary gland develops between 5-9 wks gestation in humans and embryonic day 10-19 in mice [1]. An invagination of oral ectoderm, called Rathke's pouch, forms the anterior and intermediate lobes of the pituitary gland, and evagination of the neural ectoderm forms the posterior lobe of the pituitary gland and pituitary stalk. The posterior lobe contains the axon terminals for oxytocin and vasopressin and pituicytes. The anterior lobe is comprised of cells specialized in the secretion of polypeptide hormones (**Fig. 1**). Hypothalamic neurons secrete factors into the hypophyseal portal system that regulate pituitary function. In the past three decades, a great deal of progress has been made in understanding the mechanisms that drive the differentiation of hormone-producing cells of the anterior pituitary gland during development. Multiple transcription factors and signaling pathways are involved, and defects in the genes that encode these factors and pathways are an important contributor to congenital pituitary hormone deficiency [2-5]. The focus of this chapter will be on the pituitary transcription factors that drive the differentiation of pituitary hormone-producing cells with an emphasis on the history of discovery for those that are most relevant to human pituitary

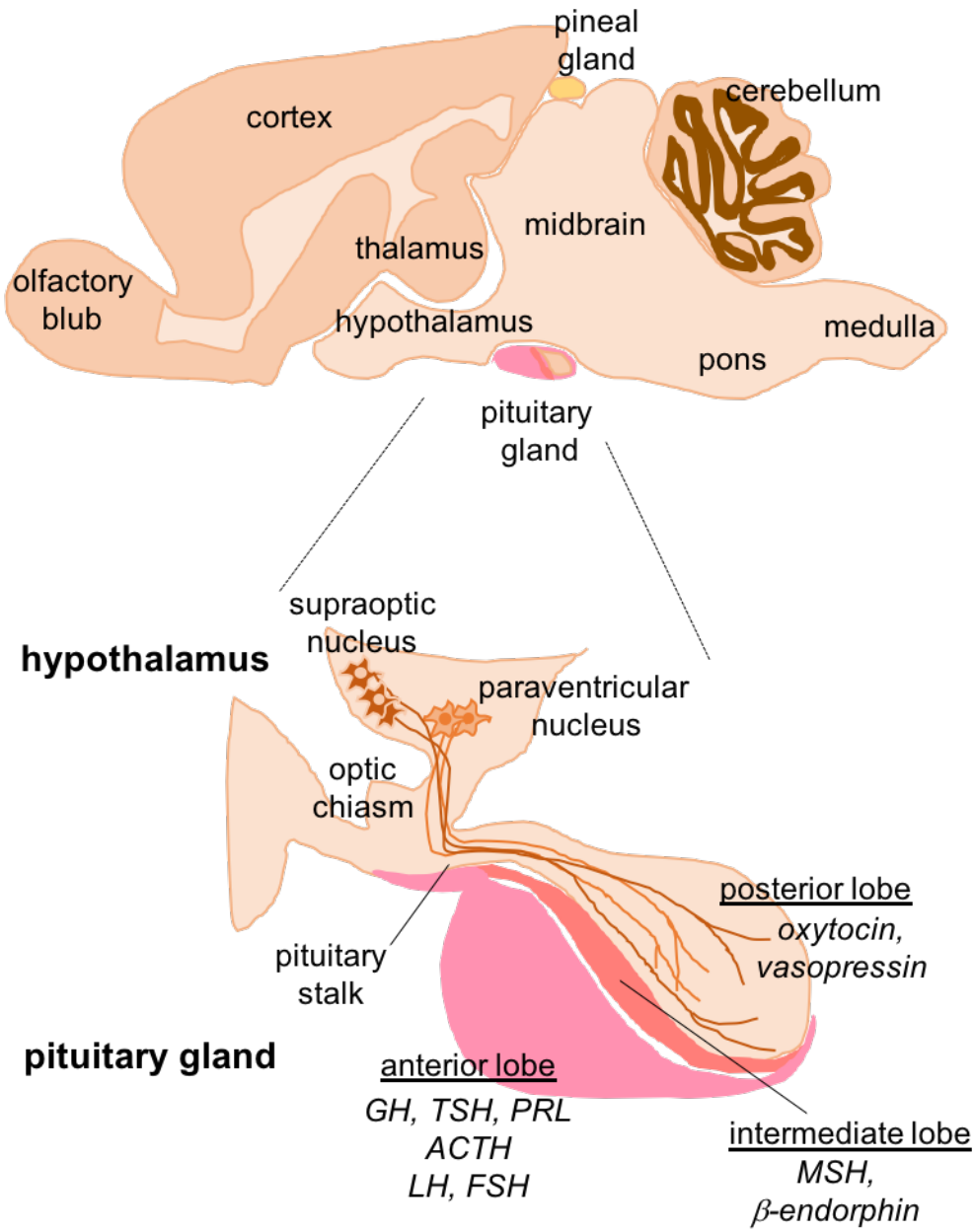

Figure 1: Anatomy of the murine pituitary gland and base of the hypothalamus.

The pituitary gland contains anterior (ant) and intermediate (int) lobes derived from the oral ectoderm that forms Rathke's pouch. The posterior lobe (post) and pituitary stalk are derived from neural ectoderm of the ventral diencephalon, and they contain the axon terminals of vasopressin and oxytocin neurons that project from both the supraoptic nucleus and the paraventricular nucleus of the hypothalamus. Hypothalamic peptides regulate the release of anterior pituitary hormones into the hypophyseal portal system.

[1]

[1] This introduction has been published: Alexandre Z. Daly and Sally A. Camper, "Pituitary Development and Organogenesis: Transcription factors in development and disease," in Developmental Neuroendocrinology, Ed: Susan Wray, Seth Blackshaw. In Masterclass in Neuroendocrinology, Vol. 9. Series Ed: John A. Russell, William E. Armstrong, Springer, 2020.

insufficiency. Other chapters in this volume review the development of the hypothalamus and its regulation of pituitary function (See the reviews by Placzek and Towers on the development of the hypothalamus, the review from Alvarez-Bolado on SHH and GLI in the hypothalamus and Lee's review on the arcuate nucleus)

The hypophyseal portal system, pituitary vasculature, and accessory cells of the pituitary gland

The hypophyseal portal system refers to the blood vessels that provide connections between the hypothalamus and the anterior pituitary gland. This vasculature develops e14.5-e18.5 in mice and appears complete by 12 wks gestation in humans [1]. The capillaries are highly fenestrated, facilitating rapid molecular exchange between the hypothalamus and pituitary lobes. Oxygen levels and blood flow are regulated and have an effect on pituitary hormone production and secretion [6, 7].

The mature pituitary gland has six distinct hormone-producing cell types, as well as folliculo-stellate cells and pituicytes (**Fig. 2**). The hormone-producing cell types in the anterior lobe include corticotropes that produce adrenocorticotropin (ACTH) from the pro-hormone pro-opiomelanocortin (POMC), somatotropes that produce GH, lactotropes that produce prolactin, gonadotropes that produce the heterodimeric glycoprotein hormones luteinizing hormone (LH) and follicle stimulating hormone, (FSH) and thyrotropes that produce the heterodimeric glycoprotein hormone thyroid stimulating hormone (TSH). The intermediate lobe, which remains distinct in rodents, contains melanotropes that produce melanocyte stimulating hormone from POMC. Folliculo-stellate (FS) cells are non-endocrine cells that were named because of their star-like morphology of cytoplasmic processes [8]. FS cells appear between postnatal day 10-20 in the rat, throughout the anterior lobe parenchyma, directly adjacent to the hormone-producing cells [9]. FS cells serve a support function for hormone-producing cells through the release cytokines and growth factors. FS cells are excitatory and are involved in the coordinated, pulsatile release of hormones from the hormone-producing cells, which

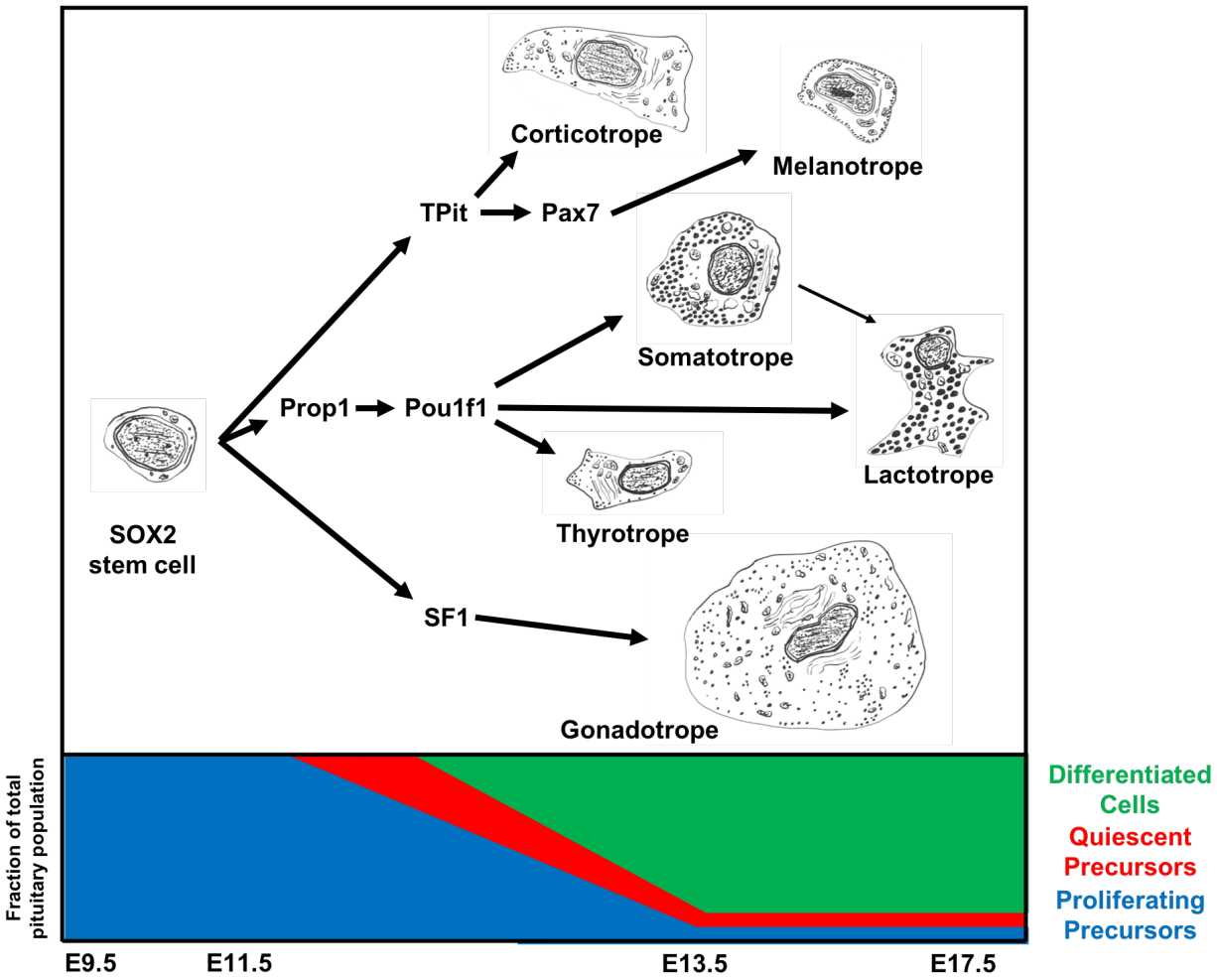

Figure 2: Critical transcription factors control the development of specialized hormone-producing cells.

The major hormone-producing cell types of the anterior and intermediate lobes of the pituitary gland are derived from SOX2-expressing progenitor cells. Combinations of transcription factors drive specific cell fates and antagonize differentiation into alternate fates. Each cell type has distinctive secretory granules and shape [10]. Proliferating precursors leave the cell cycle and differentiate into hormone-producing cells during gestation.

themselves form homotypic networks [11, 12]. Pituicytes are glial-like cells located within the posterior lobe. The larger parenchymatous pituicytes regulate hormone output by completely enveloping the neurosecretory processes of the oxytocin and vasopressin axons when hormone secretion is low, and they recede as hormone secretion increases. They also regulate hormone output by secretion of taurine [13]. The smaller fibrous pituicytes do not appear to be involved in this regulatory function and are less well understood [14].

The vasculature is important for pituitary gland function because it transports molecules from pituitary target organs that feed back at the level of the pituitary gland and hypothalamus, maintaining homeostasis. This multi-organ feedback regulation is called an axis. The best known of these axes are the hypothalamic-pituitary-gonadal axis, hypothalamic-pituitary-adrenal axis and the hypothalamic-pituitary-thyroid axis, although axes involving bone, liver and other organs also exist [15-19].

Cell signaling during pituitary gland development

Some of the major signaling pathways that have been implicated in pituitary development are SHH, FGF, BMP, Wnt, Notch, Hippo, EGF, and retinoic acid [20-23]. Hypothalamic SHH is necessary for inducing expression of the pituitary transcription factors LHX3 and LHX4, which drive progenitor proliferation and prevent cell death [24]. FGF8 and FGFR1 mutations cause pituitary hormone deficiency in humans [5], and mouse studies show reduced cell proliferation and enhanced cell death in the pituitary primordia of *Fgf8, Fgf10,* and *Fgfr2* mutants [25]. BMP and the antagonist noggin affect pituitary growth and shape during development, and altered BMP signaling is associated with pituitary adenomas [26-29]. Similarly, WNT signaling regulates pituitary organogenesis and acts in a paracrine manner to stimulate excess cell proliferation in adenomas [30]. The ligand, beta-catenin, is a cofactor for several key pituitary transcription factors including PITX2, TCF7L2 (TCF4), LEF1, NR5A1, and PROP1. Notch signaling regulates the timing of pituitary progenitor cell cycle exit and differentiation [31-33]. YAP and TAZ are transcriptional regulators downstream of the Hippo

signaling pathway, which suppresses their function by phosphorylation. This pathway plays an essential role in regulation of pituitary progenitor expansion and normal organ size [23]. There is a great deal of crosstalk between these pathways, in that perturbation of one signaling pathway typically affects the other signaling pathways. EGF and retinoic acid signaling are recognized as important signaling pathways but their precise roles during organogenesis have not been established [34, 35].

Hypopituitarism

The major pathologies associated with the pituitary are adenomas, which can be associated with either over- or under-production of hormones, and congenital or acquired hypopituitarism [36, 37]. The main emphasis of this review will be on congenital hypopituitarism, which had an estimated prevalence of 45.5 per 100,000 people [38]. This is a genetically heterogeneous condition that can present with a single pituitary hormone deficiency or with multiple deficiencies. About 50% of cases that originally present with isolated growth hormone deficiency (IGHD) progress to combined pituitary hormone deficiency (CPHD). CPHD is defined as a reduction of at least two pituitary hormones, and usually GH is one of them. It has a prevalence of 1 in 8,000 individuals, and more than 30 genes have been implicated as causal factors for CPHD [5].

Overview

Here we review the transcription factors that are critical for developing the specialized cells of the anterior and intermediate lobes of the pituitary gland, emphasizing the history of scientific discovery surrounding each factor, from its discovery through to its most recent characterization. This reveals the continuing evolution and diversity of effective technical approaches. These include identification of cis-acting sequences important for regulation of hormone gene expression and identification of the trans-acting factors that bind those sites, positional cloning of mutations in mice and human patients, and exploration of epigenomic regulation of chromatin accessibility. We also highlight areas for future discovery that may take

advantage of high-throughput sequencing and high-efficiency, targeted germline disruption tools.

SOX2 (LCC, YSB)

Gene discovery

Sox2 was first discovered in a whole-embryo cDNA screen in search of genes similar to the male, sex-determining gene *Sry*, which binds DNA through a motif or box characteristic of high mobility group proteins [39]. *Sox2* is expressed in progenitor cell populations in many tissues, and its expression is negatively correlated with differentiation [40-42]. SOX2 is one of the factors that, along with OCT3/4, c-MYC, and KLF4, were demonstrated by Yamanaka and colleagues to be sufficient to induce pluripotency in differentiated cells from mice and humans [43, 44].

Knockout mouse phenotype, Down-stream targets, Interacting factors

Sox2 is expressed in the developing pituitary and hypothalamus, and it has a role in pituitary development [43, 44]. Embryos homozygous for *Sox2* loss of function alleles die around implantation, and heterozygous mice have genetic background-dependent reduction in body size and male infertility [42]. The developing pituitaries of heterozygous mutants are bifurcated, similar to the dysmorphology observed in *Wnt5a* mutants, and both males and females exhibit reduced differentiation into somatotropes and gonadotropes (**Fig. 3**) [45, 46]. About ⅔ of the heterozygotes survive to adulthood, and in these survivors, the reduction in pituitary size is modest, and GH and LH content is only significantly reduced in males.

Martinez-Barbera and colleagues generated a conditional deletion of *Sox2* using the *Hesx1-cre* strain, deleting *Sox2* in the pituitary gland and areas of the brain between e10.5 and

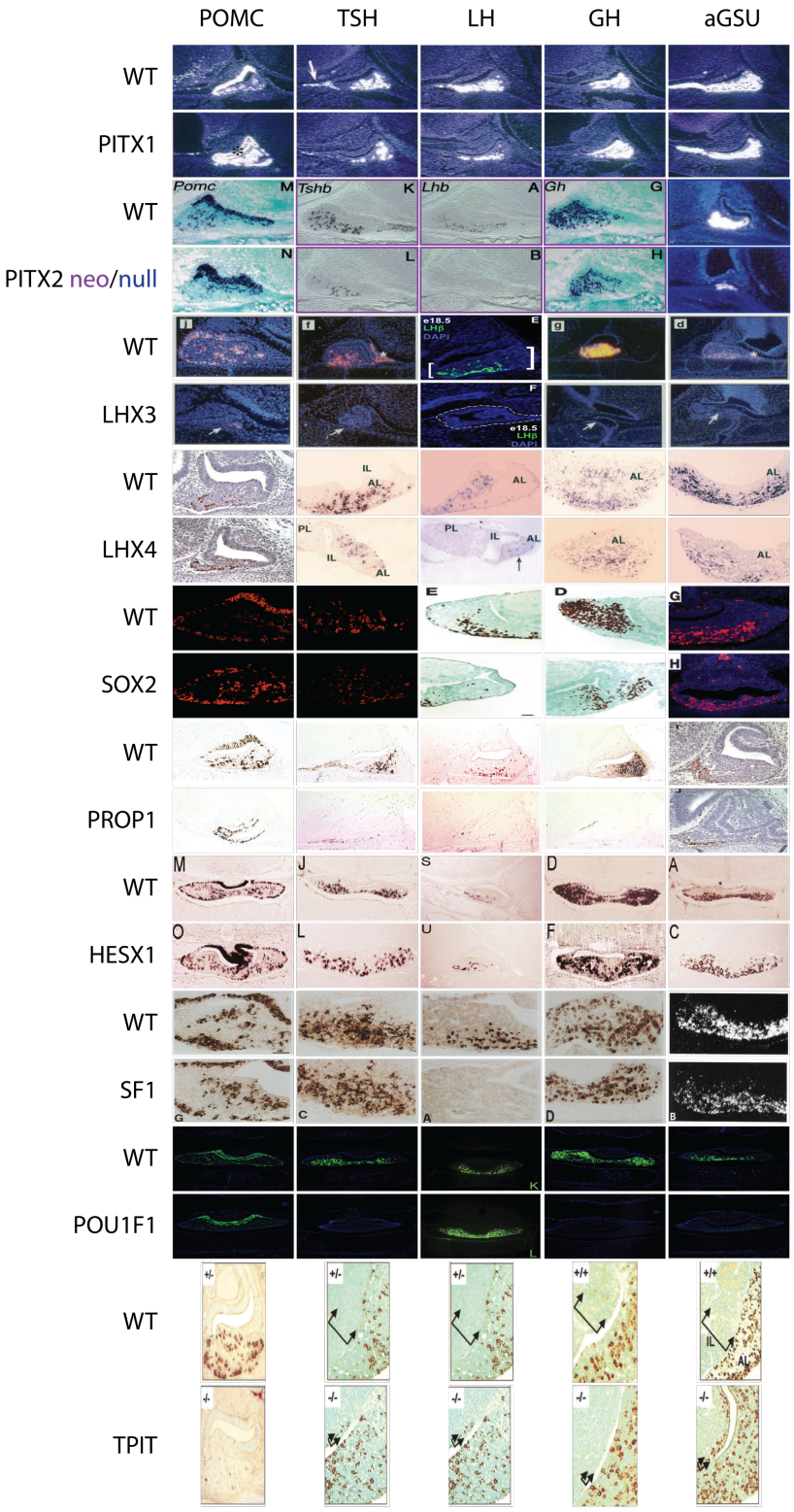

Figure 3: The effect of transcription factor mutations on pituitary development has been revealed using genetically engineered and spontaneous mutant mice.

Deletion of Pitx1 has modest effects including slight reduction of TSH and LH, slight increase in POMC and no change in GH and αGSU, as observed by in situ hybridization in P0 animals [47]. In situ hybridization in newborn

mice homozygous for a hypomorphic allele of *Pitx2*, *Pitx2* $^{neo/neo}$, revealed normal *Pomc* expression, reduction in *Gh* and *Tshb* expression, and no detectable *Lhb* or *Fshb* transcripts (panels bordered in purple) [48]. *Pitx2*$^{-/-}$ embryos had arrested the development of Rathke's pouch and reduced expression of αGSU at e13.5 mice [49]. Trace amounts of *Pomc* transcripts were present, but all other hormones were not detectable (not shown). In situ hybridization in the *Lhx3* knockout mice revealed a near-total loss of *Pomc*, *Tshb*, *Gh*, and *Cga* (αGSU) transcripts, and immunohistochemistry failed to detect significant amounts of LH. In situ hybridization of *Lhx4* knockout pituitaries revealed a significant reduction in *Tshb, Lhb, Gh*, and *Cga* transcripts at e18.5 and immunohistochemistry showed largely similar POMC expression in e14.5 mice [50]. Immunohistochemistry of *Sox2* heterozygous null mice revealed reduced staining for GH and LH at e18.5 [51]. There is no detectable POU1F1 staining in *Hesx1*$^{cre/+}$; *Sox2*$^{flox/flox}$ mice at e14.5 or later in gestation (not shown) [52]. The staining for αGSU and POMC was somewhat normal at e15.5, considering the hypoplasia of the organ. Only *Pou1f1*-independent TSH-expressing cells were detected. Immunohistochemistry of *Prop1*$^{-/-}$ pituitaries revealed POMC expression but little or no detectable caudomedial staining for TSH, LH, or GH at e18.5 [53]. αGSU staining was modestly reduced at e14.5 in *Prop1*$^{df/df}$ mice, but NR5A1 cells were normal at birth [54]. In situ hybridization analysis of e17.5 *Hesx1*$^{R160C/R160C}$ mutants revealed approximately normal levels of *Pomc, Tshb, Lhb, Gh*, and *Cga* expression, although the pituitaries were dysmorphic [55]. These missense mutant mice have similar pituitary features to mice homozygous for a null allele, but the forebrain is less affected. Analysis of newborn SF1-mutant mice revealed undetectable LH, diminished *Cga* transcripts and normal immunostaining for ACTH, TSH, and GH [56]. *Pou1f1*$^{dw/dw}$ mutant newborns have normal POMC immunostaining, undetectable TSH and GH, and increased LH [57]. CGA appeared reduced. Immunohistochemical analysis of *Tpit* knockouts revealed undetectable POMC, no effect on caudomedial staining of GH, TSH, LH, or αGSU in the anterior lobe, but ectopic expression of TSH, LH, and αGSU in the intermediate lobe [58].

e12.5 [46]. This resulted in severe pituitary hypoplasia and greatly reduced expression of *Pou1f1*, *Gh,* and *Tshb.* Gonadotropin deficiency appeared to be secondary to the reduction in GnRH neurons in these mice. Cell proliferation is significantly decreased in the conditionally deleted *Sox2* pituitary glands, and it appears that the progenitors have not migrated from the progenitor zone of Rathke's pouch to colonize the anterior lobe. This suggests that *Sox2* has an important role in pituitary progenitor proliferation and transition to differentiation.

Robinson and colleagues discovered that *Sox2*-expressing cells in the adult mouse pituitary were still mitotically active and that, given appropriate culture conditions, these SOX2 positive cells can self-renew and differentiate *in vitro* into all of the hormone producing cells of the anterior lobe of the pituitary gland [59]. Both Lovell-Badge and Martinez-Barbera and colleagues used lineage tracing to demonstrate that SOX2-positive cells give rise to all of the different hormone-producing cells in the pituitary gland in vivo [60, 61]. SOX2-positive cells contribute to tissue homeostasis, and they are involved in responding to end-organ ablation, such as adrenalectomy and gonadectomy. Mice with a constitutively active allele of β-catenin exhibit clusters of pituitary cells that over-express β-catenin, express *Sox2,* and induce transformation of neighboring cells that mimic craniopharyngioma, a childhood tumor [62].

Taken together these studies established that SOX2-expressing cells represent progenitors of the hormone-producing cells the developing pituitary.

Patient mutations

Most patients with *SOX2* mutations have serious eye abnormalities that can include anophthalmia, microphthalmia, and/or optic nerve hypoplasia, and hypopituitarism characterized by pituitary gland hypoplasia and hypogonadotropic hypogonadism [39, 51, 62, 63]. While all of the patients with *SOX2* mutations exhibited reduced gonadotrope function, the degree of GH deficiency varied. The response of patients to GnRH stimulation was also variable.

PITX Factors (PITX1: Ptx1, Bft, P-OTX; PITX2: Brx, Munc30, Otlx2, Rieg)

Gene Discovery

The PITX transcription factors, PITX1 and PITX2, are expressed early in pituitary gland development and persist through adulthood. Their names derive from their pituitary expression and paired-like homeobox DNA binding domains, and they have important functions in the hindlimb, heart, eye, and other tissues [47, 49, 64-66]. These factors were found in very different ways, and they have overlapping functions within the pituitary gland [67].

Pitx1 was discovered by searching for factors that bind the regulatory elements of the pro-opiomelanocortin gene (*Pomc*). POMC is a pro-hormone that is expressed in both corticotropes of the anterior lobe and melanotropes or the intermediate lobe. POMC undergoes differential cleavage to produce adrenocorticotropin (ACTH) in corticotropes and melanocyte stimulating hormone (MSH) and β-endorphin in melanotropes. *In vitro* analysis revealed that the major regulatory region of the *Pomc* promoter-proximal region was between 166 and 480 bp upstream of the transcription start site [68]. Drouin and colleagues found that deleting a small section from the middle of this element nearly ablated *Pomc* expression [69]. They screened a

cDNA expression library from AtT-20 cells, an immortalized corticotrope-like cell, for factors that bind this element, and identified *Pitx1*, which has high homology with the mouse *Otx* genes. *Pitx1* was identified independently by screening the same cDNA expression library for factors that interact with POU1F1 [70], a pituitary transcription factor described below.

PITX2 was discovered as one cause of Rieger syndrome, which was first described in the 1800s as a genetic disorder characterized by eye malformations, dental hypoplasia, craniofacial dysmorphism, and umbilical stump abnormalities. The causal gene was mapped to a 50kb region on chromosome 4 [71]. Genomic DNA from CpG islands in this region were used to screen human craniofacial and fetal brain cDNA libraries, and a contig of *RIEG* cDNAs were obtained [72]. *RIEG* was most closely related to *Pitx1,* and it was later renamed *PITX2*. Murray and colleagues reported mutations in six families with Rieger syndrome. *Pitx2* was discovered independently by screening an adult mouse pituitary cDNA library for homeobox genes [73]. It was predicted to be a regulator of anterior structure formation in mice based on its expression pattern and its location on mouse chromosome 3 within a region of synteny homology to the region of human 4q25 where Rieger syndrome had been mapped.

Gene Expression

The expression patterns of *Pitx1* and *Pitx2* differ, but there are some regions of striking overlap. *Pitx1* is expressed in the pituitary, intestine, tongue, oral epithelium, the mandible, salivary glands, duodenum, nasal epithelium, and the hindlimb [69, 70, 74]. *Pitx1* is expressed in the pituitary primordia by embryonic day 9.5 (e9.5) [75]. *Pitx2* is expressed in the eye, the dental lamina, limb mesenchyme, umbilical vessels, and in Rathke's pouch as early as e8.5 [72]. The early expression of both PITX factors suggested their importance for pituitary development.

Down-stream Targets

PITX1 binds the promoters of several genes that encode pituitary hormones, including *Cga* (chorionic gonadotropin alpha, the common subunit of the heterodimeric hormones LH,

FSH and TSH), *Gh*, and *Prl*, and induces their transcription [70]. PITX1 was also implicated in the transcription of *Gnrhr*, *Pou1f1*, *Tshb, Nr5a1,* and *Lhx3* using cell transfection assays [76]. However, immunostaining suggests that the gonadotropes and thyrotropes have the most abundant expression of PITX1 and PITX2 in the adult pituitary gland [77]. PITX2 activity is enhanced by β-catenin, and the complex regulates Cyclin D2 expression [78].

Knockout Mice

Mice homozygous for *Pitx1* deletion had disrupted hindlimb formation and a very mild pituitary phenotype with a slight reduction of gonadotropes and thyrotropes [47]. All of the major transcription factors were largely unaffected, and *Pomc* expression was normal.

By comparison, *Pitx2* had a much stronger effect on the developing pituitary. Four independent *Pitx2* knockout mouse lines were published in 1999 [49, 64-66]. Camper and colleagues developed several alleles, which included a hypomorphic or reduced function allele, $Pitx2^{neo}$, a null allele, $Pitx2^{-}$, and an inducible null allele [48]. Various combinations of these alleles were used to assess dosage sensitive effects of *Pitx2* loss of function, i.e. an allelic series. $Pitx2^{-/-}$ and $Pitx2^{neo/neo}$ embryos die *in utero*, at e13.5 and e18.5 respectively. Both exhibit right lung isomerism, and dosage sensitive effects on eye, pituitary gland, and heart development. The ventral body wall of $Pitx2^{-/-}$ embryos fails to close, resulting in externalization of the heart, liver, and abdominal organs. *Pitx2* heterozygotes accurately model the ocular features of Rieger syndrome [79].

The initial induction of Rathke's pouch occurs at e10.5 in $Pitx2^{-/-}$ embryos, but there is extensive cell death and reduced cell proliferation, resulting in a very small pituitary primordium at e12.5 [64, 67]. *Hesx1, Prop1,* and *Lhx4* are not expressed in these mutants, but *Lhx3* is activated. Little or no hormone cell specification is detected [49]. In contrast to the small pituitaries in $Pitx2^{-/-}$ and $Pitx2^{neo/-}$ embryos, there was no obvious reduction in the size of $Pitx2^{neo/neo}$ pituitaries [48]. Somatotropes and thyrotropes were reduced, and gonadotropes

were ablated. *Pitx2*$^{neo/neo}$ pituitaries had reduced expression of the transcription factors *Gata2*, *Egr1*, *Nr5a1,* and *Pou1f1.*

The overlapping expression patterns of *Pitx1* and *Pitx2* suggested the possibility of compensatory function. Indeed, double heterozygotes (*Pitx1*$^{+/-}$, *Pitx2*$^{+/-}$ and *Pitx1*$^{+/-}$, *Pitx2*$^{+/neo}$) have very poor viability, and hypoplastic pituitaries [67]. *Lhx3* expression was not detectable in rare double mutants, suggesting that *Pitx* genes are required for *Lhx3* expression.

Human mutations

Heterozygous *PITX1* loss of function mutations have been reported in two families with lower extremity abnormalities [80-82]. Genomic rearrangements that result in ectopic expression of PITX1 in the developing forelimbs cause Liebenberg syndrome, a homeotic transformation of the arms to a leg morphology [83, 84].

Rieger syndrome is a rare, autosomal dominant disorder affecting development of the eyes, teeth and abdominal wall. It can be caused by mutations in *PITX2* or *FOXC1.* The majority of patients with Rieger syndrome have normal height, although there are some anecdotal reports of Rieger syndrome patients with growth insufficiency. For example, a three-generation family with Rieger syndrome and either short stature or growth hormone deficiency was reported [85]. The proband responded to GH replacement therapy. The nature of the mutation in this family and other historical cases are unknown. Many Rieger syndrome patients have been screened for *PITX2* mutations, but no systematic screening of CPHD patients without eye defects has been reported.

LIM homeodomain proteins: LHX2 (ap, apterous, Lh-2, LH2A), LHX3 (P-LIM, Lim3), LHX4 (Gsh-4)

Gene Discovery

LHX proteins contain both **L**IM-domains, comprised of two contiguous zinc fingers, and a **H**omeobo**x**-domain. Three LHX factors involved in pituitary development, *Lhx2, Lhx3* and *Lhx4*, and they were discovered independently. *Lhx2* was discovered in a screen of cell lines for VDJ recombinase activity [86]. *Lhx3* was discovered in a screen for *Lhx* factors in a cDNA library generated from *Xenopus* gastrula (called Xlim3 in *Xenopus*) [87]. *Lhx4* (previously known as Gsh-4) was discovered in a screen for homeobox genes in mouse genomic DNA [88]. *Lhx2* is expressed in developing B cells, telencephalon, retina, ventral diencephalon, posterior pituitary gland and infundibulum [89]. *Lhx3* is expressed in the pituitary and pineal glands, the retina, spinal cord, and hindbrain. *Lhx4* is expressed in the developing pituitary, neural tube, hindbrain, spinal cord [50, 90].

Knockout Mice

Mouse knockouts of *Lhx2, Lhx3* and *Lhx4* revealed the importance of each gene for pituitary development [50, 54, 90-93].

Lhx2 is expressed in the developing ventral diencephalon from e9.5-e12.5, in regions that become the pituitary infundibulum and posterior lobe [91]. Embryos homozygous for *Lhx2* null alleles have pituitary dysmorphology including bifurcation of Rathke's pouch, excess proliferation in the infundibular area, and failure of the neural ectoderm to evaginate. Despite this, all hormone producing cell types of the anterior lobe are detectable, consistent with the expression of critical signaling molecules such as BMP and FGFs by the abnormal infundibular structure. The mice are not viable and also have anophthalmia, anemia and malformations of the cortex [89]. A cohort of 59 patients with pituitary deficiency and eye abnormalities were negative for *LHX2* mutations [94].

Lhx3 is expressed in the pituitary placode at e9.5 and persists through adulthood [92]. *Lhx3*$^{+/-}$ mice are phenotypically normal and fertile, but mice homozygous for the null allele were either stillborn or died within 24 hours after birth. Rathke's pouch formed in *Lhx3*$^{-/-}$ embryos but failed to expand. The thin, underdeveloped pouch fails to separate from the oral ectoderm.

These mutant pouches exhibited reduced cell proliferation and enhanced cell death, and there is evidence of abnormal dorsal-ventral polarity [93]. The cyclin dependent kinase inhibitor *Cdkn1a* (p21) is expressed more dorsally than normal, and *Cdkn1c* (p57) is absent in the caudal region of the pouch [95]. *Hesx1* and *Isl1* expression were initiated at e10.5 but failed to be sustained at e12.5. Induction of lineage-specific transcription factor gene expression -- *Tbx19, Neurod1, Nr5a1,* and *Pou1f1* -- were very poor. *Lhx3*$^{-/-}$ embryos contained a few differentiated corticotropes but no other differentiated hormone producing cells were detected.

Lhx4 is expressed in the pituitary primordium between e9.5 and e12.5, and it is restricted to the prospective anterior lobe at e12.5 [50]. Expression diminishes at e15.5, but it is detectable in adult pituitary anterior and intermediate lobes. *Lhx4*$^{-/-}$ newborns appear normal but die shortly after birth due to failure of the lungs to inflate [90]. Dexamethasone treatment, used to accelerate lung development, improved but did not completely rescue survival. Pituitary insufficiency can result in poor lung development in certain genetic backgrounds [53]. *Lhx4*$^{-/-}$ embryos have anterior pituitary lobe hypoplasia [50]. Enhanced cell death is evident at e12.5, and *Lhx3* expression is significantly delayed [54, 95]. *Isl1* expression does not become ventralized at e11.5 and it is not detected at e12.5. *Pitx2* expression is also not maintained. Expression of pituitary hormone genes is reduced but detectable.

The functions of *Lhx3* and *Lhx4* overlap [50]. Both *Lhx3*$^{+/-}$, *Lhx4*$^{-/-}$ and *Lhx3*$^{-/-}$, *Lhx4*$^{+/-}$ embryos can form Rathke's pouch, but it fails to expand and is more severely affected than in either single mutant. *Lhx3*$^{-/-}$, *Lhx4*$^{-/-}$ double mutants have a very severe pituitary phenotype [50]. The double mutants form a pouch rudiment, and invagination of the oral ectoderm occurs, but the rudiment fails to separate from the oral ectoderm and remains at the pharyngeal cavity beneath the palate.

Human mutations

Following characterization of the *Lhx3*$^{-/-}$ mice, patients with **C**ombined **P**ituitary **H**uman **D**eficiency (CPHD) were screened for *LHX3* mutations. Loss of function mutations were found

in several unrelated patients [96-106]. Generally, the mutations were recessive and associated with multiple pituitary hormone deficiencies. Limited neck rotation, hyperplastic anterior pituitary gland, sensorineural hearing impairment, respiratory problems, and skeletal abnormalities were found in some cases. Heterogeneity in the presentation of pituitary size is observed in CPHD patients with mutations in other genes including *PROP1* [107].

Mutations in *LHX4* have been identified in multiple unrelated patients with CPHD. One is a homozygous lethal missense variant (p.T126M) [104], but the rest are heterozygous loss of function mutations with incomplete penetrance [108-113]. This indicates that the dosage sensitivity to *LHX4* loss of function is more extreme in humans and mice.

In conclusion, LHX3 and LHX4 have essential and overlapping roles in anterior pituitary development in mouse and man, while LHX2 has a role in posterior pituitary lobe development.

HESX1 (Rpx)

Gene discovery and Gene expression

Hesx1 was discovered by a screen for **H**omeobox factors in an **E**mbryonic **S**tem cell cDNA library, and independently, in a screen for homeobox factors expressed during gastrulation, at e7.5 [114-116]. *Hesx1* is expressed sequentially in the anterior visceral endoderm, anterior definitive endoderm and the cephalic neural plate. While officially known as *Hesx1,* it was also named **R**athke's **P**ouch homeobo**x** (*Rpx1*) because of its robust expression in the developing pituitary primoridia at e9.5. Its expression in the developing pituitary gland is extinguished by PROP1 at e14.5 [117, 118].

Knockout mouse phenotype, Down-stream targets, upstream regulators

Robinson and colleagues generated a *Hesx1* deletion in mice and demonstrated that 93% of homozygous mutants died before weaning [119]. The phenotype was variable and

included developmental abnormalities of the forebrain, eye, and pituitary gland. The pituitary glands were missing (5%), misplaced, dysmorphic and/or small [118]. *Hesx1* deficiency permits excessive FGF signaling, resulting in multiple invaginations of oral ectoderm instead of a single Rathke's pouch [118]. Most mice heterozygous for the deletion were normal, but 1% displayed mild abnormalities of the same organs affected in homozygous mice.

Rosenfeld and colleagues demonstrated that HESX1 acts as a repressor of *Pou1f1* expression by binding the *Pou1f1* early enhancer [118, 120]. HESX1 binds the co-repressor transducin-like enhancer of split 1 (TLE1) through its engrailed homology domain and also interacts with a co-repressor, histone deacetylase complex containing Nuclear Receptor Co-Repressor (NCoR). Forced expression of HESX1 and TLE1 during pituitary development is sufficient to suppress POU1F1-dependent cell lineages. Both HESX1 and PROP1 are paired type homeodomain transcription factors that can compete for the same DNA binding sites. In the presence of beta-catenin, PROP1 binds the early enhancer of *Pou1f1* and initiates *Pou1f1* gene expression.

Both *Lhx3* and *Pitx2* are necessary upstream regulators of *Hesx1* in the developing pituitary gland [64, 92]. A 100 bp element that directs spatial expression of *Hesx1* in Rathke's pouch lies ~3.3 kb 3' of the gene and is bound by PITX2 and GATA2 [121]. The promoter proximal -570 bp, exons 1 and 2 and intron 1 of *Hesx1* are sufficient for transgene reporter expression in the anterior visceral endoderm, anterior neural ectoderm, and anterior neural plate. A negative element that suppresses *Hesx1* expression in the hypothalamus, and responds to inductive signals from Rathke's pouch, has been mapped -568 to-532 bp upstream of the gene.

Patient mutations

The phenotypes of *Hesx1* knockout mice suggested that *HESX1* mutations might cause pituitary and anterior structure malformations in humans. A screen of 61 patients with holoprosencephaly, Septo-Optic Dysplasia (SOD), or pituitary insufficiency uncovered two

siblings with agenesis of the corpus callosum and panhypopituitarism that were homozygous for a missense mutation in *HESX1,* p.R53C, which abrogates DNA binding [119]. This disease association was confirmed by screening a larger cohort of 228 patients with congenital pituitary defects for mutations in *HESX1* [122]. Three heterozygous missense mutations were identified, p.S170L, p.C509T, and p.A541G, which were associated with incomplete penetrance and variable phenotypic presentation from SOD to hypopituitarism, or Isolated Growth Hormone Deficiency (IGHD).

Summary

Hesx1 was discovered in two independent cDNA screens for homeobox transcription factors. LHX1*,* LHX3*,* and LMX1B activate its expression in early head development, and PITX2 and GATA2 activate its expression in Rathke's pouch. Pituitary expression is extinguished by PROP1*,* which also releases HESX1-mediated repression of *Pou1f1,* activating the development of somatotropes, lactotropes and thyrotropes. Homozygous mutations in mice and heterozygous mutations in humans cause variable phenotypes that include reduced forebrain, anophthalmia, and pituitary dysfunction. The cause of variable presentation is not known.

PROP1

Gene discovery

Prophet of Pit1 or PROP1 is a pituitary specific transcription factor that was identified by positionally cloning a spontaneous dwarf mouse mutant, Ames dwarf, df [123]. These mice were first described phenotypically 58 years ago by Drs. Schaible and Gowen at Iowa State University in Ames, Iowa, as they studied the descendants of an irradiation experiment [124]. Homozygous mutant mice have anterior pituitary hypoplasia, growth insufficiency,

hypothyroidism and infertility, which are attributed to lack of growth hormone, prolactin and thyroid-stimulating hormone [125-127]. *Hesx1* expression was not properly repressed in the df/df mutant pituitaries, placing the df locus downstream of *Hesx1* [127]. No expression of *Pou1f1* could be detected in the pituitaries of developing *df/df* mutants by in situ hybridization, indicating that *Prop1* is required for activation of *Pou1f1* [117, 128]. However, small clusters of cells expressing *Pou1f1* and GH, PRL or TSH could be detected in adult *df/df* mutant pituitaries by immunohistochemistry [127]. These committed somatotropes did not express detectable levels of *Ghrhr* and were insensitive to increased stimulation by growth hormone releasing hormone [127].

Genetic mapping placed the *df* locus on mouse chromosome 11 in a region of synteny homology with human chromosome 5q [129]. Using genetically directed representational difference analysis, the critical region was narrowed to a 400-600 kb window [123]. Genomic clones from this region were probed with cDNA from the developing pituitary, resulting in the identification of *Prop1,* which encodes a 233 amino acid paired homeodomain containing protein. The Ames dwarf mice had a missense mutation in the homeodomain, p.S83P, that abrogates DNA binding. A null allele of *Prop1* was genetically engineered by inserting a LacZ/Neo cassette into the first exon of *Prop1* [53]. These *Prop1*$^{-/-}$ mice essentially phenocopy the *Prop1*$^{df/df}$ mice when compared on the same genetic background. *Prop1* expression is highly restricted to the pituitary, beginning at embryonic day 10.5, reaching a peak at e12.5, declining through development, and remaining detectable in the postnatal period [123, 130].

Down-stream targets

PROP1 binds β-catenin and competes with the HESX1-co-repressor complex for binding at the early enhancer of *Pou1f1* to induce *Pou1f1* expression [118, 120, 123]. Deletion of β-catenin before the expression of *Pou1f1* blocks *Pou1f1* expression, while deletion of β-catenin after the onset of *Pou1f1* expression had no effect, suggesting a narrow critical window of β-catenin expression in lineage determination. This β-catenin phenotype occurs independent of

LEF1, TCF3, or TCF4 action. PROP1 interacts directly with the co-repressors TLE, Reptin, and HDAC1 to bind and repress the expression of *Hesx1*.

Lineage tracing reveals that all hormone-producing cell types of the anterior and intermediate lobes of the pituitary descend from *Prop1*-expressing cells [131]. This places *Prop1* just downstream of *Sox2* expression in pituitary progenitors [130] (**Fig. 2**). *Prop1*$^{df/df}$ mice have a vascularization defect, reduced expression of cyclin D1 and cyclin D2 in pituitary progenitors, and a failure of proliferating cells to migrate away from the stem cell niche into the parenchyma, which appears to be a failed epithelial to mesenchymal-like transition [132]. Many mutant cells undergo apoptosis. Notch signaling is normally active in the transitional zone between the stem cell niche and the differentiating cells, but *Prop1* mutants do not express *Notch2* [31, 133]. Colony forming assays and RNA-Seq were used to assess the effect of *Prop1* deficiency on stem cells. Mutants had a reduced stem cell pool, abnormal colony morphology, and changes in gene expression consistent with a failed epithelial to mesenchymal transition. To identify additional downstream targets of *Prop1* that might underlie the features of mutant pituitaries, Pérez Millán and colleagues developed a biotin-tagged allele of PROP1 in an immortalized pituitary cell line, facilitating direct identification of PROP1 binding sites in chromatin [130]. Binding sites were identified in or near *Notch2, Gli2* and *Zeb2. Zeb2* activation appeared to be an essential step in the process of engaging progenitors to undergo EMT.

Upstream regulators

Multiple species alignment of PROP1 genomic sequences from a variety of mammals revealed three areas of high conservation: upstream, downstream, and within intron 1 of *Prop1* [134]. In the context of the *Cga* promoter, the intronic enhancer is sufficient to drive expression in the stem cell niche, located in the dorsal aspect of the pituitary gland in transgenic mice. The *Cga* promoter alone drives expression in the more ventral aspect of the organ, consistent with the location of differentiating gonadotropes and thyrotropes. This enhancer sequence is bound by RBpJK, indicating that Notch signaling feeds back to upregulate *Prop1* expression [32].

Patient mutations

Quickly after the discovery of mouse *Prop1* by positional cloning, the human ortholog was identified and recessive loss of function mutations were found in four unrelated families with CPHD [135]. All three mutations either reduced or completely eliminated PROP1's ability to bind DNA, convincingly implicating these lesions as the cause of CPHD. Mutations in *PROP1* are the most common, known cause of CPHD [136, 137]. The most frequent mutations are frameshifts causing premature termination; many patients are homozygous for c.[301-302delAG] or c.[150delA]. Portuguese [138], Lithuanian [139] and Czech [140] cohorts have a high incidence of the 2 bp deletion, and the 1 bp deletion is common in Croatia [141]. A thorough investigation of the haplotype revealed that the 2 bp deletion founder mutation arose approximately 101 generations ago in central eastern Europe, and it either re-occurred or was transferred to the Iberian peninsula approximately 23 generations ago [141]. The Iberian haplotype and mutation were subsequently transferred to Latin America. Combining all population groups analyzed so far, *PROP1* mutations are estimated to cause ~11% of familial and sporadic cases of CPHD [5]. All mutations discovered to date are recessive, and the phenotype includes deficiency of GH, TSH, gonadotropins, and progressive loss of ACTH. We speculate that the progressive hormone loss may result from depletion of the pituitary stem cell pool.

POU1F1 (PIT-1, GHF-1)

Gene discovery

Karin and Rosenfeld independently discovered the first pituitary-specific transcription factor, demonstrated that it regulated expression of the *Gh* and *Prl* genes, and named it GHF1 and PIT1, respectively [142, 143]. It was later renamed POU1F1. Rosenfeld's group identified

cis-acting sequences in the *Gh* and *Prl* genes that were necessary for their expression in pituitary cell cultures and used them as probes to screen a pituitary cDNA expression library [143, 144]. They identified the *Pou1f1* cDNA, detected transcripts only in pituitary gland, and showed that *Pou1f1* expression vectors were sufficient to activate *Gh* and *Prl* reporter genes in transfected, heterologous cells. Karin's group took the approach of biochemically purifying the protein that bound the cis-acting sequences in the *Gh* promoter and obtaining the amino acid sequence of a peptide from the binding protein [142, 145]. Probes complimentary to the peptide sequence were used to screen pituitary cDNA libraries and GHF1 was identified. Loss of GHF1 resulted in loss of *Gh* expression [146]. Subsequent structure-function analyses revealed the presence of the nuclear localization signal and the roles of the homeodomain and POU-specific domain in specificity of DNA binding [147].

Knockout Mice

George D. Snell described the phenotype of an autosomal recessive, spontaneous dwarf mouse mutant in 1929, and it was named dw [148]. The growth insufficiency of the mutant mice is evident fourteen days postnatally, and adult mutants also exhibit hypothyroidism and hypogonadism. Tissue transplantation experiments demonstrated that the multi-organ defects were rescued by pituitary tissue, and mutant pituitaries did not improve function when implanted in the sella of normal mice, pinpointing the pituitary as the root cause of the hormone deficiencies [149, 150].

Finally, sixty-one years after the dw Snell dwarf mutation was described phenotypically, lesions in *Pou1f1* were implicated as causal [151, 152]. *Pou1f1* was tightly linked genetically to the *dw* locus, and the gene was rearranged in an allelic variant, dw^J [153]. DNA sequencing revealed a G→T missense mutation, resulting in a p.W251C change of a highly conserved residue in the homeodomain that abrogates DNA binding. These findings extended the role of *Pou1f1* from direct activation of *Gh* and *Prl* gene expression to include stimulating the

development and specification of cells that express *Gh, Prl,* and *Tshb.* These three specialized cell types became known as the *Pou1f1* lineage.

Patient mutations

Two years after linking the mouse dwarfism phenotype to lesions in *Pou1f1*, Khono and colleagues identified the first *POU1F1* mutation found in a patient with TSH, GH, and prolactin deficiencies [154]. This c.C638T nonsense mutation resulted in a truncation, p.R172X, N-terminal to the homeodomain of POU1F1. Numerous *POU1F1* mutations have been described in patients with CPHD (reviewed in [5]). The majority are recessive loss of function mutations that present with deficiency of GH, PRL and TSH. However, there are a few notable exceptions. The p.R271W mutation is dominant negative and incompletely penetrant, possibly due to variability in mono-allelic expression of the mutant vs. normal allele [155-157]. The p.R271W mutation interferes with binding to C/EBP□, and it permits recruitment to centromeric heterochromatin [158]. The mutation also interferes with tethering of POU1F1 dimers to the nuclear matrix via interactions with β-catenin, SATB1 and matrin-3 [159]. A p.K216E mutation in the homeodomain is also a dominant cause of CPHD [20]. This mutation acts by interfering with the ability of POU1F1 to autoactivate its late enhancer in response to retinoic acid stimulation (see below). A p.P76L mutation in the transactivation domain causes dominant IGHD in humans and recessive growth insufficiency in mice [160]. TSH and PRL were not measured in the mouse model. The amino acid substitution increases DNA binding at the human *GH1* locus control region and increases binding to several transcription factors, including PITX1, LHX3a, and ELK1. The p.P76L change decreases transactivation of *Gh*, but it has no effect on the *Prl* promoter. Two other proline substitutions in the transactivation domain have been reported in children with GH, PRL and TSH deficiency: p.P14L and p.P24L [156, 161]. Detailed functional studies were not carried out. The p.P14L variant appears dominant with incomplete penetrance, and no inheritance data were presented for the p.P24L allele. In sum,

mutations in *POU1F1* can cause CPHD or IGHD and be recessive or dominant, and dominant mutations are informative about the normal mechanism of action.

Upstream regulators

Pou1f1 expression is selectively high in the anterior lobe of the pituitary. The cis-acting sequences necessary for *Pou1f1* expression were mapped extensively in transgenic mice [34]. A 390 bp enhancer located ~10.4-10.2 kb upstream of the *Pou1f1* transcription start site is sufficient for *Pou1f1* expression postnatally in the context of the minimal 327 bp *Pou1f1* promoter [162]. This distal or 'late enhancer' is bound by POU1F1 in an autoregulatory loop necessary for maintaining expression. Another enhancer element located between ~8 kb upstream of *Pou1f1* is bound by PROP1 and β-catenin, inducing initial expression of *Pou1f1*, but this proximal or 'early enhancer' is not sufficient for the sustained expression of *Pou1f1* into adulthood [120, 123, 162].

Down-stream targets

The role of POU1F1 in establishing thyrotropes and *Tshb* expression was discovered later [77, 163, 164]. Ridgway and colleagues mapped cis-acting sequences necessary for *Tshb* expression in thyrotropic tumor cells and identified binding sites for POU1F1 and GATA2 within -133 to -88 of the *Tshb* transcription start site. Neither transcription factor had a major impact on *Tshb* transcription individually, but together they synergistically activated *Tshb.* Using dominant negative and ectopic gene expression transgenic approaches, Rosenfeld and colleagues discovered that POU1F1 and GATA2 interact to promote thyrotrope development, while GATA2 alone promotes gonadotrope development. Specifically, they showed that broadly expressing *Gata2* throughout the developing pituitary blocks *Pou1f1* expression, reduces thyrotrope and somatotrope differentiation, and increases gonadotrope specification. Conversely, expressing *Pou1f1* broadly throughout the developing pituitary drives high levels of thyrotrope and somatotrope differentiation, and blocks gonadotrope specification. Camper and Ridgway collaborated to show that a pituitary-specific knockout of GATA2 diminished thyrotrope

and gonadotrope differentiation. At birth, the mice have very few thyrotropes, but they recover as the mice age, likely through sensitive feedback loops that maintain thyroid hormone production at the proper level. These mice also became fertile. Marked upregulation of *Gata3* was observed, which may compensate for loss of *Gata2.* A pituitary-specific *Gata2, Gata3* double knockout would be necessary to assess whether loss of both GATA factors is sufficient to block gonadotrope and thyrotrope development. Nevertheless, these studies established an important role for both *Pou1f1* and *Gata2* in pituitary development.

POU1F1-mediated regulation of gene expression and cell fate requires interaction with chromatin modifying factors. POU1F1 binds to the *Gh* promoter by e13.5-e14.5, but *Gh* transcription is not activated until a complex containing the histone lysine demethylase, LSD1 is recruited [165]. A pituitary-specific deletion of *Lsd1* has little effect on *Pou1f1* expression, but there is little or no expression of *Gh, Tshb,* or *Prl.* Differentiation appears to be suppressed because Notch signaling fails to be silenced. LSD1 binds and activates the *Gh* promoter through interaction with an MLL1 co-activator complex. A region of the *Gh* promoter located at -161 to -146 is necessary for silencing *Gh* expression in lactotropes postnatally. ZEB1, a homeodomain transcription factor with seven Zn fingers, binds this element with a constellation of co-factors including LSD1 and co-repressors. Estrogen, an activator of *Prl* expression, enhances the recruitment of LSD1 and ZEB1 mediated repression of *Gh* in lactotropes during the postnatal period in mice.

Recently, other POU1F1 binding partners were identified, shedding light on its mechanism of action [159]. Using immunoprecipitation and mass spectrometry, POU1F1 was discovered to interact with matrin-3, β-catenin, and SATB1. The dominant negative *POU1F1* p.R271W mutation interferes with POU1F1's interaction with β-catenin and SATB1 which, in turn, results in the failure to interact with matrin-3 and reduced expression of POU1F1 target genes. Gene expression is rescued by fusing POU1F1 (p.R271W) with matrin-3. This shows

convincingly that the multi-protein complex must be tethered to the nuclear matrix for optimal activity.

NR5A1 (Steroidogenic Factor 1, SF1, Ftz-f1, adrenal 4-binding protein)

Gene discovery

NR5A1 is considered to be the signature transcription factor for driving pituitary gonadotrope cell fate. It was initially discovered in the search for transcription factors regulating steroidogenic enzyme biosynthesis in the adrenal cortex. Parker and Morohashi independently made the observation that multiple cis-regulatory elements driving expression of steroidogenic enzyme genes and cytochrome P450 genes in the adrenal cortex had highly similar AGGTC motifs, suggesting that a single factor might regulate the expression of these proteins [166, 167]. In support of this, the factor(s) that bound all six of these elements were the same molecular weight and had identical chromatographic properties. They took a biochemical purification approach to identify the transcription factor binding these elements. Y1 adrenocortical tumor cells did not produce sufficient protein for purification and characterization. To circumvent this limitation, they took advantage of evolutionary conservation of regulatory networks among mammals. The promoters of these three genes have high sequence similarity in cows and mice [168], and the bovine factor that binds the mouse regulatory elements is the same size as the mouse factor [169, 170]. They collected bovine adrenal cortex tissues, purified the binding protein, and named it steroidogenic factor 1 or SF1. This 53kD protein could bind all six regulatory elements. Because the AGGTC motif is similar to the binding sites of nuclear hormone receptors, they predicted that SF1 would have a DNA binding domain similar to the nuclear hormone receptor family. They screened a Y1 cDNA library with a probe designed to hybridize to the consensus sequence encoding a nuclear hormone receptor DNA binding

domain. One of the cDNAs fit the expected expression profile of SF1, namely expression in the adrenal glands, the corpus luteum, and the testis. They proved that they had cloned the correct cDNA by expressing the protein in bacteria and demonstrating that it had the same binding affinity as that of SF1 purified from the bovine adrenal gland. The SF1 cDNA sequence encoded an orphan nuclear hormone receptor related to the *Drosophila* segmentation gene, fushi tarazu or ftz, which also specifies neuronal identity in flies. The gene was renamed *NR5A1* according to the nomenclature for orphan nuclear receptors.

Gene expression

In mice, *Nr5a1* transcripts were detected by *in situ* hybridization in the developing hypothalamus and the urogenital ridge, which is the precursor to the adrenal glands and gonads [171]. *Nr5a1* sustains high expression in the adrenal glands through adulthood. Conversely, it is expressed highly in the developing bipotential gonad, and it is maintained in testes, particularly in Sertoli cells. Meanwhile its expression in ovaries is reduced when the ovary first becomes morphologically distinct from the testis. *Nr5a1* expression in the bipotential gonad suggested a function in sexual development. *Nr5a1* was expressed in the ventromedial hypothalamus (VMH), which is involved in feeding, fear, thermoregulation, and sexual activity [172]. These studies indicated that *Nr5a1* was expressed early in organ development and could therefore be a driver of cell fate in mammals.

Down-stream targets

Mellon and colleagues identified a DNA element that regulates gonadotrope expression of *Cga,* which encodes the alpha-subunit of the heterodimeric glycoprotein hormones, luteinizing hormone (LH), follicle stimulating hormone (FSH), and thyroid stimulating hormone (TSH) [173]. Mellon showed that this element (which they called GSE for **G**onadotrope-**S**pecific **E**lement) was bound by a 54 kD protein, which they labeled GSEB-1 (GSE-**B**inding factor 1). They demonstrated that GSEB-1 is NR5A1 by showing that NR5A1 binds specifically to the

GSE *in vitro* and that NR5A1-specific antibodies antagonize GSEB-1 function [174]. This was the first evidence that NR5A1 had a role in the pituitary gland.

Mellon discovered that NR5A1 regulates the transcription of *Lhb*. This represented the second known direct target of NR5A1 in the pituitary gland. NR5A1 binds a GSE in the promoter region of *Lhb* and increases its expression [173, 175]. Nilson and colleagues showed that 776 bp of the bovine LHB proximal promoter region was sufficient to drive gonadotrope-specific expression in transgenic mice [176]. This sequence contained the GSE, was responsive to GnRH regulation but was not androgen or estrogen responsive. A mutation in the GSE element reduced transgene expression ten-fold [177]. This suggested that NR5A1 stimulates LHB expression by binding the promoter proximal GSE in cell culture and *in vivo*.

Morohashi and colleagues found two regulatory elements of *Nr5a1*, showing that NR5A1 binds one of them to stimulate its own expression in adrenal cells [170], while Clay and colleagues demonstrated that NR5A1 directly regulates expression of *Gnrhr* via a GSE in the promoter proximal region [178].

Interacting factors

NR5A1 interacts with other transcription factors to promote gene expression. The Drouin lab demonstrated that PITX1 and NR5A1 interact directly and synergize to activate *Lhb* promoter but not *Cga* gene expression [76, 179]. The PITX1 binding site is not required for this activity. NR5A1 also interacts with the zinc-finger transcription factor EGR1 to regulate the expression of *Lhb* [180, 181]. Both the NR5A1 and EGR1 binding sites are required for the synergism. Milbrandt and Charnay independently demonstrated that EGR1 is necessary for *Lhb* expression in mice [180, 182]. There are no exact obvious NR5A1 binding sites in the *Fshb* promoter, but Mellon and colleagues found two sites bound by NR5A1 [183]. NR5A1 interacts with Nuclear Factor Y (NFYA) on the *Fshb* promoter to synergistically activate *Fshb* transcription.

Knockout mouse phenotype

Nr5a1 knockout mice were generated by homologous recombination in embryonic stem (ES) cells [184]. Homozygous mutant mice lack adrenal glands and gonads, revealing that NR5A1 is not only critical for expression of steroidogenic enzymes in these tissues, but it has a critical role early in adrenal and gonadal organogenesis. Moreover, the pituitaries of *Nr5a1*-null mice lack detectable transcripts for *Lhb, Fshb,* and the gonadotropin releasing hormone receptor, *Gnrhr* [56]. Expression of other pituitary hormones was normal. *Nr5a1* transcripts were detected at e13.5-e14.5, prior to expression of other gonadotrope markers, suggesting that NR5A1 could be involved in gonadotrope differentiation, but it was still unclear whether *Nr5a1* was involved in differentiation or maintenance.

Nr5a1 mutants had structural abnormalities in the VMH, implicating NR5A1 in three levels of the reproductive axis: hypothalamus-pituitary-gonad [185]. However, the GnRH neurons were normal. A 24 hr treatment regime of GnRH injections can rescue expression of *Lhb* and *Fshb* in hypogonadal mutants, *Gnrh*$^{hpg/hpg}$, and *Nr5a1* knockout mutants, suggesting that the gonadotrope progenitors are present in *Nr5a1* mutants, and that NR5A1 is not strictly required for gonadotrope fate [185]. GnRH induces expression of many transcription factors in the pituitary gland, including *Egr1, Atf3,* c-Jun, and TCF/LEF, and increased expression of these factors may compensate for NR5A1 deficiency [181, 186-188].

To distinguish direct effects of NR5A1 on the pituitary gland from indirect effects resulting from altered hypothalamic and or gonadal inputs to the pituitary gland, researchers developed a floxed allele of *Nr5a1* and induced deletion in the pituitary with a *Cga-cre* transgene [189, 190]. This ablated expression of *Fshb*, *Lhb*, and *Gnrhr*. These deficiencies caused failure to develop mature reproductive organs and infertility. Injection of these pituitary-specific knockout mice with pregnant mare serum gonadotropin (PMSG), a hormone produced by the equine placenta that has luteinizing and follicle stimulating activity, was sufficient to induce pituitary expression of *Lhb* and *Fshb.* This demonstrated that *Nr5a1* deficiency impacts

pituitary development and function directly, but it can be overcome by supra-physiologic hormonal stimulation.

Patient mutations

The first patient with an *NR5A1* mutation was reported in 1999 [191]. The patient presented with primary adrenal failure, complete XY sex reversal, and streak-like gonads. Her pituitary gland responded to GnRH stimulation. She was heterozygous for a two bp mutation that causes a p.G35A missense in the first zinc finger of NR5A1 that abrogates DNA binding. Her phenotype is consistent with NR5A1's role in adrenal function and stimulation of LH and FSH expression. The sex reversal was surprising because mice heterozygous for a null allele of *Nr5a1* are phenotypically normal. Loss of function mutations have been associated with other cases of 46XY sex reversal [192-195], 46XX sex reversal [196, 197], under-virilization [198], adrenocortical insufficiency [199, 200], premature ovarian failure [201] and spermatogenic failure [202]. Most mutations were dominant, some were associated with incomplete penetrance, and some were recessive [203-206].

Upstream regulators

Mice homozygous for a hypomorphic *Pitx2*^{neo} allele have no *Nr5a1* expression and, consequently, no *Lhb*, *Fshb* or *Gnrhr* expression [48]. This suggests that *Pitx2* is upstream of *Nr5a1* in the transcriptional hierarchy regulating pituitary development. Later, PITX2 was shown to bind a pituitary gonadotrope-specific enhancer within intron 6 of the *Nr5a1* gene [207]. Several groups used transgenic mice to localize elements necessary for *Nr5a1* expression in various tissues [172, 208, 209]. The action of *Nr5a1* in promoting gonadotrope fate is antagonized by TBX19 [58].

POMC transcription in corticotropes (TBX19, NEUROD1)

Factor discovery

Pro-opiomelanocortin (POMC) is a pro-hormone that is cleaved in anterior pituitary corticotropes to become adrenocorticotropic hormone (ACTH) and in melanotropes of the intermediate lobe into melanocyte stimulating hormone (MSH) and beta endorphin. Drouin used the AtT-20 mouse corticotrope tumor cell line to identify cis-acting elements that regulate *Pomc* expression. One element contained an E-box motif, which is typically bound by helix-loop-helix (HLH) transcription factors [210]. The beta HLH factor NeuroD1 is expressed in corticotrope cells and binds this element, acting together with PITX1 to activate *Pomc* expression [211]. The detection of *Neurod1* expression in the developing pituitary gland from e12-e16 is consistent with a role in initiating *Pomc* expression. *Neurod1* is transiently expressed in corticotropes, suggesting that there are other factors involved in sustained *Pomc* transcription [212].

PITX1 was identified in an effort to identify a trans-acting factor that bound another cis-acting sequence within the promoter proximal region of *Pomc* [69]. This element was sufficient to confer reporter gene expression in AtT-20 cells but not heterologous cells. Drouin and colleagues used this sequence to screen a cDNA expression library for DNA binding proteins, which led to the discovery of a novel homeodomain transcription factor PTX, now known as *Pitx1*. *Pitx1* is expressed in the pituitary primordium, and is detected in all pituitary cell types, but it is enriched in adult gonadotropes and thyrotropes [67, 74]. Mice homozgyous for *Pitx1* knockout die at birth and have severe defects in mandible and hindlimb development, but there is little effect on pituitary development due to functional overlap with the related *Pitx2* gene [47, 67, 74].

A cis-acting sequence adjacent to the PITX1 binding site is required for *Pomc* expression, and the sequence motif, TCACACCA, is a T box transcription factor binding site [213]. PCR-amplification of *Tbox* cDNAs in AtT-20 cells identified a novel factor, TPIT (officially known as TBX19), which is expressed early in pituitary development and is enriched in corticotropes and melanotropes. Ectopic expression of *Tpit* under the control of the *Cga*

promoter in mice is sufficient to drive *Pomc* expression, but not *Neurod1* expression. Patients with isolated ACTH deficiency were screened and two unrelated individuals were identified with mutations in *TPIT*, confirming the critical role of this gene in POMC expression. Homozygous deletion of *Tpit* results in almost complete loss of POMC in both the anterior and intermediate lobes, and the intermediate lobe is hypoplastic [58]. *Neurod1* expression is not obviously affected, suggesting that the commitment to corticotrope and melanotrope fate has been initiated. In the absence of TPIT, the progenitors in the intermediate lobe express *Nr5a1* and the alpha and beta subunits of TSH, FSH, and LH, suggesting that TPIT has a repressive effect on gonadotrope and thyrotrope cell fates. TPIT interacts directly with NR5A1 to inhibit its transcriptional activity. It is noteworthy that *Pou1f1, Gh* and *Prl* are not ectopically expressed in the intermediate lobes of *Tpit* mutants. Overexpressing *Tpit* under the control of the *Cga* promoter had little effect on *Tshb* expression, but it is sufficient to suppress expression of *Nr5a1, Lhb* and *Fshb,* consistent with the idea that TPIT drives corticotrope and melanotrope fate while suppressing gonadotrope fate.

Patient mutations

TPIT mutations are the most common, known cause of congenital, isolated ACTH deficiency [214-217]. Patients with homozygous loss of function mutations typically present with undetectable plasma ACTH and corticosterone, and hypoplastic adrenal glands. Affected babies may have cholestatic jaundice and potentially fatal hypoglycemia. *Tpit* null mice have more yellow pigment than wild type mice, due to the lack of MSH, but no obvious pigment defects are present in human patients.

Summary

Pomc transcription and the corticotrope and melanotrope cell fates are promoted by several transcription factors including TPIT, NeuroD1, PITX1, and PITX2. TPIT is a T box transcription factor that binds promoter proximal region of POMC and induces its expression in concert with PITX factors. It is selectively expressed in corticotropes and melanotropes,

activating the corticotrope and melanotrope lineage while repressing the gonadotrope lineage by antagonizing NR5A1 function in a DNA binding-independent manner. Loss of TPIT results in neonatal-onset isolated ACTH deficiency, but not juvenile-onset.

PAX7

Gene discovery

Pax7$^{-/-}$ mice were generated more than twenty years ago and revealed the importance of *Pax7* for muscle and brain development [218-224]. The homozygous mutants die 3 weeks after birth, but the pituitary gland was not characterized [225]. Karlstrom and colleagues showed that the SHH-responsive gene *Pax7* is expressed in the melanotropes of the developing zebrafish pituitary gland [226]. Spatial and temporal gene expression profiling revealed that *Pax7* is expressed in progenitors that give rise to intermediate lobe melanotropes in mice, and it was hypothesized to be a critical factor for intermediate lobe cell fate through direct regulation of Notch signaling [227-229].

Down-stream targets, Pioneering activity

Drouin and colleagues showed that *Pax7*$^{-/-}$ mice lack intermediate lobe melanotropes, and the deficiency of *Pax7* permits ectopic differentiation of progenitors into corticotropes [229]. Moreover, ectopic expression of *Pax7* in the immortalized, corticotrope-like AtT-20 cells is sufficient to convert them to a melanotrope identity associated with both reduced expression of corticotrope-enriched transcripts such as the *NeuroD1*, glucocorticoid receptor, CRH receptor, and vasopressin receptor 1b and activation of melanotrope-enriched transcripts such as the dopamine receptor *Drd2* and prohormone convertase 2, *Pcsk2,* which cleaves *Pomc* to produce MSH. Thus, *Pax7* is a selector of intermediate lobe melanotrope cell identity.

To understand the underlying mechanism of PAX7 action in reprogramming AtT-20 cells to the melanotrope fate, binding sites for TPIT, PAX7 and H3K4me1 were identified by chromatin immunoprecipitation (ChIP-Seq) and open chromatin was identified using FAIRE-Seq (Formaldehyde-Assisted Isolation of Regulatory Elements). Methylation of histone H3 at lysine 4 (H3K4me1) is associated with enhancers. Drouin and colleagues demonstrated that PAX7 can bind heterochromatin and act as pioneer factors to open the chromatin, yielding a FAIRE-Seq signal and permitting the binding of additional transcription factors such as TPIT [230].

To further characterize PAX7 action, the corticotrope and melanotrope transcriptomes and epigenomes were compared. In so doing, these authors confirmed much of what they had shown previously, that PAX7 is necessary and sufficient for establishing a melanotrope transcriptome and epigenome. These authors made the interesting discovery that the majority of PAX7 action on the epigenome occurs at regions far from gene promoters, as the promoters of most genes in corticotropes and melanotropes are similar. They went on to show that the areas of the genome that PAX7 opens and activates represents a minor, but sizable fraction of PAX7 binding sites. Interestingly, they revealed a large fraction of sites containing a PAX7 binding motifs that are impervious to PAX7 binding. These sites were characterized by CTCF binding, and constitutive heterochromatin. While constitutive heterochromatin was resistant to PAX7 remodeling, facultative heterochromatin was readily bound by PAX7. Using inducible nuclear localization of PAX7 in AtT20- PAX7+ cells, these authors showed that PAX7 binds to open DNA very quickly (within 30 minutes), while it takes much longer (nearly 24 hours) for PAX7 to bind areas of closed DNA. Unsurprisingly, it takes even longer for PAX7 to remodel bound, heterochromatin sites, requiring more than 3 days to fully open these areas of DNA. Finally, areas of PAX7 binding and opening were subject to reduction in CpG methylation, a very stable form of epigenetic memory, and most sites opened by PAX7 pioneering activity remain open long after PAX7 has been removed from the nucleus. With this information, the authors put

forth a model which involves PAX7 binding to both euchromatin and facultative heterochromatin, remodeling of the areas of heterochromatin into areas of euchromatin, allowing factors like TBX19 and STAT3 to bind DNA, and drive expression. This clearly defines the function of a pioneering transcription factor, and it leaves us with the question of whether this mechanism of pioneering action represents a broader pattern of pioneer action, or whether it is specific to PAX7.

Patient Mutations

PAX7 translocations resulting in fusion with the forkhead in rhabdomyosarcoma gene, *FKHR*, can cause pediatric alveolar rhabdomyosarcoma [231]. Loss of function mutations would be expected to be lethal in the homozygous state, and none have been reported in humans [225].

Summary

PAX7 is the first validated pioneer transcription factor acting within the pituitary. Important for both muscle and brain development, it was not implicated in pituitary function until 2010. Melano/corticotrope precursor cells can become either cell type in development. The presence of PAX7 railroads the development to a melanotrope fate, whereas the absence of PAX7 results in a corticotrope fate. PAX7 does this by making melanotrope-specific TPIT binding sites available to TPIT by binding to heterochromatin and converting it to euchromatin. The Drouin lab has shown a very thorough mechanism by which PAX7 does this, revealing the amount of time this chromatin-changing process takes, and showing its stability through repeated DNA replication cycles. However, the exact complex required for this change in the epigenetic landscape is unclear. Furthermore, all of the work done to date has focused on the 'opening' of DNA that is specific to melanotropes, while it is yet unclear whether PAX7 'closes' corticotrope-specific DNA.

Current Model for the Transcription Factors of the Pituitary Gland and Open Questions

A complex cascade of transcription factors is responsible for the development and maintenance of the pituitary gland. PITX and LHX proteins are some of the earliest factors in promoting pituitary formation. *Pitx1* and *Pitx2* compensate for one another and are responsible for turning on *Lhx3*. LHX3 and LHX4 also have overlapping functions, and together, they are necessary for the pouch rudiment to expand. During these early stages, the majority of cells are undifferentiated, proliferating progenitor cells, defined by their expression of SOX2. Then, *Lhx3* activates *Prop1* throughout Rathke's pouch from e10.5 to e12.5, and *Prop1* quickly becomes restricted to the progenitors that are undergoing an epithelial to mesenchymal like transition, involving activation of *Zeb2,* and have silenced *Sox2* expression. PROP1 represses *Hesx1* expression and induces *Pou1f1*, the major lineage-determining transcription factor for somatotropes, lactotropes, and thyrotropes. POU1F1 interacts with epigenomic regulators to activate and repress expression of target genes necessary for the sub-specialization into three different hormone-producing cell fates. LSD1*,* ZEB1*,* estrogen receptor, and GATA2 are some of the factors involved in sub-specialization. During the last few days of embryogenesis, GATA2, NR5A1, and EGR1 drive gonadotrope fate, and TPIT and NEUROD1 drive corticotrope fate. PAX7 and TPIT act together to drive melanotrope fate.

This attractive model represents decades of sophisticated, pioneering work, and explains many basic steps in pituitary development. There are, however, questions that remain unanswered. How is the switch from proliferation to differentiation regulated? What additional transcription factors and signaling pathways are involved in cell specification?

SOX2 is firmly established as the marker for cycling progenitor cells in the developing mouse pituitary, and it is also expressed in the quiescent stem cell reserve in adult pituitary.

The steps involved in switching cells from their SOX2-expressing, cycling state to their specific lineage is unclear. A thorough analysis of cell cycle regulators from e11.5 through e16.5 helped clarify this, as it revealed three distinct populations [232]. There is a cycling precursor population (defined as Ki67-positive, and presumably SOX2-positive), a non-cycling precursor population (defined as p57-positive and p27-negative), and a non-cycling differentiated population (p57-negative and p27-positive). Drouin and colleagues showed that deletion of the major transcription factor TPIT resulted in an unusual population of non-cycling, undifferentiated progenitors that were p57+, p27+. This suggests that p57 marks cell cycle exit, and major factors (PROP1, TPIT, NR5A1) silence p57, permitting differentiation, and locking cells into their fate. Unlike the temporal phasing of neuronal differentiation in the brain and retina, nearly all cells in the pituitary leave the cell cycle at approximately the same time between e11.5 and e13.5 [233]. Two major questions remain: what triggers the transition from the proliferating to non-proliferating state, and how are the major transcription factors exclusively turned on in different progenitors? Notch, WNT and YAP/TAZ signaling play important roles in regulating progenitor proliferation [23, 33, 62] The second question concerning how each factor is turned on is almost certainly specific to the factor, as common regulatory networks across cell lineages would fail to explain the highly unique transcription network in the different cell types.

The prevailing model of cell-type differentiation in the pituitary involves an exit from the cell cycle with a major transcription factor that inexorably pushes it down a single path to induce a specific and exclusive fate. There is evidence to suggest, however, that the differentiation is not as linear as once thought, and the fate may be more plastic than the model suggests. Early analyses of the pituitary led Romeis to propose a “one cell one hormone” model [234]. However, a single gonadotrope can express and secrete both LH and FSH [235, 236] and GH and TSH are co-expressed in hypothyroid mice [237]. Cells that express both GH and PRL may be a transient population that represents a precursor of both somatotropes and lactotropes [238, 239]. Or, they may represent a transition from a GH-expressing cell to PRL-expressing through

the action of POU1F1, LSD1 and ZEB1 [165]. Boehm and colleagues discovered that at e17.5, nearly all cells expressing FSH also express TSH, and that many of these cells express NR5A1, suggesting a close relationship between gonadotropes and thyrotropes [240]. These studies highlight how closely related the various cell types are, challenging the idea that major transcription factors direct an inflexible cell fate.

Technical Developments and Future Directions

Four major technological innovations are now available to gain insight into cell fate decisions during development: innovative DNA library preparation methods coupled with high-throughput sequencing, single-cell sequencing, CRISPR, and organoids.

High Throughput Sequencing

Advances in sequencing technology have made genome-wide analyses of gene expression feasible. Sequencing mRNA from genetically marked pituitary cells has been invaluable to the pituitary field. Subpopulations of pituitary cells have been purified from transgenic mice with fluorescently labeled cells and fluorescence-activated cell-sorting (FACS). This approach revealed heterogeneity of gonadotrope gene expression in different sexes at different times [241] and the similarity between corticotropes and melanotropes, with only ~500 differentially expressed genes [230]. This method also revealed novel regulators of cell identity for somatotropes and lactotropes [242]. There are limitations, however, to applying this technology to small numbers of cells collected from developing pituitaries, as they may contain different factors that drive cell fate from those that are employed to maintain it in adult animals.

Identification of genome-wide regions of open chromatin and transcription factor binding sites in specialized cells is valuable for understanding cell fate decisions. DNase hypersensitivity mapping has been largely replaced by **A**ssay for **T**ransposase-**A**ccessible

Chromatin with sequencing (ATAC-seq) for identification of putative regulatory elements [243]. These powerful methods have successfully been used in the pituitary, finding regulatory elements in melanotropes and corticotropes [229], implicating PAX7 as a pioneering transcription factor, and further characterizing the speed at which PAX7 euchromatinizes DNA and the longevity of the subsequent epigenetic marks [230]. Similarly, they have shown the chromatin accessibility at STAT3 and Glucocorticoid receptor binding sites in corticotropes [244]. Software programs are available to identify footprints of transcription factors in ATAC-seq data and DNA binding motifs that underlie transcription factor binding [245]. Genome-wide binding sites for PROP1 [130] were identified using **Ch**romatin **I**mmuno**p**recipitation with sequencing (ChIP-seq) [246]. POU1F1 binding at active enhancers with Matrin3 have been reported also [159].

ChIP-seq for epigenomic marks on histones can identify putative poised enhancers (histone H3 lysine 4 methylation, H3K4me1 alone) and active enhancers (H3K4me1 coupled with histone H3 lysine 27 acetylation, H3K27ac) [247]. H3K27me3 marking is a little more nuanced, as the presence of this mark across the gene body is correlated with repression, whereas enrichment at the transcription start site or the promoter may be a sign of bivalency or even active transcription [248].

Chromatin Conformation Capture (3C) enables researchers to determine which regulatory elements and promoters are interacting. This is important because enhancer elements may not regulate the closest gene, and they may lie at substantial distance from the gene they regulate. Liebhaber and colleagues initially used traditional techniques of DNase I hypersensitivity mapping and transgenic animal models to discover and characterize the Locus Control Region (LCR) for the human growth hormone gene cluster [249]. There are several different enhancers within the LCR that selectively regulate the expression of *GH1* and the surrounding *GH*-related genes in the pituitary and the placenta, respectively. The 3C method was used to discover the interaction of different enhancers within the LCR with the promoters of

GH1 and the neighboring related genes [250-252]. This method was also used to show that the early and distal enhancers of *Pou1f1* interact with the *Pou1f1* promoter sequentially, and this shift requires POU1F1, establishing an auto-regulatory network, that results in enrichment of H3K27ac at the *Pou1f1* promoter [253]. Further application of this method will link enhancers found using ChIP-seq to the genes they regulate. A remaining challenge for the field is scaling the technology to small numbers of cells available during pituitary development and the tendency for individual enhancers to be redundant [254].

Single Cell Sequencing

RNA-sequencing of single cells (scRNA-seq) is now possible [255]. Various methods can be used to capture single cells including fluidics, manual capture, and FACS [256], and there are different approaches for obtaining the RNA sequences from individual cells, including bar-coding RNA library preparations from single cells followed by next generation sequencing [257, 258]. scRNA-seq analysis algorithms allow researchers to map out a shared differentiation pathway in an asynchronous population of cells [259]. Temporal changes in gene expression that occur as differentiation proceeds can be inferred, revealing candidate genes that may drive these differentiation pathways. The scRNA-seq methods are particularly valuable for analysis of rare cell types or situations in which the relative contribution of individual cell types to the whole is shifting. Currently, very few publications containing single-cell sequencing data from pituitary exist [260, 261]. But the work that has been done already shows that this approach is powerful and can reveal previously unappreciated sub-populations of cells and novel markers of specialized cell types.

CRISPR

Genetically engineered mice have been invaluable for understanding the role of individual genes in pituitary development [262]. Transgenic mice were used to identify the regulatory elements of the *Gh* gene [249] and *Nr5a1* [208, 209] and to tease apart the differentiation of the somatolactotrope [239]. Homologous recombination in embryonic stem

cells was used to characterize the function of *Hesx1* [118] and numerous other pituitary genes, as described earlier. Despite the importance of these technologies, there are significant shortcomings, including expense and inefficiency, and position effects associated with random integration of transgenes. CRISPR– Cas9 (clustered regularly interspersed short palindromic repeats-CRISPR-associated protein 9) technology has reduced the time and expense needed to make genetic modifications in mammalian genomes [263]. Suddenly, knockouts, knockins, conditional alleles, and even more complex tissue specific CRISPR mice were developed. This technology will have a high impact on the field as it is more broadly implemented.

Organoids

Organoids offer the opportunity to study developmental processes ex-vivo, which has helped in understanding the differentiation the gut [264], retina [265], kidneys [266], and pituitary gland [267, 268]. Pituitary *Sox2*-expressing and verapamil-sensitive cells can be cultured as pituispheres and differentiate into each of the anterior pituitary hormone-producing cell types [59, 269]. Subsequently, Sasai and colleagues demonstrated an incredible ability of mouse and human embryonic stem cells to self-organize and differentiate into functional pituitary hormone-producing cells that could rescue hormone deficiency, giving promise for future cell-based therapies for hypopituitarism [267, 268].

Future Directions

These powerful technological advances will help us clarify many questions that remain in understanding pituitary development, namely understanding the switch from proliferation to differentiation and the factors responsible for the differentiation of the cell types. Single-cell sequencing will reveal more nuanced populations of cells that will clarify the exact pathway from a *Sox2*-expressing progenitor cell, through a non-cycling intermediate precursor, to a cell-type that has some combination of major transcription factors and hormones, to finally, a

differentiated cell type that expresses high levels of hormones. Knowing exactly which factor is in which cell will rigorously generate a model for differentiation that will be less prone to revision. Highly enriched motifs and footprints in ATAC-seq data will implicate transcription factors that are critical to this process, shortening the long list of factors that will be generated by single-cell RNA-seq. ATAC-seq will also (in concert with ChIP-seq for histone marks) find the regulatory elements for these major factors, revealing transcriptional networks that are active at different timepoints during pituitary development. Using CRISPR, each factor's necessity and function will be directly assessed *in vivo*. Finally, once a larger suite of factors has been implicated, whose expression profile is clear, and whose function has been characterized, we will be able to generate highly accurate organoids, knowing which ingredients are necessary and sufficient for creating a pituitary gland.

One such area that requires further investigation are the thyrotropes. These represent ~5% of the total number of cells in the pituitary gland [270], making them difficult to study. It is clear from the *Pou1f1*-dwarfed mice that POU1F1 is required for the adult population of thyrotropes (**Fig. 3**), and it interacts with GATA2 to drive thyrotrope fate [164]. There could be additional factors that are necessary to drive thyrotrope differentiation [77]. The regulatory elements of *Tshb* are not known. POU1F1, GATA2, and MED220 all synergize on the *Tshb* promoter to activate its expression [163, 271], but these sequences are insufficient for expression in transgenic mice [262]. Using single-cell sequencing, ATAC-seq and ChIP-seq for POU1F1 and histone marks, the factors responsible for thyrotropes, and the cis-regulatory elements to which they bind will become clear.

Chapter 2: Identification of pituitary thyrotrope signature genes and regulatory elements

Abstract

Pituitary thyrotropes are specialized cells that produce thyroid stimulating hormone (*Tshb*), a critical factor for growth and maintenance of metabolism. The transcription factors POU1F1 and GATA2 have been implicated in thyrotrope fate and regulation of *Tshb* transcription, but no transcriptomic or epigenomic analyses of these cells has been undertaken. The goal of this work was to discover key transcriptional regulatory elements that drive thyrotrope fate. We identified the transcription factors and epigenomic changes in chromatin that are associated with differentiation of POU1F1-expressing progenitors into thyrotropes, a process modeled with a pair of cell lines: one that represents an early, undifferentiated *Pou1f1* lineage progenitor (GHF-T1) and one that is a committed thyrotrope (TαT1). We generated and compared RNA-seq, ATAC-seq, histone modification CUT&RUN (including H3K27Ac, H3K4Me1, and H3K27Me3), and transcription factor (POU1F1) CUT&RUN in these two cell lines to identify regulatory elements and candidate transcriptional regulators. We identified POU1F1 binding sites that were unique to each cell line. POU1F1 binding sites are commonly associated with bZIP transcription factor consensus binding sites in GHF-T1 cells and Helix-Turn-Helix (HTH) or basic Helix-Loop-Helix (bHLH) factors in TαT1 cells, suggesting that some classes of transcription factors may recruit or cooperate with POU1F1 binding to unique sites. We validated enhancer function of novel elements we mapped near *Cga, Pitx1, Gata2,* and

Tshb by transfection in TαT1 cells. Finally, we confirmed that an enhancer element near *Tshb* can drive expression in thyrotropes of transgenic mice, and we demonstrate that GATA2 enhances *Tshb* expression through this element. These results extend the ENCODE multi-omic profiling approach to an organ that is critical for growth and metabolism, which should be valuable for understanding pituitary development and disease pathogenesis.

Introduction

Recent genome-wide association studies (GWAS) have begun to identify loci that are associated with sporadic pituitary adenomas and variation in normal height, but the genes associated with many of these loci are unknown [272-274]. Nearly 90% of GWAS hits are in noncoding regions, making it difficult to transition from genetic mapping to biological mechanism [275]. Recent studies that identify enhancer regions by undertaking large scale functional genomic annotation of non-coding elements like Encyclopedia of DNA Elements (ENCODE) have begun to yield a better understanding of some complex diseases. Dense molecular profiling maps of the transcriptome and epigenome have been generated for more than 250 cell lines and 150 tissues, but pituitary cell lines or tissues were not included. This represents a major limitation, as the cell types that comprise the pituitary gland secrete hormones responsible for growth (growth hormone secreted by somatotropes), reproduction (gonadotropins secreted by gonadotropes), adrenal gland function and the stress response (ACTH secreted by corticotropes), lactation (prolactin secreted by lactotropes), and thyroid gland function (thyroid-stimulating hormone secreted by thyrotropes). Epigenomic and gene expression data are emerging for somatotropes, gonadotropes and corticotropes, but there is very little available data on thyrotropes [230, 241, 242, 276].

Thyrotropes represent ~5% of cells in the pituitary gland, and their function is to express and secrete Thyroid Stimulating Hormone (TSH or thyrotropin), which regulates thyroid gland development and thyroid hormone production. These hormones are essential for normal growth and metabolism. Up to 12% of the US population suffers from abnormal levels of thyrotropin [277]. The incidence of secondary hypothyroidism is estimated to be 1:20,000 to 1:80,000 individuals [278]. Research into the regulation of thyrotrope differentiation and function is relevant to this public health problem.

A cascade of transcription factors is responsible for the differentiation of the major pituitary hormone-producing cell types, and three transcription factors associated with thyrotrope development and function are POU1F1, GATA2, and ISL1. The pituitary transcription factor POU1F1 is essential for the differentiation of growth hormone, prolactin and TSH-producing cells [152]. It binds to the promoters of *Gh, Prl,* and *Tshb* to activate gene expression [143, 145, 163, 279, 280]. Defects in the POU1F1 gene cause severe growth insufficiency and hypothyroidism in humans and mice [5, 152]. POU1F1 and GATA2 act synergistically to activate *Tshb* expression through promoter-proximal elements [163, 164]. Defects in GATA2 and ISL1 reduce thyrotrope differentiation in mice, but they do not appear to ablate it [77, 281, 282]. Despite the important role of *Pou1f1* in thyrotrope development and function, little is known about the gene regulatory network of POU1F1 in progenitors or thyrotropes.

Due to the scarcity of the thyrotrope cell-type, classical genomic techniques are challenging to apply. Hormone-producing cell lines have been invaluable for understanding changes in chromatin and gene expression that occur during development [229, 230]. To discover thyrotrope-specific regulatory elements and potential drivers of differentiation, we generated and compared RNA-seq, ATAC-seq, histone modification CUT&RUN (including H3K27Ac, H3K4Me1, and H3K27Me3), and transcription factor CUT&RUN (for POU1F1) in two mouse cell lines, a POU1F1-expressing pituitary precursor cell line that does not express any hormones, GHF-T1, to a thyrotrope-like cell line, TαT1 [283, 284]. TαT1 cells behave much like endogenous thyrotropes in that they respond to TRH and retinoids, and secrete TSH in response to diurnal cues [285-287]. Finally, we evaluated putative enhancer elements for function using transfection assays in TαT1 cells and genetically engineered mice. Together, these studies extend ENCODE-like multi-omic analyses to generate reference maps of gene regulation for cell types critical for growth and metabolism.

Results

Comparison of transcriptomes

To identify candidate factors that drive the differentiation of thyrotropes, we performed RNA-sequencing on the GHF-T1 and TαT1 cell lines. There were many differences in their transcriptomes, consistent with their distinctive morphology, growth rate, and hormone secretion properties (**Fig. 4 A**). Eighty-two percent of genes were differentially expressed (FDR < 0.01). *Pou1f1* expression levels were nearly twice as high in TαT1 cells (160 FPKM) relative to GHF-T1 cells (85 FPKM). Other SV40 immortalized pituitary cell lines vary ten-fold in *Pou1f1* expression levels, but there was no correlation with differentiation state [288]. As expected, *Cga* and *Tshb* were expressed in TαT1 (3557 and 11 FPKM, respectively) but negligibly expressed in GHF-T1 cells (1.4 and 0 FPKM, respectively). The GHF-T1 cells had elevated expression of the transcription factors *Gli3*, *Pax3*, and *Foxg1* (**Table 1**). TαT1 cells had elevated expression of *Gata2* and *Isl1,* as expected, and *Lhx3*, *Rxrg*, *Neurod4, Ascl1,* and *Rfx1* were also significantly up regulated. While the functions of *Lhx3*, *Rxrg*, *Neurod4*, and *Ascl1* have been explored in the pituitary, RFX factors, though critical for pancreas function, have not been studied in the pituitary gland.

To uncover pathways up- and down-regulated in these cell lines, we performed GO-term (gene ontology) enrichment analysis on the top 5% of the most differentially expressed genes (by log-2 fold-change) in both lines [289, 290]. The GO

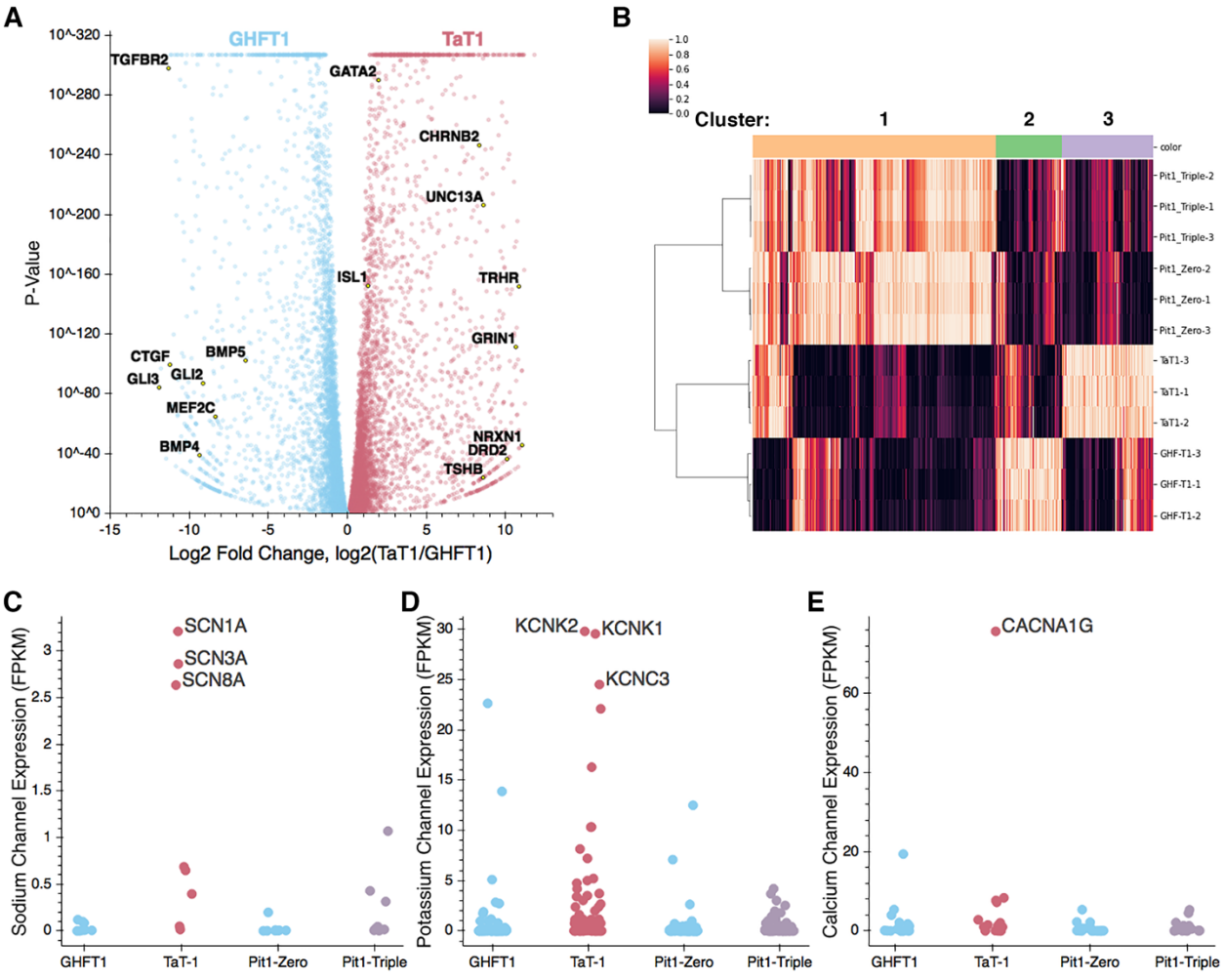

Figure 4: Differentially expressed genes in GHF-T1 and TαT1 cells.

(A) Volcano plot of differential gene expression for GHF-T1 compared to TαT1 cells. Genes upregulated in GHF-T1 cells are colored blue, and those upregulated in TαT1 cells are colored red. Labeled genes represent key thyrotrope factors, and genes associated with GO terms in Table 2. (B) Heatmap showing similarly and differentially expressed genes across GHF-T1, TαT1, Pit1-Zero and Pit1-Triple cells. Genes associated with each cluster can be found in Supplemental Table 1. (C) FPKM values of sodium channel genes. (D) FPKM values of potassium channel genes. (E) FPKM values of calcium channel genes.

Table 1. Differentially expressed transcription factors (FDR <5x10^{-14})

GHFT1 cells			TαT1 cells		
Gene	**Log2 fold change**	**rank**	**Gene**	**Log2 fold change**	**rank**
GLI3	11.90	1	LHX3	11.04	8
PAX3	10.95	12	RXRG	10.74	25
ZFHX4	10.74	21	INSM1	10.67	30
FOXG1	10.59	26	NEUROD4	10.56	37
ZFP57	10.51	29	SOX3	10.23	55
HOXC13	10.29	40	FEV	10.18	57
KDM5D	10.19	48	MYT1L	9.93	72
HMGA2	10.15	53	SCRT2	9.90	77
MSX2	10.11	54	ZFP641	9.39	126
RUNX1	10.07	55	SCRT1	9.15	145
RHOX10	9.94	60	ZIC3	8.96	168
MECOM	9.84	68	EN2	8.95	169
TEAD2	9.65	80	LIN28B	8.82	184
VAX1	9.58	85	PAX5	8.61	205
TCF7L1	9.57	87	ZFP709	8.52	218
HOXA1	9.52	91	PRDM16	8.30	249
TCF24	9.46	95	POU2F2	8.15	268
HOXC9	9.35	104	ZIM1	7.92	301
MAF	9.32	106	NHLH1	7.85	312
POU3F3	9.16	112	FOXL2	7.82	317

The most differentially expressed transcription factors by log 2-fold-change in GHF-T1 and TαT1 cells along with their log 2-fold-change and their relative rank in the list of most differentially expressed genes.

Table 2. Gene ontology term enrichment

GHFT1 cells								TαT1 cells							
Gene	**Structure & development[1]**					**Expression**		**Gene**	**Synapse development & function[2]**					**Expression**	
	A	B	C	D	E	GHFT1	TαT1		F	G	H	I	J	GHFT1	TαT1
CYR61	X	X	X	X	X	117.1	0.5	NRXN1	X	X	X	X	X	0.0	4.2
EDN1	X	X	X	X	X	7.3	0.0	UNC13A	X	X	X	X	X	0.0	19.8
BMP4	X	X	X	X	X	6.8	0.0	DRD2	X	X		X	X	0.0	12.4
TGFBR2	X	X	X	X	X	65.1	0.0	CHRNB2	X	X		X	X	0.0	12.7
FGF10	X	X	X	X	X	1.1	0.0	GRIN1	X	X		X	X	0.0	20.5
GLI3	X	X	X	X	X	13.4	0.0	SYT4	X	X		X	X	0.0	86.3
MEF2C	X	X	X	X	X	7.6	0.0	GRIN3A	X	X		X	X	0.0	11.4
CAV1	X	X	X	X	X	10.1	0.0	SNAP25	X	X		X	X	0.1	107.4
BMP5	X	X	X	X	X	3.8	0.0	SEZ6	X	X	X	X	X	0.0	39.8
CTGF	X	X	X	X	X	40.3	0.0	GABRG2	X	X	X	X	X	0.0	13.0
GLI2	X	X	X	X	X	4.2	0.0	PCLO	X	X	X	X	X	0.0	4.0
GATA6	X	X	X	X	X	1.2	0.0	ATP2B2			X	X		0.0	9.4
TBX20	X	X	X	X	X	2.2	0.0	CHRNA4	X	X			X	0.0	3.4
MSX2	X	X	X	X	X	20.1	0.0	SHISA6	X	X			X	0.0	11.3
YAP1	X	X	X	X	X	40.3	0.2	LRRC4C			X	X		0.0	1.7
SFRP1	X	X	X	X	X	7.1	0.0	THY1				X		0.0	23.3
HLX	X	X	X	X	X	1.5	0.0	GLRA3	X	X	X		X	0.0	28.1
CXCL12	X	X	X	X	X	4.2	0.0	ADGRB1			X	X		0.0	9.5
PAX3	X	X	X	X	X	9.1	0.0	GRIA1	X	X			X	0.0	11.7
FN1	X	X	X	X	X	611.8	1.0	LGI1				X		0.0	1.1

[1] A = Animal Organ Development, B = Anatomical Structure Development, C = Anatomical Structure Morphogenesis, D= Multicellular Organism Development, E= System Development

[2] F = Synaptic Signaling, G = Trans-Synaptic Signaling, H = Synapse Organization, I = Nervous System Development, J = Anterograde Transynaptic Signaling

The top five GO terms enriched in each cell type by FDR resulting from an input of the top 5% of most differentially expressed genes by log 2-fold-change. Also, the twenty genes for each condition that are present in the greatest number of the top twenty GO terms and their respective expression in TαT1 and GHF-T1 cells. X's reveal the association of each gene with a given go term. A volcano plot of the result of GO term enrichment and KEGG pathway analysis can be seen in **Supplemental Figure 1**.

terms enriched in GHFT1 cells were broadly related to development and morphogenesis (**Table 2**). Genes contributing to these GO terms include genes from the GLI family that are targets of hedgehog signaling (*Gli2*, *Gli3*, *Glipr1*, *Glipr2*, *Glis2*, *Glis3*), BMPs (*Bmp1*, *Bmp4*, *Bmp5*, *Bmpr1a*, *Bmpr2*, *Bmper*, *Bmp2k*), and FGFs (*Fgf5*, *Fgf7*, *Fgf8*, *Fgf10*, and *Fgf21*). Increased expression of these factors in GHFT1 cells is consistent with the underlying the importance of FGF, BMP, and Hedgehog signaling in early pituitary development [24, 27, 29]. In contrast, the up-regulated genes in TαT1 cells were enriched for GO terms related to nervous system development and synaptic formation. Some genes enriched in TαT1 cells that contribute to these neuronal GO terms are Neurexin, genes of the glutamate receptor family (*Grin1*, *Grina*, *Grin2d*, *Grin3a*), and the synaptic regulator *Unc13a*. KEGG-pathway enrichment analysis revealed an increase in neuroactive ligand-receptor interaction in TαT1 cells, consistent with the enrichment in GO terms found.

The function of several members of the bHLH family of transcription factors, including *Ascl1, Neurod4,* and *Neurod1* has been investigated in pituitary development [291]. Seventy-one of the ninety-three bHLH factors are differentially expressed between GHF-T1 and TαT1 cells (FDR < 0.05); NEUROD4 and ASCL1 are upregulated in TαT1 cells (**Supplemental Table 2**). *Ascl1* is essential for development of all hormone-producing cell types in fish pituitary, and in mice, *Ascl1* loss of function causes reduced production of *Pomc*, *Lhb*, and *Fshb* [291, 292]. However, these reports conflict on whether thyrotropes are affected by *Ascl1* deficiency. We performed TSH immunostaining on pituitaries from *Ascl1*-null mice and did not detect a reduction in thyrotropes at e18.5 (**Supplemental Figure 2**), suggesting *Ascl1* does not affect thyrotrope cell specification. Repressive bHLH genes of the ID family had the highest expression in both of the cell lines, but the role of these genes has not been investigated.

We compared gene expression profiles that we obtained from GHF-T1 and TαT1 cells with those of other SV40-transformed pituitary cell lines, Pit1-zero and Pit1-triple cells [288].

Pit1-zero and Pit1-triple cells were transformed using the same *Pou1f1* regulatory elements as the GHF-T1 cell line. Pit1-zero cells express *Pou1f1*, but none of POU1F1's downstream hormone genes, whereas Pit1-triple cells express *Pou1f1* and all three POU1F1-dependent hormones, GH, PRL, and TSH. In the TαT1 cell line, we found a statistically significant increase in the expression of sodium channel (p-value = 0.002) and potassium channel genes (p-value = 2.9e-05), but not in calcium channel genes (p-value = 0.26). The most highly expressed sodium channels in TαT1 cells are SCN1A, SCN8A, and SCN3A. Notably, three sodium channel genes (*Scn1a*, *Scn8a*, and *Scn9a*) are also expressed in the Pit1-Triple cell line, the only other hormone-expressing cell lineage we studied. The most highly expressed potassium channel genes in TαT1 cells are *Kcnc3*, *Kcnq2*, *Kcnk1*, and *Kcnk2*. G protein-gated ion channels are involved in regulated hormone secretion. This marked increase in ion channel genes in the TαT1 cells is consistent with their GO terms associated with synapses and neuron formation and function. The only calcium channel gene with differential expression was *Cacna1g,* which is highly expressed in TαT1 cells.

Chromatin landscape around thyrotrope-signature genes

To assess genome-wide changes in the chromatin landscape associated with thyrotrope differentiation, we performed Cleavage Under Target and Release using Nuclease (CUT&RUN) for three major histone marks: H3K27Ac, H3K4Me1, and H3K27Me3 [293]. The presence of both H3K27Ac and H3K4Me1 mark active enhancers, while H3K27Me3 marks repressed regions [247, 294-296]. We also performed an Assay for Transposase-Accessible Chromatin with High-Throughput Sequencing (ATAC-seq), a method for profiling regions of accessible chromatin,

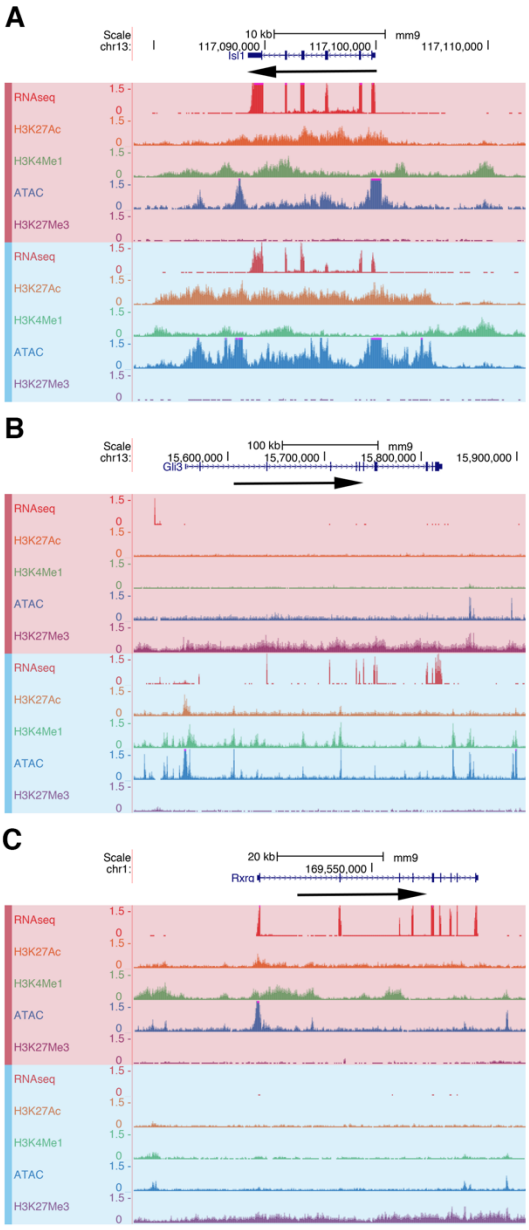

Figure 5: Expression and chromatin mark tracks at key pituitary genes.

(**A**) RNA-seq, H3K27Ac, H3K4Me1, ATAC-seq, and H3K27Me3 tracks (TαT1 in red, GHF-T1 in blue) at *Isl1*, a key pituitary transcription factor expressed in both cell lines containing active chromatin mark across the locus in both cell lines. (**B**) Tracks at *Gli3*, a gene expressed and in active chromatin in GHF-T1 cells, while not expressed and repressed in TαT1 cells. (**C**) Tracks at *Rxrg*, a gene expressed and in active chromatin in TαT1 cells, while not expressed and repressed in GHF-T1 cells.

which are often regulatory [243]. The results are shown in **Figure 5.** These data (called tracks) reveal that *Isl1* is expressed in both cell lines, and has extensive H3K27Ac, H3K4Me1, and ATAC-seq signal across the locus, revealing active enhancers and areas of open chromatin. Concretely, the stretch of H3K4Me1 and H3K27Ac signal covering *Isl1*'s last intron and penultimate exon could be indicative of an *Isl1* enhancer (**Fig. 5A**).

We visualized the expression and chromatin architecture around genes that are differentially expressed in the precursor and differentiated cell lines. Here we show the tracks for *Gli3* and *Rxrg* which are the most and second-most differentially expressed transcription factors in the GHF-T1 and TαT1 cells, respectively. *Gli3* is strongly expressed in GHF-T1 cells, and has many H3K27Ac, H3K4Me1, and ATAC-seq peaks, revealing active enhancers in areas of open chromatin (**Fig. 5B**). By contrast, *Gli3* is not expressed in TαT1 cells. The chromatin surrounding *Gli3* in the TαT1 cells is devoid of H3K27Ac, H3K4Me1, and ATAC-seq peaks and is covered with H3K27Me3, a mark of active repression. This shows that *Gli3* is not expressed and is actively repressed in the TαT1 cell line. Conversely, *Rxrg*, a gene whose deletion in mice is associated with thyroid hormone resistance, is highly expressed in TαT1 cells but not in GHF-T1 cells [297]. Consistent with this, in TαT1 cells the *Rxrg* locus is decorated with H3K27Ac, H3K4Me1, and ATAC-seq peaks, whereas the GHF-T1 line has no such peaks, and shows active repression of *Rxrg*, with a broad H3K27Me3 signal (**Fig. 5C**).

We used ChromHMM to annotate different chromatin states based on H3K27Ac, H3K4Me1, H3K27Me3, and ATAC-seq signal [298]. Iterating over increasing numbers of possible states, we found that 11 states best captured the chromatin architecture within these two cell lines (**Supplemental Fig 6**). Of these states, two had both H3K4Me1 and H3K27Ac, indicating active enhancers. The difference between the two states was the presence or absence of an ATAC-seq signal, meaning one state represented open, active enhancers, while the other represented active enhancers in a more closed state.

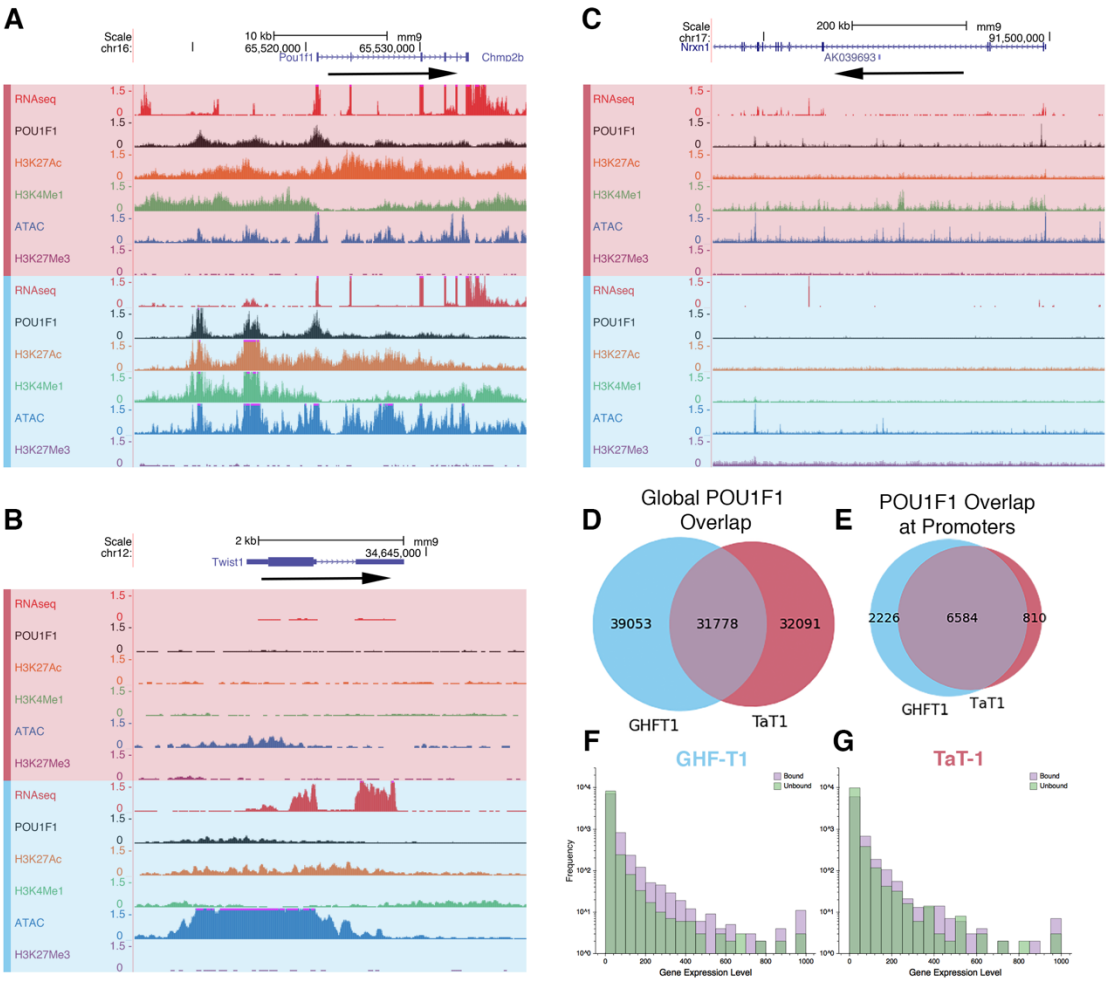

Figure 6: Comparing POU1F1 binding in GHF-T1 and TαT1 cells.

(**A**) RNA-seq, POU1F1, H3K27Ac, H3K4Me1, ATAC-seq, and H3K27Me3 tracks (TαT1 in red, GHF-T1 in blue) at *Pou1f1*, a gene expressed in both cell lines containing active chromatin marks and POU1F1 binding across the locus in both cell lines. (**B**) Tracks at *Nrxn1*, a gene whose promoter is bound only in TαT1 cells. (**C**) Tracks at *Twist1*, a gene whose promoter is bound only in GHF-T1 cells. (**D**) A Venn diagram showing shared and distinct POU1F1 binding sites. (**E**) A Venn diagram showing shared and distinct POU1F1 binding sites at promoters. (**F**) A histogram showing expression of genes in GHF-T1 cells that have POU1F1 bound to their promoters in purple and that do not have POU1F1 bound to their promoters in green. (**G**) A histogram showing expression of genes in TαT1 cells that have POU1F1 bound to their promoters in purple and that do not have POU1F1 bound to their promoters in green.

POU1F1 binding

We performed CUT&RUN for POU1F1 in both the GHF-T1 and TαT1 cell lines to identify similarities and differences in POU1F1 binding at these two stages of differentiation. *Pou1f1* has two enhancers, a proximal (5.6 kb), early-stage enhancer bound by PROP1, and a distal (10 kb), late-stage enhancer which POU1F1 binds to and drives its own expression in an auto-regulatory fashion after birth [162, 299]. In both cell lines CUT&RUN shows extensive POU1F1 binding across the *Pou1f1* promoter-proximal region and both the early and late enhancers (**Fig. 6A**). The *Twist1* promoter is an example of preferential POU1F1 binding in GHF-T1 cells relative to TαT1 cells (**Fig. 6B**). TWIST1 is a bHLH protein that plays an important role in head development and is mutated in patients with Saethre-Chotzen syndrome [300]. *Twist1* is more highly expressed in GHF-T1 than TαT1 cells (having a log-2-fold change value of 5). Of note, POU1F1 binding was detected at the neurexin promoter in TαT1 cells, and neurexin expression increased from nearly zero in GHFT1 cells to 5 FPKM in TαT1 cells (**Fig. 6C**). Neurexin is critical for proper synapse formation.

Genome-wide analysis of POU1F1 binding at promoters revealed that only 15-16% of POU1F1 binding sites in GHF-T1 cells (10980 out of 69644) and TαT1 cells (9360 out of 63036) are within 1 kb of a transcription start site (TSS). While only one third of all POU1F1 binding sites are shared between the two lines (**Fig. 6D**), nearly seventy percent of genes whose promoters are bound by POU1F1 in the differentiated line are also bound by POU1F1 in the precursor line (**Fig. 6E**). We found that POU1F1 binding is associated with higher levels of gene expression in both cell lines (**Fig. 6F, 6G**).

POU1F1 binding is associated with higher ATAC-seq signal in GHF-T1 than in TαT1 cells (**Fig. 7A**), but in both cell lines, POU1F1 is associated with less open chromatin than TPIT [276]. Despite this, sites of POU1F1 binding specific to TαT1 cells are far more open in TαT1 cells (**Fig. 7B**), sites of POU1F1 binding specific to GHF-T1 cells are far more open in GHF-T1

cells (**Fig. 7C**), and shared POU1F1 sites have similar chromatin openness signatures in both cell lines (**Fig. 7D**).

Active enhancers (states containing both H3K27Ac and H3KMe1 in ChromHMM) are heavily enriched for POU1F1 binding in both cell lines, but GHF-T1 enhancers appear to have greater POU1F1 binding than do TαT1 enhancers (**Fig. 7E, 7F**). POU1F1 binding that is specific to TαT1 cells is associated with active chromatin states in TαT1, but it is less so in GHF-T1 cells (**Fig. 7G**). Conversely, GHF-T1-specific POU1F1 binding is broadly associated with active chromatin states in GHF-T1 cells but less so in TαT1 cells, whereas sites of POU1F1 binding in both cell types share similarly active chromatin states. To identify transcription factors that may be associated with differential POU1F1 binding between the cell lines, we analyzed the chromatin states associated with shared and unique POU1F1 binding sites and screened these for binding motifs. We classified genomic sites that had POU1F1 binding exclusively in TαT1 cells, and were in active states in the TαT1 cells and in repressed states in GHF-T1 cells (Repressed to Active), POU1F1 binding sites that are shared between GHF-T1 and TαT1 and are in similarly active chromatin in both (Active to Active), and GHF-T1-specific POU1F1 binding sites that are in active chromatin in GHF-T1 sites and are repressed in TαT1 cells (labeled Active to Repressed). This revealed an expected increased POU1F1 motif density at the center of POU1F1 sites in both GHF-T1 and TαT1 cells (**Fig. 7H**). There was a striking amount of bZIP motifs at the center of GHF-T1-associated POU1F1 binding sites (**Fig. 7I**). Interestingly, there was remarkable helix-turn-helix motif density at the center of TαT1 POU1F1 binding sites, and even more so at Repressed to Active sites, suggesting HTH factors mediate POU1F1 activity in thyrotropes (**Fig. 7J**). Similarly, there was increased bHLH motif density at Repressed to Active sites (**Fig. 7K**).

Stretch Enhancers

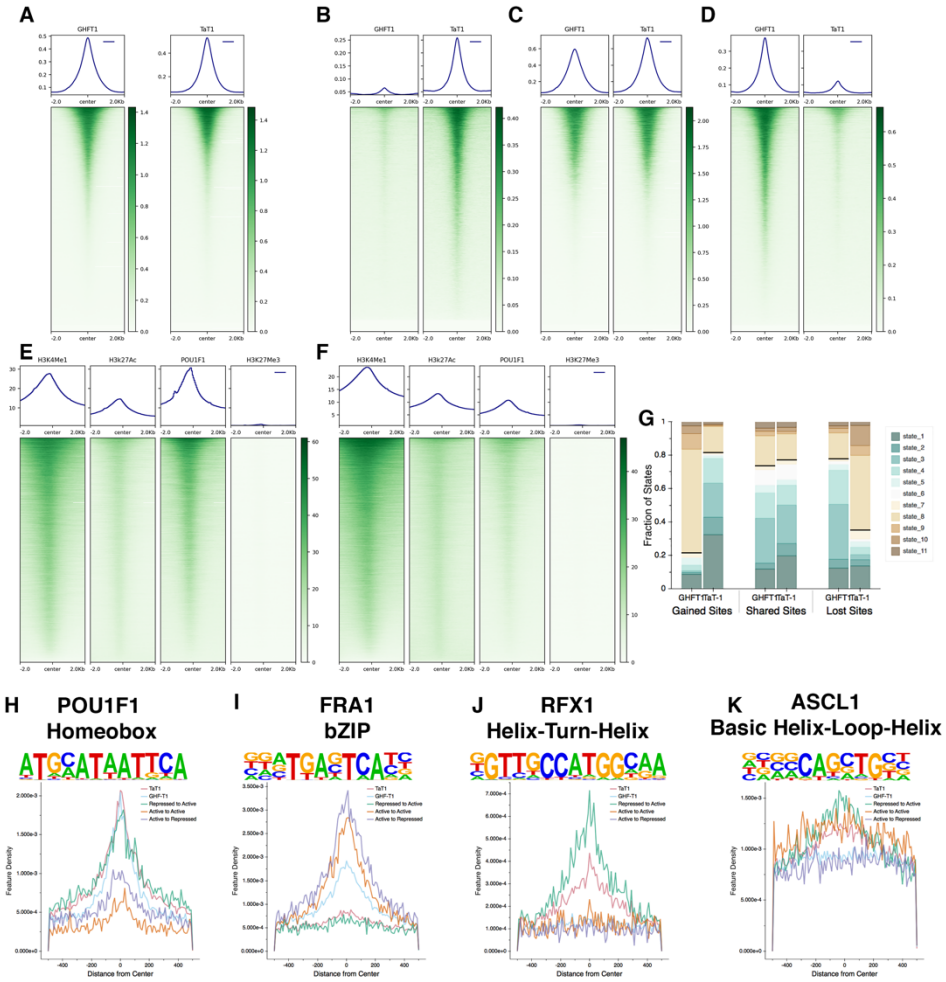

Figure 7: Characterizing POU1F1 binding at different chromatin states.

(**A**) ATAC-seq signal at POU1F1 bindings sites in GHF-T1 and TαT1 cells. (**B**) ATAC-seq signal at POU1F1 binding sites that are specific to TαT1 cells. (**C**) ATAC-seq signal at POU1F1 binding sites that are shared between Tα T1 and GHF-T1 cells. (**D**) ATAC-seq signal at POU1F1 binding sites that are specific to GHF-T1 cells. (**E**) POU1F1 signal at enhancers in GHF-T1 cells. (**F**) POU1F1 signal at enhancers in TαT1 cells. (**G**) Composition of TαT1-specific POU1F1 binding site chromatin states in GHF-T1 and TαT1 cells (gained sites, left, emissions found in **Supplemental Figure 4**), composition of shared POU1F1 binding site chromatin states in GHF-T1 and TαT1 cells (shared sites, center), composition of GHF-T1-specific POU1F1 binding site chromatin states in GHF-T1 and TαT1 cells (lost sites, right). (**H**) Density of POU1F1 motifs across POU1F1 binding sites in GHF-T1 cells (GHF-T1), TαT1 cells (TαT1), at TαT1-specific POU1F1 binding sites that are repressed in GHF-T1 cells and active in TαT1 cells (Repressed to Active), POU1F1 binding sites that are shared in GHF-T1 and TαT1 cells that are active in both (Active to Active), and POU1F1 binding sites that are specific to GHF-T1, and are in an active state in GHF-T1 cells and a repressed state in TαT1 cells. (**I**) Similar analysis as **H**, on the bZIP transcription factor, FRA1. (**J**) Similar analysis as **H**, on the HTH transcription factor, RFX1. (**K**) Similar analysis as **H**, on the bHLH transcription factor, ASCL1. **Supplemental Figure 5** shows more motifs.

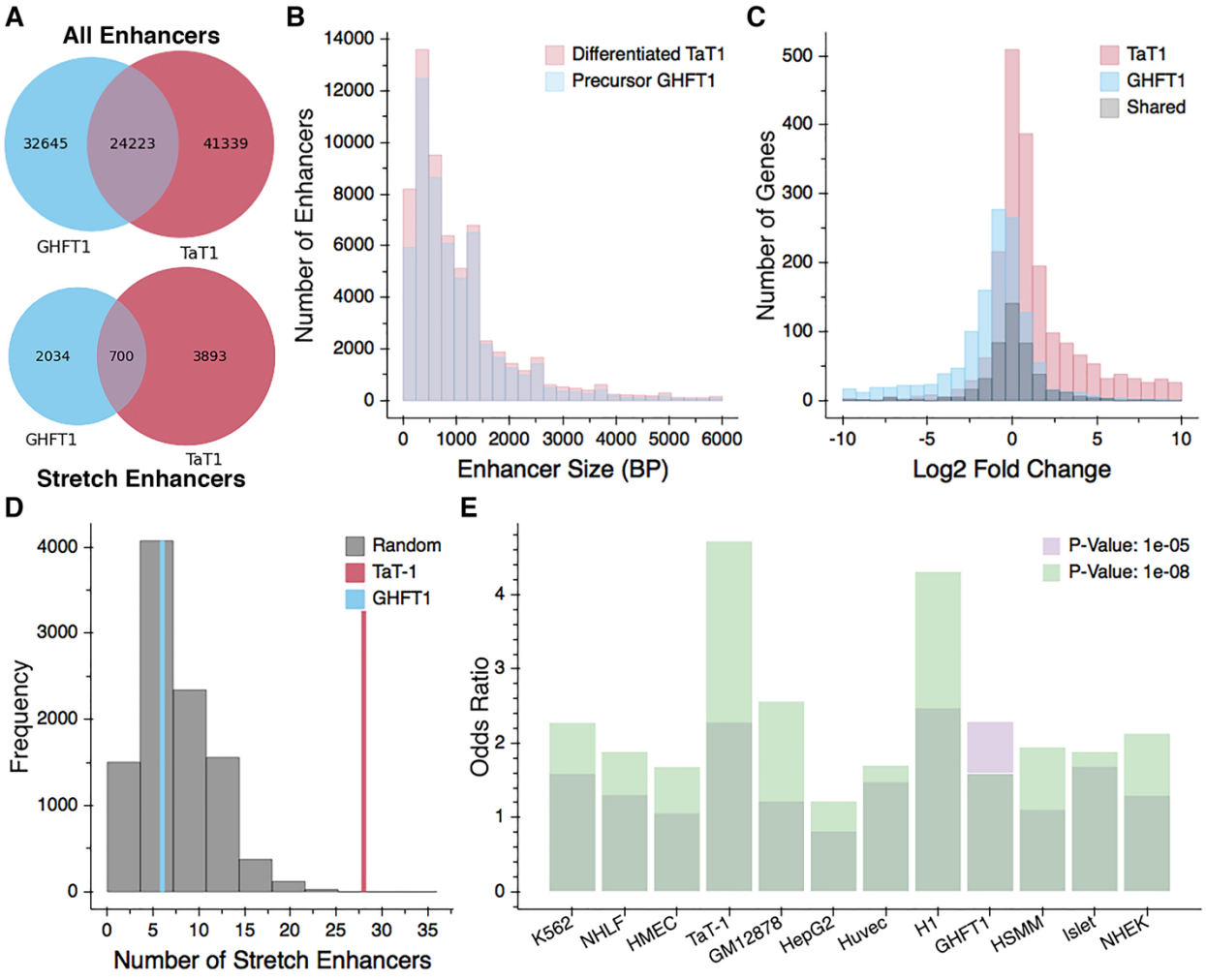

Figure 8: Characterizing stretch enhancers in GHF-T1 and TαT1 cells.

(**A**) A Venn diagram showing shared and distinct enhancers in GHF-T1 and TαT1 cells (top). A Venn diagram showing shared and distinct stretch enhancers in GHF-T1 and TαT1 cells (bottom). (**B**) A histogram showing the distribution of enhancer sizes in GHF-T1 (in blue) and TαT1 cells (in red). (**C**) A histogram showing the log 2-fold-change of the genes that are closest to GHF-T1-specific stretch enhancers (in blue), TαT1-specific stretch enhancers (in red), and shared stretch enhancers (in black). (**D**) Number of TαT1 (red) and GHF-T1 (blue) stretch enhancers within 100kb (50kb upstream or downstream) of TSS of 25 genes known to be important for thyrotrope function. Underneath is a histogram of the number of TαT1 stretch enhancers surrounding (within 100kb) 10,000 iterations of 25 randomly selected genes (normalized for gene expression). (**E**) The odds ratio of observing such an enrichment of SNPs for the neuroticism sub-phenotype of feeling miserable within stretch enhancers of all tissues tested.

Twenty-four percent of the enhancers that we identified were present in both the precursor and differentiated cell lineages, as defined by at least 25% bidirectional overlap (Fig. 8A). There were 15% more enhancers in the differentiated, thyrotrope state than the precursor state. The distribution of enhancer sizes was very similar between the two cell lines (Fig. 8B). Enhancers larger than 3 kb in length, called stretch enhancers, represent 5-10% of all enhancers, are typically cell-type specific and often enriched in disease-associated areas [301, 302]. Stretch enhancers represent 4.9% of the enhancer population in the precursor cell lineage and 7.1% of the enhancer population in the differentiated thyrotrope population. This is within the expected fraction, and the increased abundance in TαT1 cells is consistent with their more differentiated state. While GHF-T1 and TαT1 cells share twenty-four percent of all enhancers, only ten percent of stretch enhancers are shared between the two cell-types (**Fig. 8A**).

We compared the expression of the closest gene to each stretch enhancer and found that expression was highly cell-type specific. Genes closest to precursor stretch enhancers were heavily upregulated in the precursor cell line, whereas the genes closest to thyrotrope stretch enhancers were heavily upregulated in the thyrotrope cell line (**Fig. 8C**). Genes closest to shared stretch enhancers had similar gene expression in both cell lines.

We sought to determine whether genes associated with thyrotrope function in both mouse and man were closer to stretch enhancers. We generated a list of 25 candidate genes associated with thyrotrope differentiation and/or function (**Supplemental Table 3**), and we found that the TSS's of all of these genes were within 100 kb of 28 TαT1 stretch enhancers and only 6 GHF-T1 stretch enhancers (**Fig. 8D**). To determine whether this result was significant, we randomly selected 25 genes 10,000 times, ensuring the genes had similar expression levels, and we counted the number of stretch enhancers within 100 kb of the transcription start site of those randomly selected genes. The randomly selected genes were within 100 kb of 28 TαT1

stretch enhancers only 2 times out of 10,000, yielding an empirical p-value of 0.0002, which confirms the enrichment of TαT1 stretch enhancers at thyrotrope-signature genes.

To probe the potential value of these data for application to human disease studies, we mapped the mouse enhancers in TαT1 and GHF-T1 cells from the mm9 genome onto the human genome, hg19. Because ~90% of GWAS SNPs are intronic or intergenic, and stretch enhancers are heavily enriched for disease SNPs, we expected to implicate thyrotropes in disease phenotypes by uncovering enrichment of disease SNPs in TαT1 stretch enhancers [275, 301]. We used GARFIELD to measure the enrichment of these SNPs in GHF-T1 and TαT1 and stretch enhancers, while accounting for linkage disequilibrium, minor allele frequency, and distance to TSS [303]. We compared their enrichment to stretch enhancers found in heterologous cell lines including but not limited to Islet cells, GM12878 (human B-lymphocyte cells), and K562 (human myelogenous leukemia cells) cells [301]. The study that exhibited the greatest enrichment of SNPs in TαT1 stretch enhancers (odds ratio of 4.7) was from GWAS done on the neuroticism sub-phenotype of feeling miserable (**Fig. 8E**) [304]. While the significance of this is uncertain, untreated hypothyroidism can be associated with fatigue and depression. **Supplemental Figure 8** shows the enrichment odds ratios for all GWAS studies and cell line stretch enhancers, as well as their p-values.

***In vitro* validation of enhancers**

We sought to test putative enhancers of thyrotrope-signature genes, namely *Gata2*, *Cga*, and *Pitx1*, by transient transfection of TαT1 cells. We identified putative regulatory elements as regions with significantly enriched ATAC-seq signals near these genes. The promoter proximal sequences of each gene were amplified from genomic DNA and fused to a luciferase reporter gene. Putative regulator elements were amplified from genomic DNA and

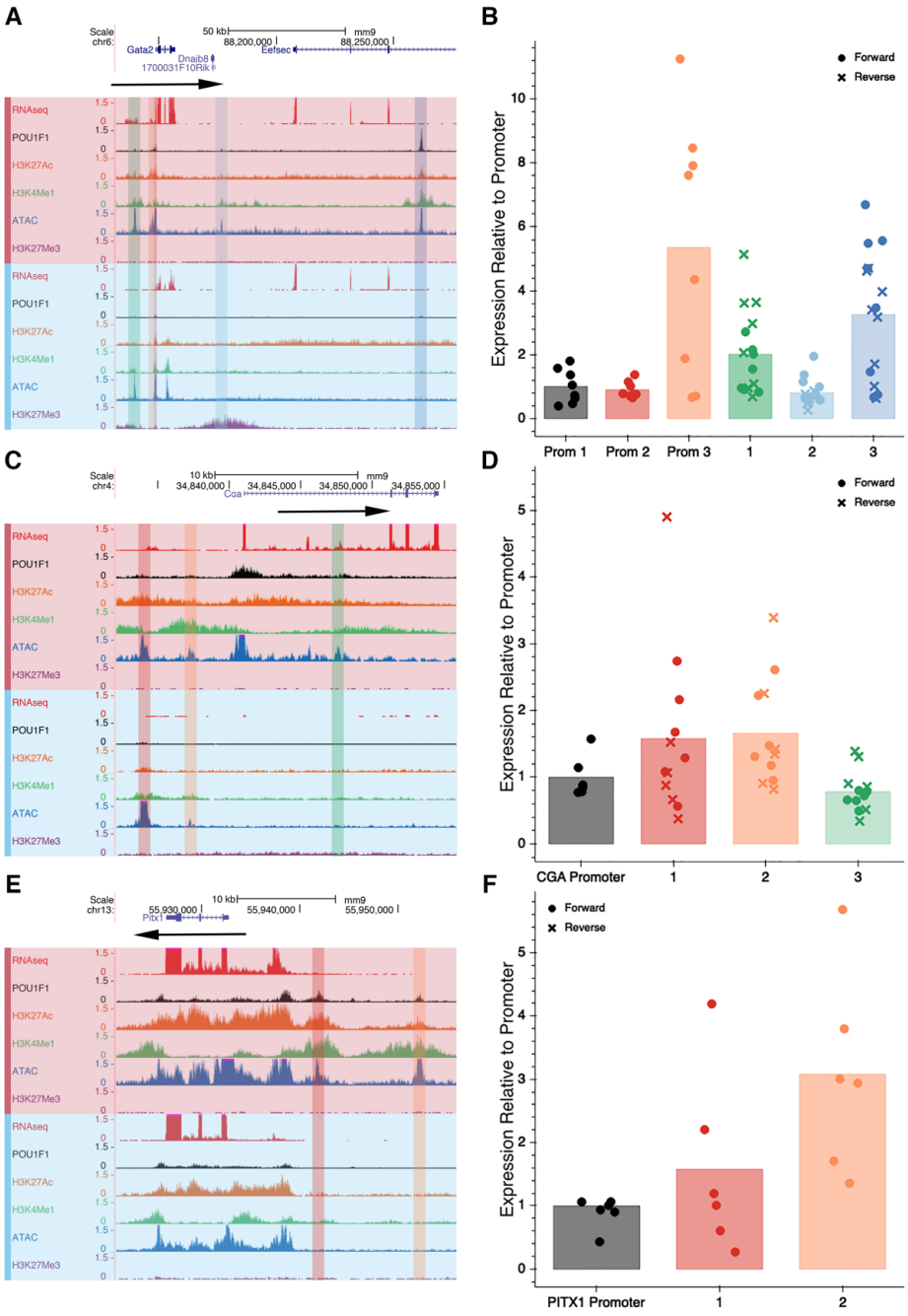

Figure 9: In vitro testing of putative regulatory elements surrounding thyrotrope-signature genes.

(**A**) RNA-seq, POU1F1, H3K27Ac, H3K4Me1, ATAC-seq, and H3K27Me3 tracks (TαT1 in red, GHF-T1 in blue) at *Gata2*, with the pieces of DNA cloned for the luciferase assay highlighted in red, orange, green, light blue and dark blue. (**B**) Level of luciferase activity of each element. Prom 1, 2, and 3 represent the 0.2, 0.9, and 2.8kb promoters tested, and 1, 2, and 3 represent the three similarly highlighted elements in **A** tested in both the forward (circles) and reverse (x's) orientation upstream of the *Gata2* 0.2kb promoter. (**C**) Same tracks as in **A**, at the *Cga* locus, where elements tested are highlighted. (**D**) Level of luciferase activity of each element, color-coordinated with the highlighted elements in **C** in both the forward (circles) and reverse (x's) orientation. (**E**) Same tracks as in **A** at the *Pitx1* locus, where elements tested are highlighted. (**F**) Level of luciferase activity of each element, color-coordinated with the highlighted elements in **F**. Elements were tested only in the forward orientation.

cloned in both the forward and reverse orientation upstream of the promoter proximal region. The transfection efficiency of TαT1 cells is low (~20%), and the results vary, likely due to their poor adherence to the plate. Thus, all experiments were performed with six replicates. We detected one enhancer element for *Gata2*, two elements that function as enhancers for *Cga*, and two elements for *Pitx1* (**Fig. 9**, position of cloned promoters and elements can be seen in **Supplemental Table 4**).

Gata2 is implicated in *Tshb* transcription and proper thyrotrope function [77, 163, 164]. *Gata2* has two promoters, and each are upstream of a non-coding exon [305]. The more distal promoter is located ~5 kb upstream of the more proximal promoter, and it drives expression in Sca-1+/c-kit+ hematopoietic progenitor cells, while the downstream promoter drives *Gata2* expression in most other tissues. The downstream promoter is the only one utilized in TαT1 and GHF-T1 cells, according to our RNA-seq data. *Gata2* expression is five-fold higher in TαT1 cells than in GHF-T1 cells and there is a larger area of accessible chromatin upstream of *Gata2* in the TαT1 cells (~2.8 kb vs 0.9 kb, **Fig. 9A**). There is no difference in activity between the 0.2 kb and 0.9 kb promoter proximal region in TαT1 cells, but the larger, 2.8 kb promoter-proximal region stimulated luciferase activity 5-fold (p-value = 0.009). This indicates the probable presence of enhancer elements between 0.9 and 2.8 kb of the common TSS for *Gata2*. We tested three distal elements, fusing them with the smallest, 0.2 kb *Gata2* promoter construct, and we discovered that the element ~100 kb 3' of the *Gata2* common promoter, that had significant POU1F1 binding, drove the highest levels of luciferase expression, increasing luciferase activity 3-fold (p-value = 0.005). Thus, we identified two enhancer elements for *Gata2* expression in thyrotropes, one in the proximal promoter region, within 2.8 kb of the TSS, and a more distal one, approximately 110 kb downstream.

Cga is the alpha-subunit of thyrotropin, the major hormone secreted by thyrotropes, and follicle stimulating hormone and luteinizing hormone, the major hormones secreted by pituitary

gonadotropes, which are responsible for stimulation of ovulation and spermatogenesis. We tested three *Cga* enhancer elements, and two appeared to have activity, although they did not reach statistical significance. The element ~7 kb upstream of *Cga* increased luciferase activity 1.5-fold, and it has not been previously described. The element located 4.6 kb upstream of the *Cga* gene increased luciferase activity 1.6-fold and approached statistical significance (p-value = 0.07). This element was previously demonstrated to be sufficient for developmental activation, cell type specific expression, and hormonal regulation in transgenic mice (**Fig. 9B**) [280, 306].

Pitx1 was initially identified as a pituitary transcription factor and demonstrated to have a role in POMC expression in cells and hindlimb formation in mice and humans [69, 307]. *Pitx1* has overlapping functions in pituitary development with the related transcription factor *Pitx2* [67]. *Pitx1* and *Pitx2* are expressed in thyrotropes and gonadotropes, and *Pitx1* expression is elevated in pituitaries of mice with *Pitx2* ablated in thyrotropes, suggesting the possibility of functional compensation [308]. The *Pitx1* regulatory landscape extends over 400 kb and includes a pituitary enhancer 110 kb upstream [309]. ATAC-seq signatures revealed two previously undescribed thyrotrope-specific regions of open chromatin 9 and 19 kb upstream of the *Pitx1* TSS (**Fig. 9C**). The proximal element did not have statistically significant enhancer activity. The distal element, however, increased luciferase activity 3-fold (p-value = 0.009).

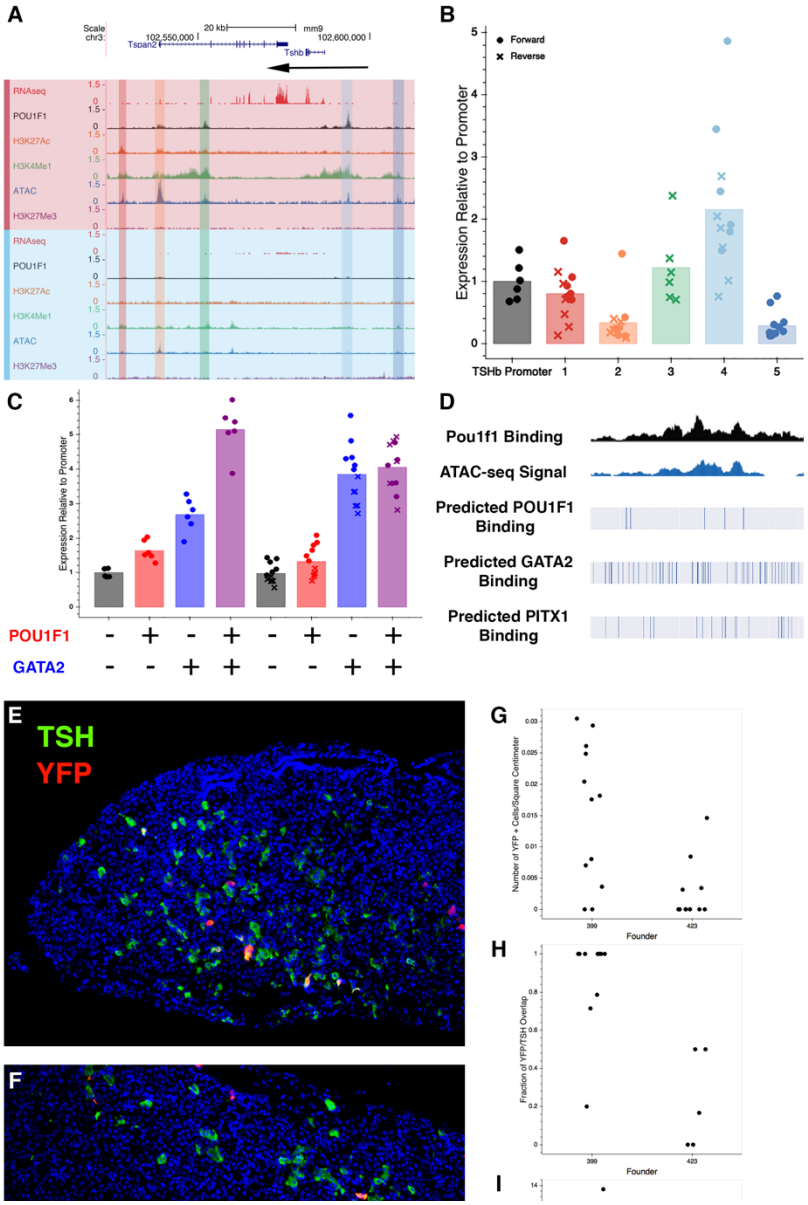

Figure 10: Characterization of Tshb regulatory element.

(**A**) RNA-seq, POU1F1, H3K27Ac, H3K4Me1, ATAC-seq, and H3K27Me3 tracks (TαT1 in red, GHF-T1 in blue) at *Tshb* where elements tested are highlighted. (**B**) Level of luciferase activity of each element, color-coordinated with the highlighted elements in **A** in both the forward (circles) and reverse (x's) orientation. (**C**) Element 4 from **B** tested in heterologous CV1 cells in the absence or presence of POU1F1 and GATA2 expression vectors either singly or together. (**D**) POU1F1 and ATAC-seq tracks across the 1.4 kb region of Element 4. Below represent rug plots of predicted POU1F1, GATA2, and PITX1 binding sites within Element 4 that reach a confidence of at least 0.8 in JASPAR. Extended list of motifs found in Element 4 are presented in **Supplemental Table 5.** (**E**) Pituitary gene expression analysis in transgenic founder 399 with co-immunostaining for YFP (red) and TSHB (green), revealing overlap in expression (yellow). (**F**) Same as **E**, in founder mouse 423. (**G**) The number of YFP-positive cells per unit area in each founder. (**H**) The percentage of thyrotropes that express YFP in each founder. (**I**) The fraction of YFP-positive cells that are thyrotropes in each founder.

Discovery of a novel TSH β-subunit enhancer

A bacterial artificial chromosome clone containing *Tshb* and 150 kb of surrounding DNA sequence was sufficient to drive expression in thyrotropes of transgenic mice [308], but there is no information about the location of key regulatory elements within this region. In fact, multiple efforts to drive expression in transgenic mice with smaller constructs were unsuccessful [262]. We sought to leverage the information we have about the chromatin states in the TαT1 cells to identify elements sufficient for *Tshb* expression in mice. Knowing that the 150 kb BAC was sufficient to drive expression in thyrotropes, we limited our search to this space, and found five areas with high ATAC-seq signal in TαT1 cells (**Fig. 10A**). We tested each of these elements both in the forward and reverse orientation fused to a 0.4 kb *Tshb* promoter proximal region driving luciferase expression (**Fig. 10B,** position of cloned promoter and elements can be seen in **Supplemental Table 4**). We discovered that an element 7 kb upstream of the *Tshb* TSS drove significant levels of luciferase (hereafter named Element 4). Element 4 had extensive ATAC-seq signal and H3K4Me1 and POU1F1 binding, consistent with the observation that POU1F1 is important for *Tshb* expression. Because GATA2 and POU1F1 synergize on the *Tshb* promoter to drive increased *Tshb* expression we tested whether they acted synergistically on Element 4 in heterologous CV1 cells [163]. We observed that GATA2 and POU1F1 independently increase expression of the *Tshb*-luc reporter gene (2.7-fold and 1.6-fold respectively), and together they drive higher expression (5-fold) (**Fig. 10C**). On Element 4, POU1F1 drives modestly increased reporter gene expression (1.3-fold increase), but GATA2 drives far higher levels (4.3-fold increase). GATA2 and POU1F1 do not have an additive effect on element 4 reporter activity (4.4-fold increase) in contrast to the promoter proximal region. This suggests that GATA2 is a powerful regulator of *Tshb* expression through interaction with Element 4. To determine which other factors may be binding Element 4, we checked for the presence of over 1,000 Jaspar motifs within Element 4 at an 80% threshold. We found

extensive predicted GATA2 and PITX1 binding (**Fig. 10D**). A more complete list of predicted binding factors is presented in **Supplemental Table 5**.

We tested whether Element 4 was sufficient to drive expression in transgenic mice by placing the Element 4 in front of the *Tshb* promoter and a YFP reporter gene. This construct was injected into fertilized eggs that were subsequently transferred to pseudopregnant surrogate females. We dissected the pituitaries of eleven founder transgenic mice at four weeks of age and examined the expression of YFP using immunohistochemistry (**Fig. 10E, 10F**). Six founders had no detectable YFP activity in the pituitary gland, three founders had low levels of YFP activity, and two founder mice had higher levels of YFP activity. We analyzed the latter two in more detail. 87% of YFP-positive cells were also positive for TSH in one founder, indicating high specificity for thyrotropes (**Fig. 10H**). 6% of the transgenic thyrotropes were also positive for YFP, suggesting low penetrance of expression (**Fig. 10I**). This represents the first regulatory element that is sufficient to drive reporter expression in thyrotropes, as several other constructs were insufficient for *in vivo* expression [262]. This serves as a proof of the principle that combined transcriptome and epigenome data can be valuable for identifying enhancer elements that function in developmentally specific cell lines and intact animals.

Discussion

Our work builds on the ENCODE effort to discover regulatory elements in diverse tissues. This represents the first systematic characterization of the epigenome and transcriptome of a thyrotrope-like cell line, providing insight into the changes that are associated with the differentiation of committed POU1F1 pituitary cells into thyrotropes. We have also performed CUT&RUN for the key transcription factor POU1F1, revealing its similar binding profile at promoters in the two cell lines, differential binding elsewhere, and clear association

with massive shifts in chromatin states between the two cell lines. CUT&RUN for histone marks (H3K27Ac and H3K4Me1) revealed active enhancers globally in the two cell lines. We demonstrated that many of the enhancers surrounding thyrotrope-signature genes drive expression in a thyrotrope cell line. Furthermore, an enhancer element upstream of *Tshb* proved to be sufficient to drive expression in thyrotropes in transgenic mice. The transcriptomic, epigenomic, and POU1F1 binding data here contributes significantly to our understanding of thyrotropes, which are key cells for regulation of thyroid gland development and regulation of thyroid hormone production.

As hormone-producing cells mature, they ramp up translational machinery for robust hormone production, and CREB3L2 is a master regulator of this process in the pituitary corticotropes [310]. While *Creb3l2* is not highly expressed in TαT1 cells, *Creb3l1* is expressed nearly 30-fold higher in TαT1 cells than in GHF-T1 cells (172.5 FPKM vs. 5.9 FPKM). It is possible thyrotropes use a similar mechanism of increasing translation to meet the demand for thyrotropin. Consistent with this, *Creb3l1* is upregulated in a model of thyrotrope adenoma [311].

Pituitary endocrine cells are electrically excitable, and voltage-gated calcium influx is the major trigger for hormone secretion [312]. G-protein coupled receptors, ion channels, and hormones all are considered components of cellular identity. For example, thyrotropes have unique electrical activity relative to other pituitary hormone-producing cell types. TαT1 cells exhibit a bursting pattern of action potentials that are affected by exposure to TRH and thyroid hormone, but the nature of the ion channels regulating TSH secretion is not understood [313, 314]. The involvement of ion channels in excitation-secretion coupling is an area of active study. The hypothalamic factors CRH, TRH, GHRH and somatostatin have an effect on electrical activity in corticotropes, lactotropes and somatotropes. Thyrotropes have not been well studied in this regard. Our study provides evidence for the acquisition of ion channel gene expression

as progenitors adopt the thyrotrope fate. Voltage gated potassium channels *Kcnc3*, *Kcnq2*, *Kcnk1*, and *Kcnk2* were highly expressed in TαT1 cells. Interestingly, *KCNQ1* missense mutations cause growth hormone deficiency [315]. We found that sodium channel genes are upregulated in two cell types that express hormones, Pit1-triple and TαT1. Calcium channel gene expression was not different amongst the four cell types: Pit1-zero, GHFT1, Pit1-triple and TαT1. The most highly expressed calcium channel was CACNA1G, a low-voltage activated, T-type channel. This suggests that the previously proposed model, in which ion channel expression is pruned as differentiation proceeds, needs to be updated [312]. Knowing which ion channels are expressed in thyrotrope cells is the first step in understanding the mechanism whereby TRH stimulates TSH release in a pulsatile manner and according to the appropriate diurnal rhythm.

Two pituitary cell types express POMC, corticotropes and melanotropes, and they process the protein differently to make adrenocorticotropin and melanocyte-stimulating hormone, respectively. Although there are very few differences in the transcriptomes of these cells, a single pioneering transcription factor, PAX7, remodels the chromatin landscape and provides access to new binding sites for TBX19 (Tpit), which drives melanotrope fate [229, 230, 276]. We observed far more differences in gene expression between an undifferentiated GHF-T1 cells and differentiated TαT1 cells, however, suggesting that a single factor may not responsible for all of differences.

Several transcription factors were strongly upregulated in TαT1 cells relative to GHFT1, including ISL1, RXRG and LHX3. Upregulation of *Isl1* and *Rxrg* was expected because pituitary-specific deletion of *Isl1* causes reduced thyrotrope differentiation [281], and several lines of evidence support a role for *Rxrg*. RXRG suppresses serum TSH levels and *Tshb* transcription, *Rxrg* deficient mice have central resistance to thyroid hormone, and loss of retinoic acid signaling suppresses thyrotrope differentiation [297, 316]. *Isl1* had extensive

POU1F1 binding across the 1 MB region surrounding it. *Lhx3* expression is detectable at e9.5 in the mouse pituitary placode and expression persists though adulthood [50]. Thus, we expected to detect *Lhx3* transcripts in all pituitary cell lines. *Lhx3* transcripts were nearly undetectable in Pit1-zero cells and in the precursor GHF-T1 lineage, transcripts were higher in Pit1-triple (1.6 FPKM), and highest in TαT1 cells (44.2 FPKM). Recently, an SV40-transformed pituitary precursor cell line was developed that expresses the stem cell marker SOX2 but not LHX3 [317]. There may be dynamic changes in *Lhx3* expression during development that have not been documented.

SHH signaling is critical for establishing the pituitary placode and induction of *Lhx3* expression [24]. The GHFT1 precursor lineage expressed GLI2 and GLI3, the downstream targets of SHH, at higher levels than TαT1 cells. This is suggestive of active SHH signaling. *Gli2* and *Gli3* promoters are associated with extensive H3K4Me1 and H3K27Ac, and active enhancers can be found upstream, downstream, and within their introns. By contrast, *Gli2* and *Gli3* have broad stretches of H3K27Me3 in the TαT1 line, a mark of active repression. The active expression of these elements in GHF-T1 cells underline how well these cell types represent the early pituitary state, and suggest they could be for valuable for identifying GLI target genes that underlie pituitary developmental abnormalities [5].

POU1F1 is critical for development of thyrotropes, somatotropes and lactotropes, and it likely interacts with other factors that specify the three different cell fates. The work done here may give insight into which other factors may be involved. While POU1F1 binding is associated with the homeobox motif, sites of TαT-1-specific POU1F1 binding that are repressed in GHF-T1 cells and active in TαT1 cells are heavily enriched for bHLH and HTH motifs. This raises the possibility that bHLH and HTH factors pioneer the binding of POU1F1 which then activates thyrotrope-specific expression.

Members of the RFX family of transcription factors are attractive candidates for interaction with POU1F1 to drive thyrotrope fate. These HTH factors contain DNA binding and heterodimerization domains and regulate cell fate in many organ systems, including the pancreatic islets and the sensory cells of the inner ear [318, 319]. They interact with other POU and SIX factors to direct fate. *Rfx1, Rfx2, Rfx3, Rfx5,* and *Rfx7* are expressed in both GHF-T1 and TαT1 cells. *Rfx3, Rfx4, Rfx5* and *Rfx7* are expressed in pituitary development between e12.5 and e14.5, a time when progenitors leave the cell cycle and initiate differentiation [320]. Future studies will be necessary to define the role of these genes in pituitary development.

POU1F1 binding sites unique to TαT1 cells are enriched for bHLH binding sites, suggesting that bHLH factor(s) might drive thyrotrope fate. However, thyrotrope commitment is normal in *Ascl1* knockout and in triple knockout mice deficient in *Ascl1* (*Mash1*)*, Neurod4* (*Math3*)*,* and *Neurod1.* These bHLH activating factors have overlapping functions in promoting somatotrope, gonadotrope, and corticotrope development [291, 292, 321, 322]. They promote pituitary stem cell exit from the cell cycle and act as selectors of cell fate, as triple knockout mice have more SOX2-positive cells and more lactotropes. We discovered expression of numerous bHLH factors that are candidates for driving thyrotrope fate. Given their electrical activity, it is possible that the factors regulating differentiation of thyrotropes and TαT1 cells may have some similarity to the factors that are involved with neuronal differentiation, which rely heavily on bHLH factors. Marius Wernig convincingly showed that ASCL1 (in addition to BRN2 and MYT1L, called BAM factors) are sufficient to transdifferentiate mouse embryonic fibroblasts (MEFs) into neurons, and he comprehensively characterized the mechanisms by which these factors act [323, 324]. MYT1L is a zinc finger transcription factor. ASCL1 and MYT1L represent two of the most highly upregulated transcription factors in TαT1 cells. BRN2 barely reaches the limit of detection in TαT1 cells, however it is a POU factor, and POU1F1 is critical for expression and regulation in TαT1 cells. While we showed definitively that loss of ASCL1 has no effect by

e18.5, it is possible that ASCL1, acting in concert with MYT1L and POU1F1 may be important for the neuron-like fate of the TαT1 cells. While the knockout of ASCL1 alone has no apparent effect on thyrotrope differentiation in mice, ASCL1 is critical for zebrafish pituitary development, and there are many other bHLH factors expressed in thyrotropes (and TαT1 cells) that could have overlapping function with ASCL1.

The top three most highly expressed bHLH factors in both of pituitary cell lines are the repressive bHLH factors in the ID family. The role of these genes in pituitary development has not been studied, but they may be important in regulating progenitor differentiation and cell fate selection. For example, a proper balance of activating and repressive bHLH factors is critical for cortical development [325]. Repressive ID and Hes factors are expressed in cortical progenitors, and induction of key activating bHLH factors drive these progenitors to differentiate. Astrocytes, however, require continued repressive bHLH factor expression. The interplay of active and repressive bHLH factors in pituitary development is likely complex.

We identified many putative enhancers in both the precursor and thyrotrope cell line by epigenomic marks and assessment of open chromatin. To facilitate utilization of these data for analysis of human genome wide association analysis hits, we mapped the putative mouse regulatory elements onto the human genome. We discovered that SNPs associated with a neuroticism subphenotype described as feeling miserable were enriched in TαT1 stretch enhancers. Thyrotrope dysfunction can lead to hypothyroidism, which is associated with depression and lethargy [326]. Thus, these stretch enhancers may be important for proper regulation of thyroid function in humans.

We carried out functional testing of putative regulatory elements in and around the thyrotrope-signature genes *Tshb*, *Gata2*, *Cga*, *Pitx1*, and *Trhr*. We tested twenty-five elements around these genes, and found that eight drove luciferase expression, One element for *Tshb*, two for *Gata2*, two for *Cga*, two for *Pitx1*, and one for *Trhr*. We show here the first regulatory

element that is sufficient to drive reporter expression in thyrotropes in genetically engineered mice. Previous promoter-proximal elements have been reported to have activity in thyrotrope cell lines, however, have failed to drive expression in murine models. This represents a significant improvement in our understanding of thyrotrope regulation. In vitro studies in TαT1 cells showed that POU1F1 binds this element and GATA2 drives *Tshb* expression via this element. Further motif analysis suggests that PITX factors may also be binding this element. Full characterization of the transcription factors binding this element would give insight into the broader thyrotrope regulation network.

This work represents the first thorough characterization of the epigenome and transcriptome in Pou1f1 lineage progenitors and thyrotropes. We used this genome-wide catalog and demonstrated enhancer function for elements in genes encoding thyrotropin, *Cga* and *Tshb*, the receptor for the hypothalamic releasing hormone that regulates thyrotropin, *Trhr*, and two crucial transcription factors, *Gata2* and *Pitx1*. This provides proof of the principle that the catalog is valuable for dissecting gene regulation. In addition, we demonstrate that the *Tshb* enhancer element is sufficient for expression in thyrotropes in transgenic mice and is directly regulated by GATA2. We discovered that unique POU1F1 binding sites are associated with bZIP factor binding motifs in *Pou1f1* lineage progenitors and bHLH or bHTH binding motifs in thyrotropes. This suggests candidate gene families for regulating thyrotrope differentiation, such as the RFX family. Of the more than 30 known genes that are mutated in patients with hypopituitarism, 18 are transcription factors that regulate pituitary development and cell specification, indicating the clinical importance of this field of study. The overwhelming majority of patients with hypopituitarism have no molecular diagnosis, suggesting additional genes remain to be discovered. We provide a rich selection of candidate transcription factors that are differentially expressed in progenitors and thyrotropes. Amongst the top 40 of these, 9 are already implicated in pituitary development and disease. Future analysis of the remaining 31 candidates may uncover additional disease genes.

Methods

Cell culture and transfection

GHF-T1 and TαT1 cells were provided by Dr. Pamela Mellon at University of California San Diego and grown on uncoated 100mm dishes and Matrigel-coated 60mm dishes, respectively. They were grown in DMEM (Gibco, 11995-065) with 10% Fetal Bovine Serum (Corning, 35016CV) and 1% Penicillin Streptomycin (Sigma-Aldrich P4333). Cells were split 1:10 once they achieved 80% confluence. Six replicates of TαT1 cells were transfected using FuGENE 6 with a 3:1 transfection reagent/DNA ratio. Cells were collected 48 hours post-transfection for collection and luciferase measurement was performed using Promega Dual-Glo (Promega #E2920), and a GloMax 96 microplate luminometer.

Cloning

The DNA prepared for the plasmids used in the transfection experiments and transgenic mice was amplified from TαT1 DNA. Primers were designed to work with Phusion Green Hot Start II High-Fidelity PCR Master Mix (catalog # F566S). Two methods were employed to clone plasmids containing the regulatory element, the respective promoter, and the YFP reporter. The first method involved adding 10-15 nucleotides onto the insert that overlapped with the pCDNA3-YFP Basic plasmid that had been cut with Kpn1 and Xho1. The amplicon and linearized plasmid backbone were combined using the NEB HiFi DNA Assembly Master Mix (catalog # E2621L) with 1:2 vector:insert ratios, and 60 min incubation time at 50°C. The subsequent plasmid was transformed into DH5α cells. The second method was to insert the amplified construct into a Zero Blunt TOPO vector (ThermoFisher #450245), select clones that are in the forward and reverse orientation, then cut the TOPO vector containing the insert with Kpn1 and Xho1. The resulting fragment is then ligated into a digested pCDNA3-YFP Basic

plasmid that had been cut with Kpn1 and Xho1 using a standard T4 DNA Ligase protocol (NEB #M0202). Once the insert, plasmid, and breakpoint sequences were confirmed by Sanger sequencing, the plasmids were extracted from overnight 1 L cultures of DH5α cells using Qiagen Plasmid Maxi Kits (catalog #12163). Endotoxins were removed from the plasmids using the Endotoxin removal Solution (Sigma, E4274-25ML).

RNA Seq

One million GHF-T1 and TαT1 cells were collected for each of the three replicates for each cell line. Once collected, the RNA was extracted using the RNAqueous™ Total RNA Isolation Kit (catalog #AM1912). The RNA was prepared by the University of Michigan Advanced Genomic Core for mRNA enrichment followed by 50-cycle, paired-end sequencing on the Illumina HiSeq-4000. The RNA was checked for quality using FastQC and mapped and analyzed using the VIPER Snakemake pipeline [327]. Briefly, VIPER aligns the files to the mm9 transcriptome using STAR, followed by differential expression analysis using DESeq2 and cell type clustering and expression quantification using QoRTs [328]. The quality of the alignment was also analyzed using QoRTs.

We measured the significance of the increase in expression of sodium, potassium, and calcium using a one-way ANOVA. This demonstrated the significance of the increase in expression of the sodium and potassium, but not the calcium channel genes.

GO Term and KEGG Pathway Enrichment

We performed GO-term enrichment on the top 5% of most differentially expressed genes (by log-2 fold-change) in both lines [289, 290]. This represented 453 genes in GHFT1 cells, and 490 genes in TαT1 cells. We used the default settings on the web-based Gene Ontology Resource (geneontology.org), using the biological process and Mus Musculus options. The resulting GO terms were plotted by their log2 fold enrichment, and their p-values.

We also performed a directional Kyoto Encyclopedia of Genes and Genomes (KEGG) pathway enrichment analysis on all of the genes using RNA-enrich [329]. We set the maximum number of genes per concept to 500 and the minimum number of genes per concept to 5, and otherwise used the default settings. The resulting KEGG pathways were plotted by their coefficients and p-values.

ATAC-Seq

The Assay for Transposase Accessible Chromatin with high-throughput sequencing (ATAC-seq) was performed as previously described [243, 330]. Briefly, 50,000 nuclei were extracted from collected GHF-T1 and TαT1 cells. The cells were transposed with Illumina transposase (Illumina #FC-121-1030) for 30 minutes at 37°C while shaking at 250 RPM. The resulting fragmented DNA was amplified using ¼ of the cycles required to reach saturation in the described qPCR QC. The final amplified DNA library was purified using the Qiagen PCR purification kit (catalog #28104) and sequenced on the Illumina HiSeq platform. The quality of the reads was checked using FastQC, aligned to the mm9 genome, and had its peaks called using the Parker lab's Snakemake pipeline [331].

CUT&RUN

CUT&RUN was performed under high-digitonin conditions as described with few exceptions, namely all steps with < 1 ml of liquid requiring mixing were done by 500 RPM shaking instead of inversion [293]. Briefly, 250,000 cells per sample, and one sample per cell line-antibody pair were collected, washed, and bound to Concavalin A beads (Bangs Laboratories, BP531). The cells attached to beads were incubated at 4°C overnight with the respective antibodies (POU1F1 – this antibody was a kind gift from Dr. Simon Rhodes, University of North Florida, Jacksonville, FL [332], H3K27Me3 – Cell Signal #C36B11, H3K27Ac – Abcam ab4729, H3K4Me1 – Abcam ab8895, Rabbit IGG – R&D AB-105-C). The antibodies were washed, and no secondary antibody was used. The protein A/MNAse fusion protein was

added, followed by Ca^{2+}-induced digestion at 0°C for 30 minutes. The fragmented chromatin was then collected and purified using Macherey-Nagel NucleoSpin Gel and cleanup columns (catalog #740609). Libraries of this DNA was prepared using the Kapa Biosystems library prep kit (catalog #KK8702) at a 100:1 adapter:sample ratio. The libraries were paired-end sequenced on a single lane of the Illumina HiSeq-4000 for 50 cycles. The resulting data was then checked for quality using FastQC, aligned to the mm9 genome using Bowtie2 using the flags recommended for CUT&RUN (--local --very-sensitive-local --no-unal --no-mixed --no-discordant --phred33 -I 10 -X 700), and peaks were called using MACS2.

ChromHMM

ChromHMM was performed on both cell lines using H3K4Me1, H3K27Ac, ATAC-seq and H3K27Me3 as input. The number of states was iteratively increased to find the number of states that resulted in the fewest number of states with the best log-likelihood. An eleven-state model was selected as a result. Association of each state with the various marks and genomic features can be seen in **Supplementary Figure 6**. Contiguous states of value two and three were stitched together as enhancers using bedtool's mergeBed function with a -d 1 flag [333].

Association Enrichment Test

Enrichment analysis of disease SNPs at stretch enhancers in GHFT1, TαT1 and heterologous cell lines was performed using GARFIELD and stretch enhancers published previously [301, 303]. To find the human sequences orthologous to GHFT1 and TαT1 stretch enhancers we used a conversion file generated using bnMapper and an mm9 to hg19 chain file [334]. We selected associations that had association counts of at least 50, that had a full complement of summary statistics, had more than three million tested SNPs, and were in the harmonized data format were chosen from the GWAS catalog [335]. The resulting heatmap of odds ratios and p-values for each association, tissue-type pair is shown in **Supplementary Figure 8**.

Transgenic mice

All mice were housed in a 12-h light, -12 h dark cycle in ventilated cates with unlimited access to tap water and Purina 5020 chow. All procedures were conducted in accordance with the principles and procedures outlined in the National Institutes of Health Guidelines on the Care and Use of Experimental Animals and approved by our Institutional Animal Care and Use Committee.

Recombinant DNA was generated by amplifying genomic mouse DNA regions in **Supplemental Table 4**, and the previously described Phusion polymerase. The putative regulatory element was then combined with 438 base pairs of the TSHβ promoter (chr3:102,586,594-102,587,032), and a YFP reporter. These elements were combined using the DNA Hifi reaction into a pGEM-T Easy plasmid. The putative regulatory element, the promoter, the YFP, and the breakpoints were checked for accuracy with Sanger sequencing. Once the plasmid was confirmed, larger quantities of the plasmid were generated from overnight 1L cultures of DH5α cells using Qiagen Plasmid Maxi Kits (catalog #12163). To reduce the effect of the plasmid backbone on the viability of injected eggs, the enhancer, promoter, and YFP were amplified from the plasmid. The resulting amplicon was gel purified and injected into fertilized eggs of mice on a C57BL/6 and SJL mixed background. The resulting mice were genotyped for the YFP allele according to the Jackson Laboratory recommended primers and conditions [336]. We dissected the pituitaries from mice that were positive for the YFP transgene (and four age-matched, negative, control littermates) at three weeks of age.

Tissue Preparation and Immunohistochemistry

Mouse pituitaries were fixed in 4% formaldehyde in PBS overnight at 4°C. The tissue was washed three times in PBS and put in 10% EDTA for 3 hours. They were then dehydrated by putting them in 25%, then 50%, then 70% ethanol for one hour each. The pituitaries were embedded in paraffin with four-hour cycles using a Tissue Tek VIP Paraffin tissue processing

machine (Miles Scientific). The embedded pituitary was cut into coronal, six-micron sections, and was analyzed by immunohistochemical markers as previously described [308, 337]. Anti-YFP and anti-*Tshb* were used (from Abcam ab6556 and National Hormone and Peptide Program, respectively).

Antibodies were detected using either the tyramide signal amplification (TSA) (33002 CFF488A Streptavidin HRP, Biotium, Fremont, CA) and streptavidin-conjugated Alexa-fluor 488 (1 : 200, S11223, Invitrogen). DAPI (1:200) was incubated on the slides for five minutes to stain nuclei. DABCO-containing permount was used to mount the slides, which were then imaged using a Leica DMRB fluorescent microscope.

Data Access

All raw sequencing data generated in this study have been submitted to the NCBI Sequence Read Archive (SRA, https://www.ncbi.nlm.nih.gov/sra) under accession number PRJNA643917, and will be released once published.

Supplemental Figures

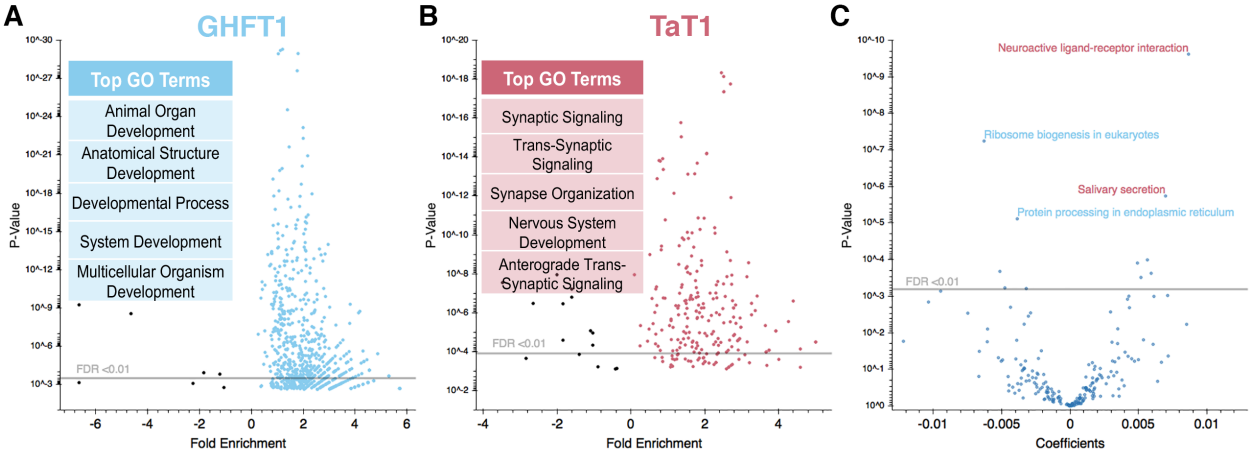

Supplemental Figure 1: GO term enrichment and KEGG pathway analysis.

(A) Volcano plot of GO Terms from the top 5% of the genes most highly expressed in GHF-T1 cells. (B) Volcano plot of GO Terms from top 5% of the most highly expressed genes in TαT1 cells. (C) KEGG pathway enrichment done on all genes.

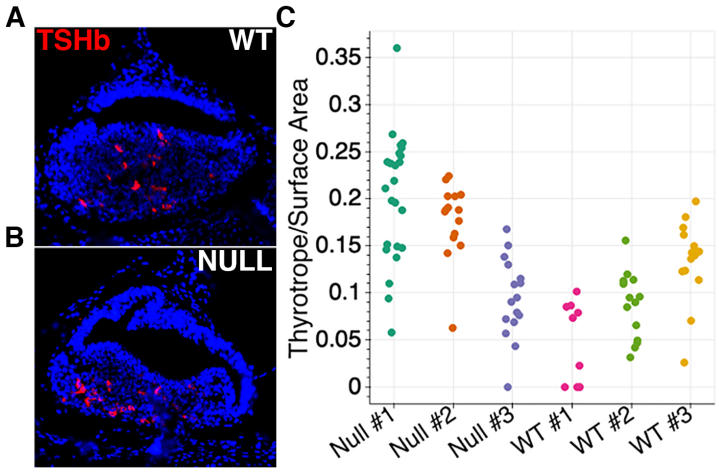

Supplemental Figure 2: Loss of ASCL1 has minimal impact on thyrotrope number.

(A) Immunostain for TSH in wild type e18.5 pituitary. (B) Immunostain for TSH in *Ascl1*$^{-/-}$ e18.5 pituitary. (C) Number of thyrotropes per surface area in six e18.5 mice (three wild type, three null) revealing no significant difference between the genotypes (p-value 0.71).

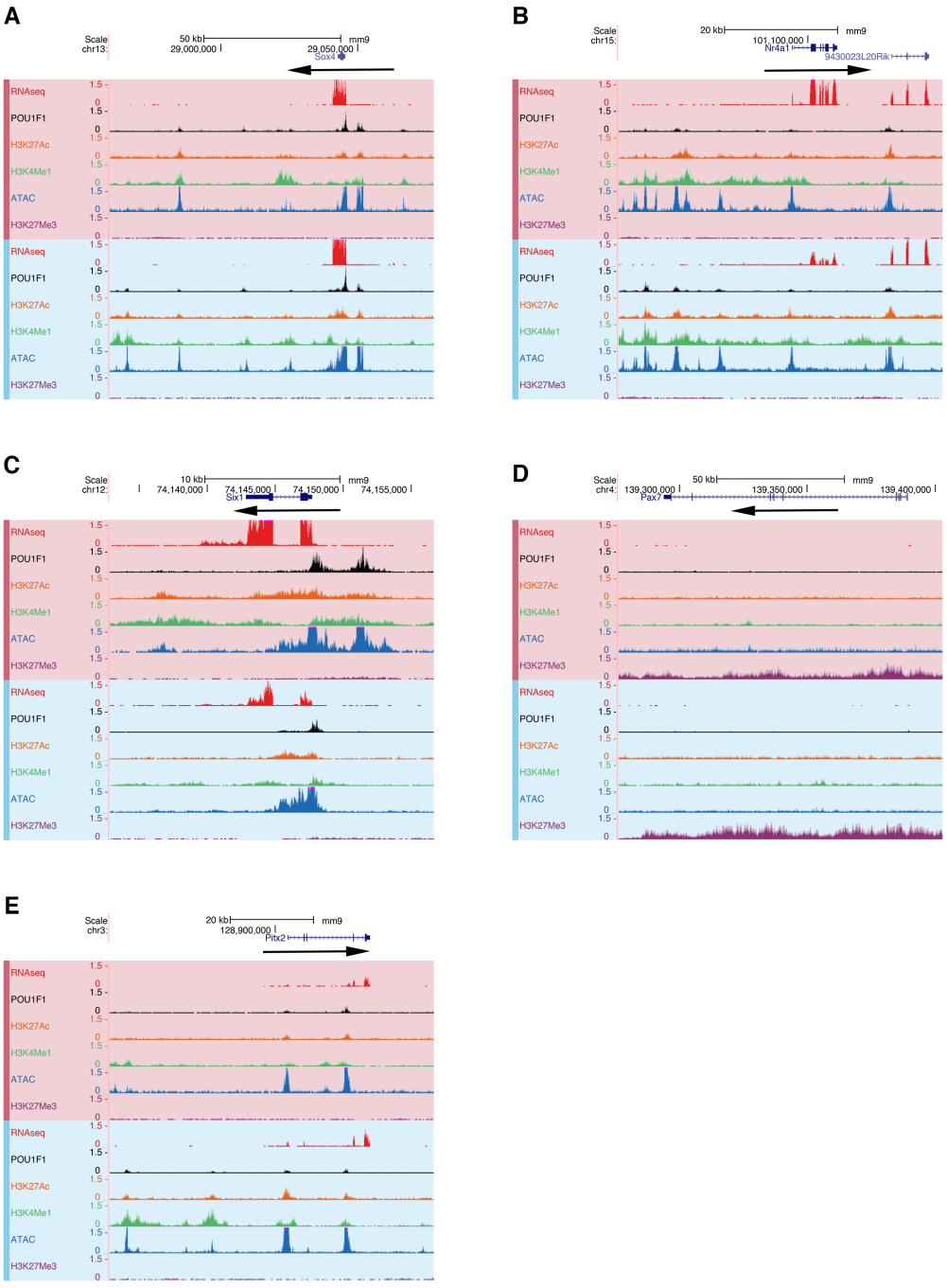

Supplemental Figure 3: Multi-omics tracks for loci with similar levels of expression and chromatin landscapes in both cell types.

RNA-seq, POU1F1, H3K27Ac, H3K4Me1, ATAC-seq, and H3K27Me3 tracks at (**A**) *Sox4*, (**B**) *Nr4a1*, (**C**) *Six1*, (**D**) *Pax7*, and (**E**) *Pitx2* loci in TαT1 cells (red) and GHF-T1 (blue).

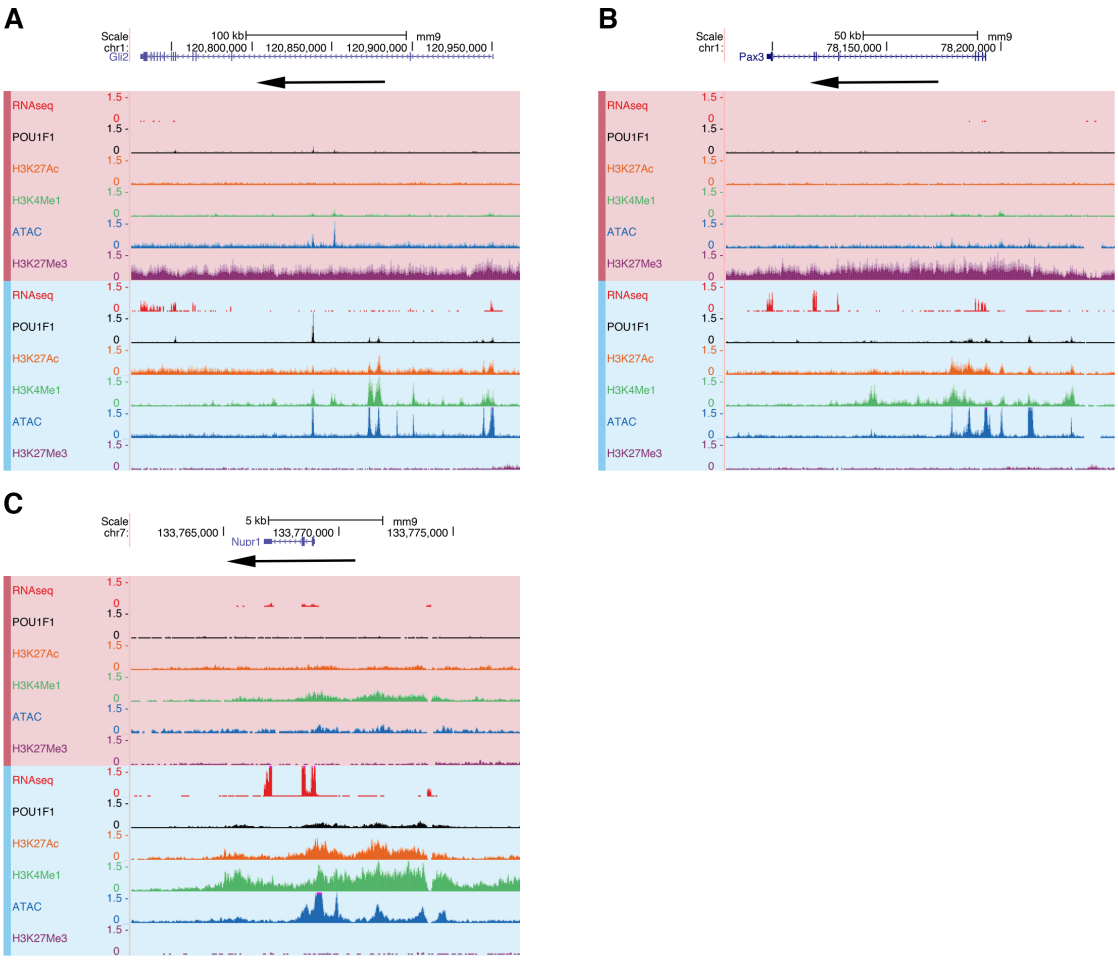

Supplemental Figure 4: Multi-omics tracks for selected genes with higher levels of expression in GHF-T1 cells.

RNA-seq, POU1F1, H3K27Ac, H3K4Me1, ATAC-seq, and H3K27Me3 tracks in TαT1 (red) and GHF-T1 (blue) cells for (**A**) *Gli2*, (**B**) *Pax3*, and (**C**) *Nupr1*.

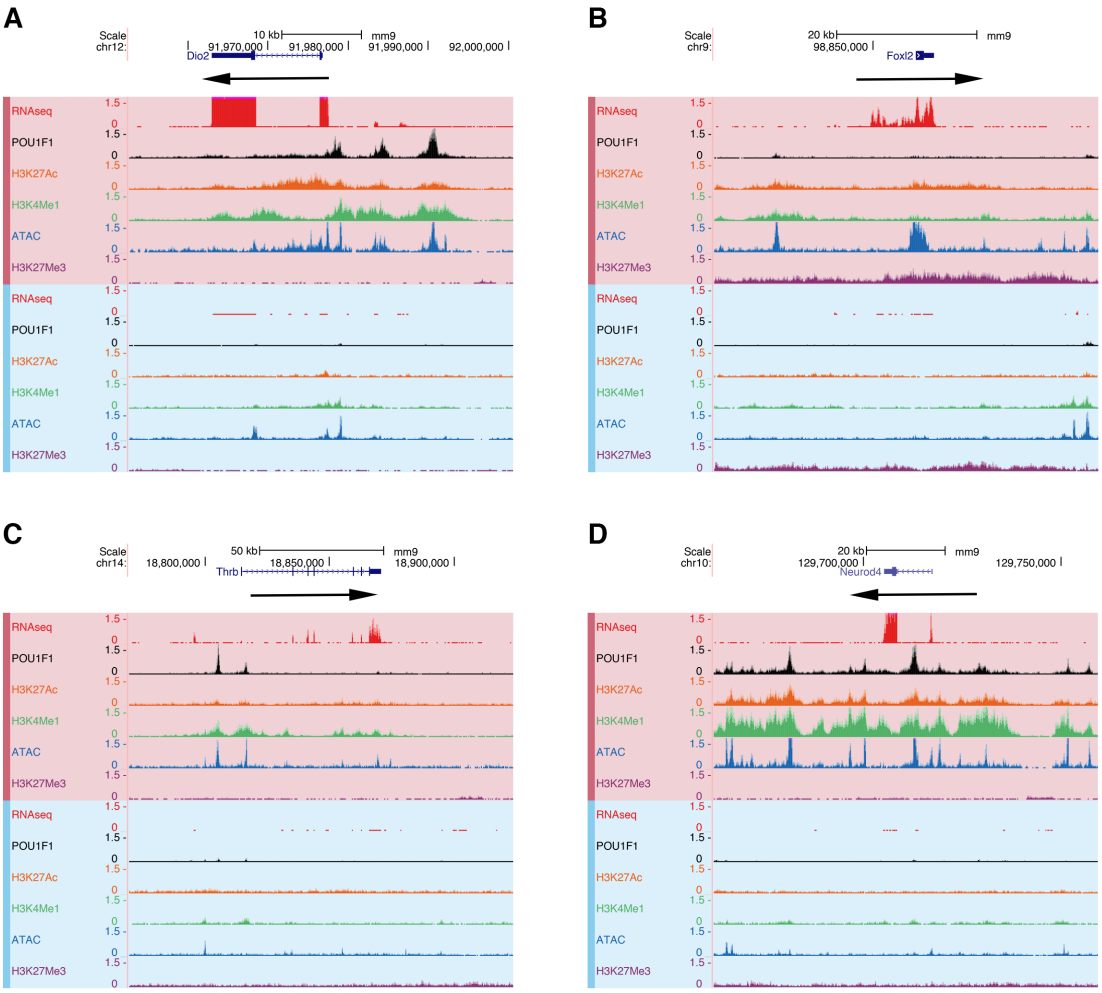

Supplemental Figure 5: Multi-omics tracks for selected loci with higher levels of expression in TαT1 cells.

RNA-seq, POU1F1, H3K27Ac, H3K4Me1, ATAC-seq, and H3K27Me3 tracks from TαT1 (red) and GHF-T1 (blue) cells at (**A**) *Dio2*, (**B**) *Foxl2*, (**C**) *Thrb*, and (**D**) *Neurod4*.

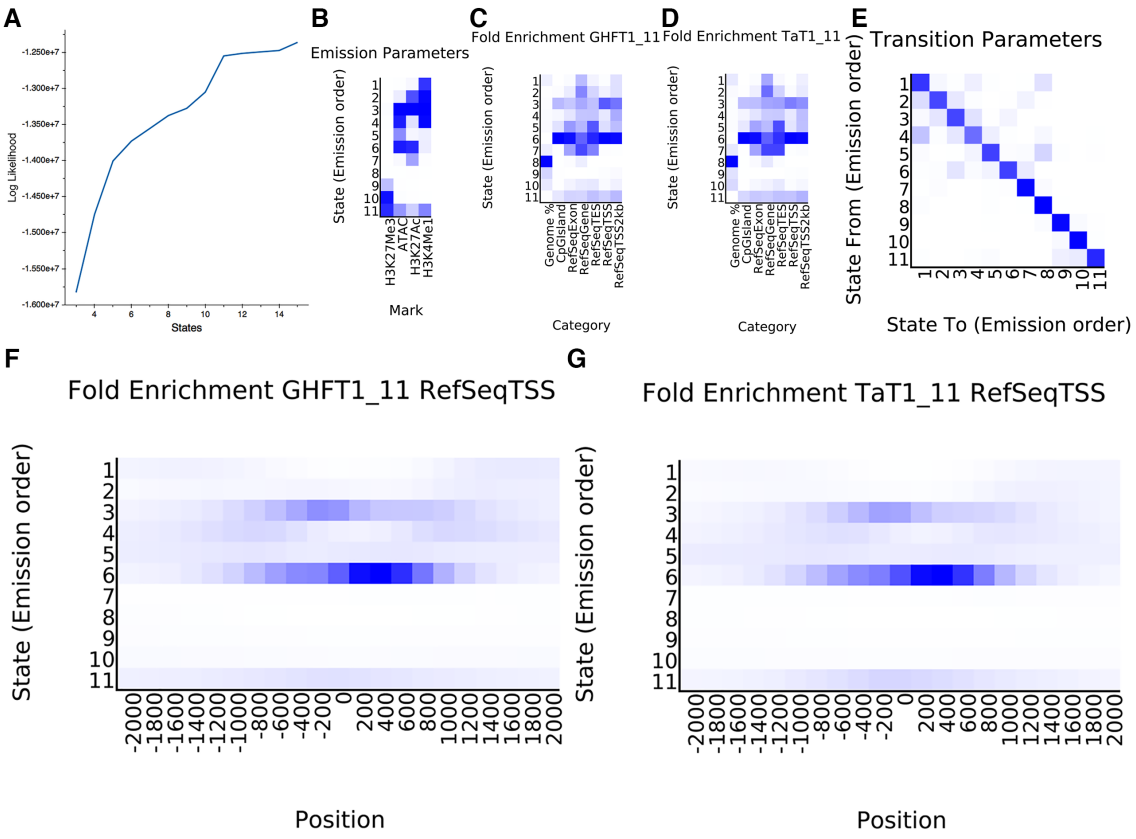

Supplemental Figure 6: ChromHMM summary data.

(A) Log likelihood of the resulting ChromHMM performed for each number of states. Eleven states had the best combination of the fewest states and most favorable log likelihood. (B) The emission parameters reveal the presence of each histone mark and the level of ATAC-seq signal for each state with darkest blue being the highest enrichment. (C) Genomic features of each state in GHF-T1 cells. (D) Genomic features of each state in TαT1 cells. (E) A plot revealing the degree of transition from each parameter to each other parameter. (F) Degree of enrichment of each state at TSS's in GHF-T1 cells, revealing that state six is heavily enriched at promoters. (G) Degree of enrichment of each state at TSS's in TαT1 cells, revealing that state six is heavily enriched at promoters.

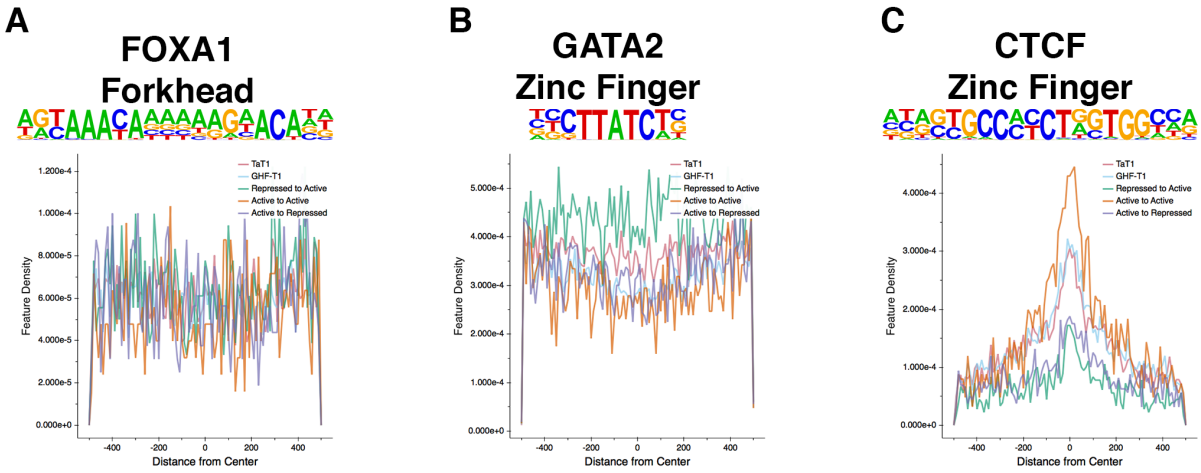

Supplemental Figure 7: Motif density at POU1F1 binding sites in GHF-T1 and TαT1 cells.

(A) Motif density of the representative forkhead factor FOXA1 at all TαT1 POU1F1 binding sites (TαT1), at all GHF-T1 POU1F1 binding sites (GHF-T1), at POU1F1 binding sites that are specific to TαT1 that have repressed repressive marks in the precursor, GHF-T1 cells and active chromatin in the differentiated, TαT1 cells (Repressed to Active), at POU1F1 binding sites that are shared between both lines and have similarly active chromatin marks in both (Active to Active), and POU1F1 binding sites that are specific to GHF-T1 that have active chromatin in GHF-T1 cells, and repressed chromatin in TαT1 cells (Active to Repressed). (B) Motif density of GATA2 at the same POU1F1 binding domains as in (A). (C) Motif density of CTCF at the same POU1F1 binding domains as in (A).

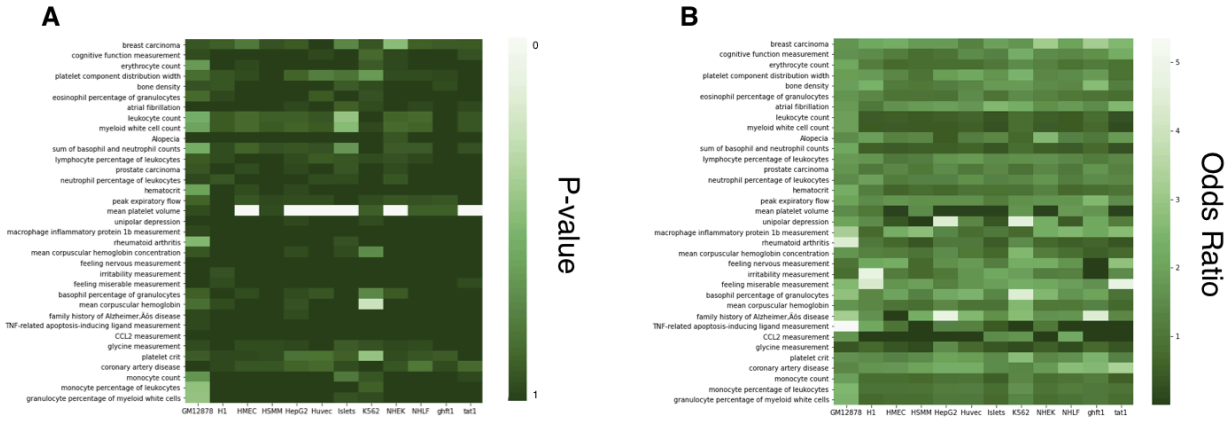

Supplemental Figure 8: Heatmap of associations with each cell type.

(A) P-value for each enrichment test performed for each association and cell type pair. (B) Odds ratio for each enrichment test performed for each association and cell type pair.

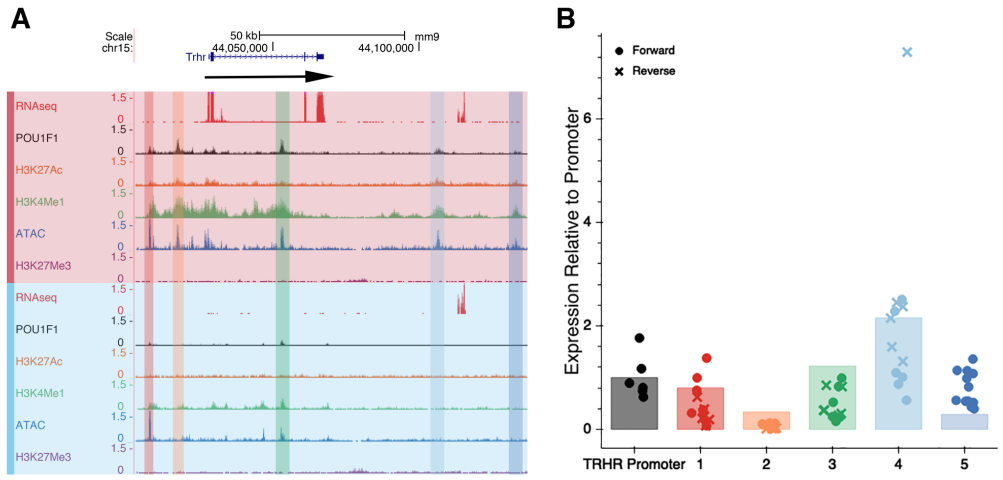

Supplemental Figure 9: Functional enhancer testing of elements of open chromatin in and around *Trhr*

(A) RNA-seq, POU1F1, H3K27Ac, H3K4Me1, ATAC-seq, and H3K27Me3 tracks (TαT1 in red, GHF-T1 in blue) at the *Trhr* locus where elements tested are highlighted. (B) Level of luciferase activity of each element, color-coordinated with the highlighted elements in **A** in both the forward (circles) and reverse (x's) orientation.

Supplemental Tables

Supplemental Table 1: Genes Associated with SV40 Immortalized Pituitary Cell Lines.

Cluster 1 (Pit1-Zero + Pit1-Triple	Cluster 2 (GHF-T1)	Cluster 3 (TαT1)
LXN	FABP7	CGA
TBX18	SDPR	NNAT
MIR692-1	VAX1	PCP4
GYPC	SHTN1	SMTNL2
ARSJ	BST2	CHGA
PBP2	TUBA8	CHGB
LCE1G	GAS7	PNMAL1
EREG	TPRG	RESP18
LOX	COX7A1	ELAVL3
NID1	LDHB	PCSK2
CES1G	LRRC17	SYP
GREM1	1700019N19RIK	SCG3
BGN	CHRNB1	SCG2
GJA1	CGNL1	SEZ6L2
CHRNA1	CLVS2	CELF3
CASP8	BTBD3	SNAP25
HEBP2	RCN3	CDK5R2
PDGFRB	HOTAIRM1	ZIM1
PTX3	CREB5	SCG5
TPM2	MEIS2	INSM1

Supplemental Table 2: bHLH genes expressed in GHF-T1 and TαT1 cells.

Factor	GHF-T1 Expression (FPKM)	TαT1 Expression (FPKM)
Shared Expression		
ID2	155.4	253.8
ID1	121.2	203.8
TCF4	99.6	166.6
HIF1A	49.92	103.4
TCF12	48.4	83.2
BHLHB9	33.1	82.6
SREBF2	61.1	44.7
TCF3	50.2	41.9
BHLHE40	23.3	69
MAX	45.4	41.1
Up in GHF-T1		
TCF24	2.3	0
TWIST2	6.6	0
BHLHE22	4.8	0.1
TWIST1	17.3	0.5
ATOH8	42.2	2.9
MSC	3.2	0.3
HEY2	2.3	0.3
HES1	16.6	2.6
EPAS1	3.3	0.7
ID3	226.7	63.5
TCF24	2.3	0
Up in TαT1		
NEUROD4	0	31.9
ASCL1	0.2	25.3
OLIG1	0.1	3.7
MYCN	0.3	13.9
HEYL	0	1.3
ID4	3.3	81.3
TAL1	0.1	2.7
MLXIPL	0.3	2.6
NCOA1	2.1	13.5
ARNTL	10.4	41.5

Supplemental Table 3: Thyrotrope signature genes.

Gene	Protein	References (PMIDs)
Cga	Chorionic gonadotropin alpha	7544315
Tshb	Thyroid stimulating hormone beta subunit	2792087
Trhr	Thyrotropin releasing hormone receptor	9141550, 14988432
Thrb	Thyroid hormone receptor beta	22570333, 32122258
Dio2	Deiodinase 2	11731615, 5007895
Pou1f1	POU homeobox transcription factor (PIT1)	1302000, 15928241, 1981057, 1977085
Gata2	GATA binding protein 2	16543408, 12385825, 10367888
Gata3	GATA binding protein 3	16543408, 10935639
Isl1	Islet 1	32453714, 27580811
Lhx3	LIM homeobox protein 3	8638120, 16394081
Pitx1	Paired homeodomain transcription factor 1	21775501, 10049363, 10101115, 15761027
Pitx2	Paired homeodomain transcription factor 2	8944018, 10498698, 11807026
Foxl2	Forkhead transcription factor FOXL2	11175783, 12149404, 15056605, 14736745, 29800110, 16840539
Sox4	SRY-box 4	22543271, 30661772, 9815146
Rxrg	Retinoid receptor X gamma	16306084, 108800050
Nr4a1	Nuclear receptor subfamily 4, group a, member 1 (Nurr77)	22792320, 30093910
Creb3l	cAMP-responsive element-binding protein 3-like 1	29311806, 27580811
Eya3	Eyes absent transcriptional co-activator and phosphatase 3	21129973
Six1		9020840, 1978983, 14628042
Tef	Thyrotroph embryonic factor	1916262, 15175240
Nupr1	Nuclear protein transcriptional regulator 1	12429736, 18495683, 27580811
Tceal5	Transcription elongation factor A (SII)-like 5	27580811
E2f1	E2F transcription factor 1	27580811, 18794899
Etv5	Ets variant 5	27580811, 19898483, 16107850
Msx1	Muscle segment homeobox 1	12807959, 7914451, 23371388, 1837990/0, 16703404
Lhx2	LIM homeodomain transcription factor 2	7513049, 19900438

Supplemental Table 4: Mm9 Genomic coordinates for promoter and enhancer elements tested in transfection.

Gene	Element	Chrom	Start	Stop
Gata2	200 bp Promoter	chr6	88148535	88148762
Gata2	900 bp Promoter	chr6	88147851	88148762
Gata2	2.8 kb Promoter	chr6	88145925	88148762
Gata2	Element 1	chr6	88139279	88141082
Gata2	Element 2	chr6	88176353	88177232
Gata2	Element 3	chr6	88261331	88262559
Cga	486 bp Promoter	chr4	34840577	34841063
Cga	Element 1	chr4	34833573	34835422
Cga	Element 2	chr4	34836822	34837786
Cga	Element 3	chr4	34846587	34847868
Pitx1	377 bp Promoter	chr13	55932587	55932964
Pitx1	Element 1	chr13	55941401	55944503
Pitx1	Element 2	chr13	55951439	55953329
Tshb	438 bp Promoter	chr3	102586594	102587032
Tshb	Element 1	chr3	102527463	102529377
Tshb	Element 2	chr3	102536553	102540450
Tshb	Element 3	chr3	102550639	102553942
Tshb	Element 4	chr3	102592924	102594331
Tshb	Element 5	chr3	102605012	102609378
Trhr	957 bp Promoter	chr15	44027215	44028172
Trhr	Element 1	chr15	44007238	44011587
Trhr	Element 2	chr15	44016635	44021495
Trhr	Element 3	chr15	44050106	44054542
Trhr	Element 4	chr15	44105357	44109171
Trhr	Element 5	chr15	44132604	44133764

Supplemental Table 5: Factors that may be binding *Tshb* Element 4.

Gene	Number of Motifs	Top Motif Score	Average Motif Score	TαT1 Expression
Sorted by TαT1 Expression				
PITX1	31	8	5	363.5

MAZ	2	16	11	187.3
TCF4	21	13	5	166.6
POU1F1	5	10	10	159.6
ATF4	7	10	8	147.2
CENPB	2	5	5	114.4
HIF1A	4	6	5	103.4
TFDP1	1	9	9	97.6
TCF12	17	15	5	83.2
PLAGL1	1	7	7	78.6
JUND	19	8	3	77.5
BHLHE40	6	8	4	69
MEF2A	27	11	7	66.4
SMAD4	6	5	5	58.2
STAT5A	7	11	10	57.1
PKNOX2	2	11	11	53.5
CTCF	1	9	9	51.4
E2F1	3	6	5	50.1
VEZF1	4	7	6	47
ISL1	15	11	6	45.7
Ranked by Number of motifs (TαT1 FPKM >=1)				
FOXD2	76	7	4	2
LHX9	76	11	5	1.3
HOXA5	75	11	5	1.3
GATA2	65	14	5	34.8
FOXC1	60	9	4	4.8
LHX4	60	10	5	1.1
LHX1	58	9	5	8.5
ARID3A	51	9	5	1.2
STAT3	50	11	4	30
LIN54	49	13	6	22.6
HLTF	49	8	5	6.1
DLX1	48	9	5	2.1
HLF	47	12	7	36.7
ETS1	47	12	5	3.1
NKX3-2	47	12	6	1.7
TBP	46	10	7	24.9
VAX2	43	11	5	10.6
ZEB1	43	11	5	9.4
KLF4	43	10	6	7.7
HOXA6	42	9	5	1.3
FOXD2	76	7	4	2

Chapter 3: Pituitary tumors and immortalized cell lines generated by cre-inducible expression of SV40 T antigen

Abstract

Targeted oncogenesis is the process of driving tumor formation by engineering transgenic mice that express an oncogene under the control of a cell-type specific promoter. Such tumors can be adapted to cell culture, providing immortalized cell lines. To make it feasible to follow the process of tumorigenesis and increase the opportunity for generating cell lines, we developed a mouse strain that expresses SV40 T antigens in response to cre-recombinase. Using CRISPR/Cas9 we inserted a cassette with coding sequences for SV40 T antigens and IRES-GFP into the *Rosa26* locus, downstream from a stop sequence flanked by loxP sites: *Rosa26*$^{LSL\text{-}SV40\text{-}GFP}$. These mice were mated with previously established *Prop1-cre* and *Tshb-cre* transgenic lines. The majority of *Rosa26*$^{LSL\text{-}SV40\text{-}GFP/+}$; *Prop1-cre* and all *Rosa26*$^{LSL\text{-}SV40\text{-}GFP/+}$; *Tshb-cre* mice developed dwarfism and large tumors by 4 weeks. *Prop1*-cre-mediated activation of SV40 expression affected cell specification, reducing thyrotrope differentiation and increasing gonadotrope differentiation. Flow-sorted GFP-positive cells from *Rosa26*$^{LSL\text{-}SV40\text{-}GFP/+}$; *Prop1-cre* and *Rosa26*$^{LSL\text{-}SV40\text{-}GFP/+}$; *Tshb-cre* mice express PROP1 and TSH, respectively. Tumors from both of these mouse lines were adapted to growth in cell culture. We have established a progenitor-like cell line (PIT-P1) that expresses *Sox2* and *Pitx1*, and a thyrotrope-

like cell line (PIT-T1) that expresses *Cga* and *Pou1f1.* These studies demonstrate the utility of the novel, *Rosa26*$^{LSL\text{-}SV40\text{-}GFP}$ mouse line for reliable targeted oncogenesis and development of unique cell lines.[2]

[2] This chapter has been submitted and is under revision: Alexandre Z. Daly*, Amanda H. Mortensen*, Hironori Bando, Sally A. Camper, "Pituitary tumors and immortalized cell lines generated by cre-inducible expression of SV40 T antigen" *Endocrinology.* (*indicates co-first authors). Ms. Mortensen conducted the histological staining and immunohistochemical analyses and assisted with animal colony management. Dr. Bando assisted with cell line development.

Introduction

Immortalized cell lines have been invaluable tools for understanding the molecular mechanisms that underlie the pituitary gland's response to hypothalamic regulation, feedback from end organs, and intracellular signaling. They have also been useful in understanding the formation of pituitary adenomas [338]. Cell lines offer the ease of manipulation and obviate the need to rely on primary tissues. This is particularly true for small organs like the pituitary gland. Additional pituitary cell lines would be useful for dissecting the changes associated with stem cells transitioning to differentiation and commitment to the thyrotrope fate.

Pituitary and hypothalamic cell lines have been developed by targeted oncogenesis. This involved using cell-specific transcriptional regulatory sequences to drive expression of large and small SV40 T antigens in transgenic mice. Invariably, tumors develop in some of the mice, and the cells in these tumors can sometimes be adapted to grow in culture into stable, immortalized cell lines that maintain some of the features of differentiated cells. Tumors often develop early and cause infertility or death, making it difficult to generate cell lines from a single founder mouse. For this reason, we generated a mouse line that can express SV40 T antigen in response to cre-recombinase excision of a stop sequence flanked by loxP sites.

Both the SV40 large and small T antigen contribute to immortalization. The large T antigen causes transformation by binding to and disrupting the function of HSC70, Rb, p300, and p53, whereas the small t antigen binds to pp2A to contribute to the transformation, characterized by uncontrolled proliferation [339]. The ability of SV40 to inactivate p300-related activity is critical to its capacity to immortalize cells [340]. SV40-mediated immortalization has been used to create cell lines that represent pre-gonadotropes (αT3-1), gonadotropes (LβT2), precursors of the POU1F1 lineage (GHF-T1, Pit1-zero), differentiated cells of the POU1F1 lineage (Pit1-triple, TαT1, and Pit1-PRL), and GnRH neurons (GT1-1) [283, 284, 288, 341, 342].

αT3-1 cells were developed by driving SV40 T antigen expression with 1.8 kb of the *CGA* promoter. *CGA* encodes a common alpha subunit of three heterodimeric pituitary hormones: FSH and LH, which are expressed in the gonadotropes, and TSH, which is expressed in thyrotropes. The αT3-1 cells do not express any beta subunits, but they do express *Cga* and the GnRH receptor, indicating commitment to the gonadotrope fate. These cells have been invaluable for studying GnRH mediated cell signaling and regulation of gene expression [343-346]. A more differentiated gonadotrope-like cell line, the LβT2 cell line, was generated by driving SV40 T antigen expression from the rat LHβ gene regulatory elements. LβT2 cells express GnRH receptor, CGA, LH, and FSH. They secrete LH in response to GnRH stimulation and respond appropriately to steroid hormone feedback [347]. These cells have been used widely to study regulation of gene expression in response to various stimuli [348-352]. The TαT1 cell line was generated from a tumor produced by driving SV40 T antigen expression with an expanded, human *CGA* regulatory region. These thyrotrope-like cells respond to TRH and retinoids, and they secrete TSH in response to diurnal cues [285-287]. Several cell lines were generated using the *Pou1f1* regulatory elements to drive T antigen. While each of these cell lines express *Pou1f1,* they vary in hormone expression from none (GHF-T1 and Pit1-zero) to three hormones (Pit1-triple), including GH, TSH and PRL. These cell lines were valuable for studying regulation of the human GH gene cluster, which was introduced as a transgene, and for studying interactions between POU1F1 and the CCAAT enhancer binding protein, CEBPα [353]. A GnRH neuronal-like cell line, GT1-7, was generated by driving SV40 T antigen from GnRH promoter elements, and these cells were used to study GnRH expression and responsiveness to external stimulation [354-356]. Despite these success stories, pituitary tumors often lead to dwarfism, infertility and sudden death, and it can be difficult to adapt tumors to culture.

Additional pituitary cell lines would be valuable for understanding the process of differentiation from progenitors to hormone producing cells. Pituitary stem cells express the common pluripotency factor *Sox2.* SOX2-positive cells are capable of giving rise to all hormone-producing cells within the pituitary [59-61]. The commitment to pituitary fate is associated with expression of the transcription factors PITX1, PITX2, LHX3, and LHX4 [59, 357]. *Prop1* is initially co-expressed with *Sox2*. *Prop1* is a pituitary-specific transcription factor necessary for the POU1F1 lineage, which comprises thyrotropes, somatotropes and lactotropes [130]. Lineage tracing suggests that all cells of the anterior and intermediate lobes of the pituitary gland pass through a *Prop1*-expressing progenitor [131]. Pituitary stem cells can be grown as organoids and stimulated to differentiate into all hormone-producing cell types [267, 268, 358]. This process is inefficient, making it difficult to get enough material to analyze chromatin accessibility and epigenomic marks. There are currently no *Sox2*-expressing pituitary progenitor cell lines.

To expand the repertoire of cell lines available for study, we generated a mouse line that conditionally expresses SV40 T antigen from the *Rosa26* locus: *Rosa26*$^{\text{LSL-SV40-GFP}}$. Well-characterized cre strains can be used to initiate cell-type specific oncogenesis, and the development of tumors can be followed because targeted oncogenesis is initiated with two different transgenes. This approach also provides multiple opportunities to adapt tumors to culture. As rare, novel pituitary cell populations have been discovered with the use of single-cell RNA-seq, we have created a reagent for the generation of limitless immortalized cell lines that permits characterization of these elusive populations.

Results

Constructing mice with an inducible knock-in of SV40 at the *Rosa26* locus

Our objective was to create a mouse line with inducible oncogene expression and a fluorescent marker for tracking induction and generating immortalized cell lines. We chose to use the SV40 large and small T Antigens (SV40 TAg) as the oncogene, given their ability to immortalize cells with high penetrance and their track record of successful transformation [359]. We selected the *Rosa26* locus for targeting because it has nearly ubiquitous expression (including in the pituitary), is a non-essential gene, and has been optimized for targeting. We used a targeting vector (pR26 GFP Dest) that had arms of homology with the first intron of the *Rosa26* locus [360]. It contains a splice acceptor sequence, a floxed-stop sequence, an internal ribosome entry site (IRES), and a green fluorescent protein (GFP) coding region. We used the gateway recombination method to add the large and small SV40 T antigen coding sequences to this vector (**Fig. 11**). This vector was injected into fertilized eggs together with CRISPR-Cas9 and the short guide RNA, sgRosa26-1, to produce transgenic mice. Genomic DNA of potential founder mice was genotyped by PCR. The knock-in was highly efficient, as 16 of 79 (20%) potential founders had the correct allele, verified by PCR amplification and DNA sequencing.

Cre-recombination results in dwarfed mice

We selected two *cre* transgenic lines to cross with the new *Rosa26*$^{LSL\text{-}SV40\text{-}GFP/+}$ strain. *Prop1-cre* genetically labels a few pituitary cells in Rathke's pouch at e11.5 and completely labels cells in the anterior and intermediate lobes by e12.5 [131]. *Tshb-cre* labels thyrotropes beginning at e14.5 [308]. Both *Rosa26*$^{LSL\text{-}SV40\text{-}GFP/+}$; *Prop1-cre* (hereafter referred to as *SV40*; *Prop1*-cre) and *Rosa26*$^{LSL\text{-}SV40\text{-}GFP/+}$*; Tshb-cre* (hereafter referred to as *SV40*; *Tshb*-cre) mice and their littermates were weighed at 2, 3, and 4 weeks (**Fig. 12**). There were no significant

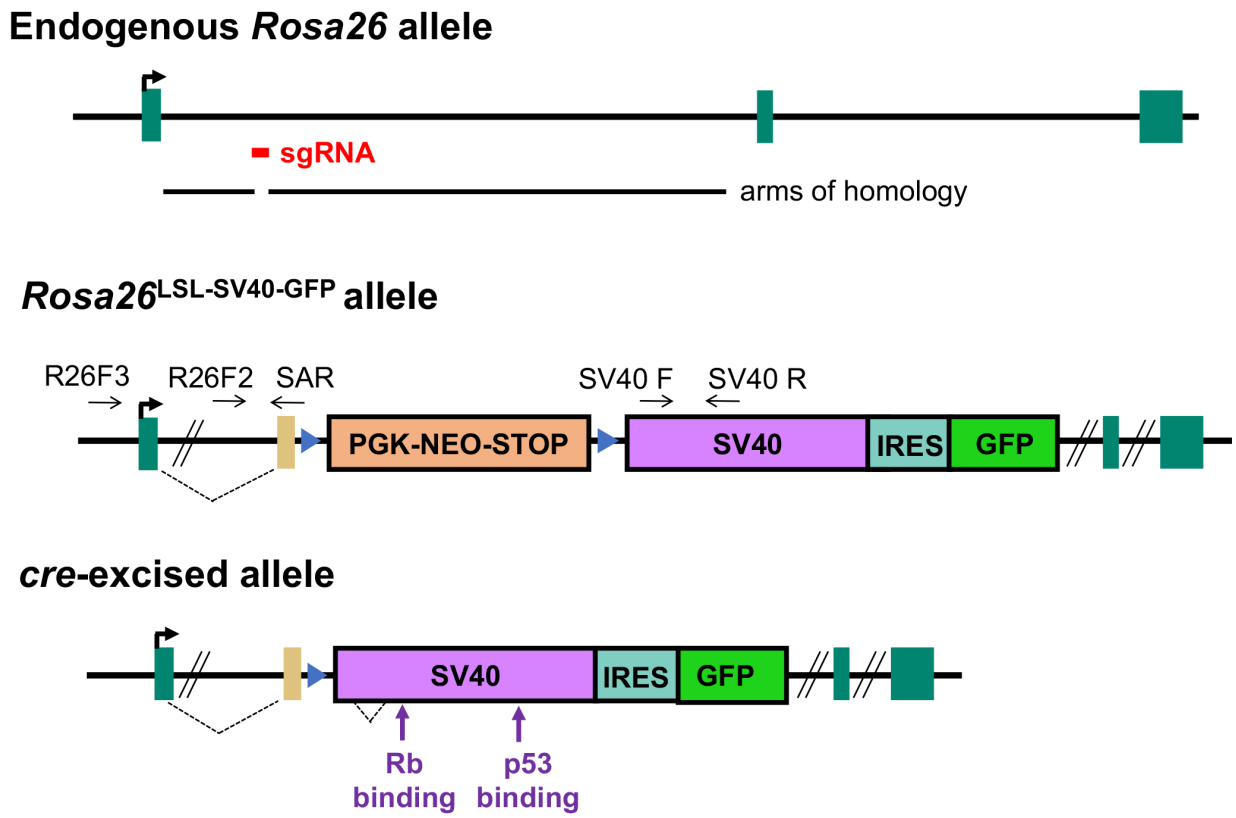

Figure 11: Development of *Rosa26*$^{LSL\text{-}SV40\text{-}GFP}$ mice.

The endogenous *Rosa26* allele is shown with the arms of homology in the targeting vector and the location targeted by the small guide RNA (sgRNA). *Rosa26*$^{LSL\text{-}SV40\text{-}GFP}$ knock-in allele contains the *Pgk-neo* stop sequence flanked by loxP sites and the downstream SV40 coding region, internal ribosome entry site (IRES), and GFP coding region. Primers used to verify that the allele was properly integrated were R26F3 and SAR, as well as R26F2 and SAR. Genotyping was conducted with the primers SV40F with SV40R. After cre-mediated excision of the stop sequence, SV40 and GFP will be expressed from the *Rosa26* regulatory sequences. Dotted lines indicate splice donors and acceptors for *Rosa26* and the gene trap splice acceptor region (SAR) and for the SV40 small T antigen.

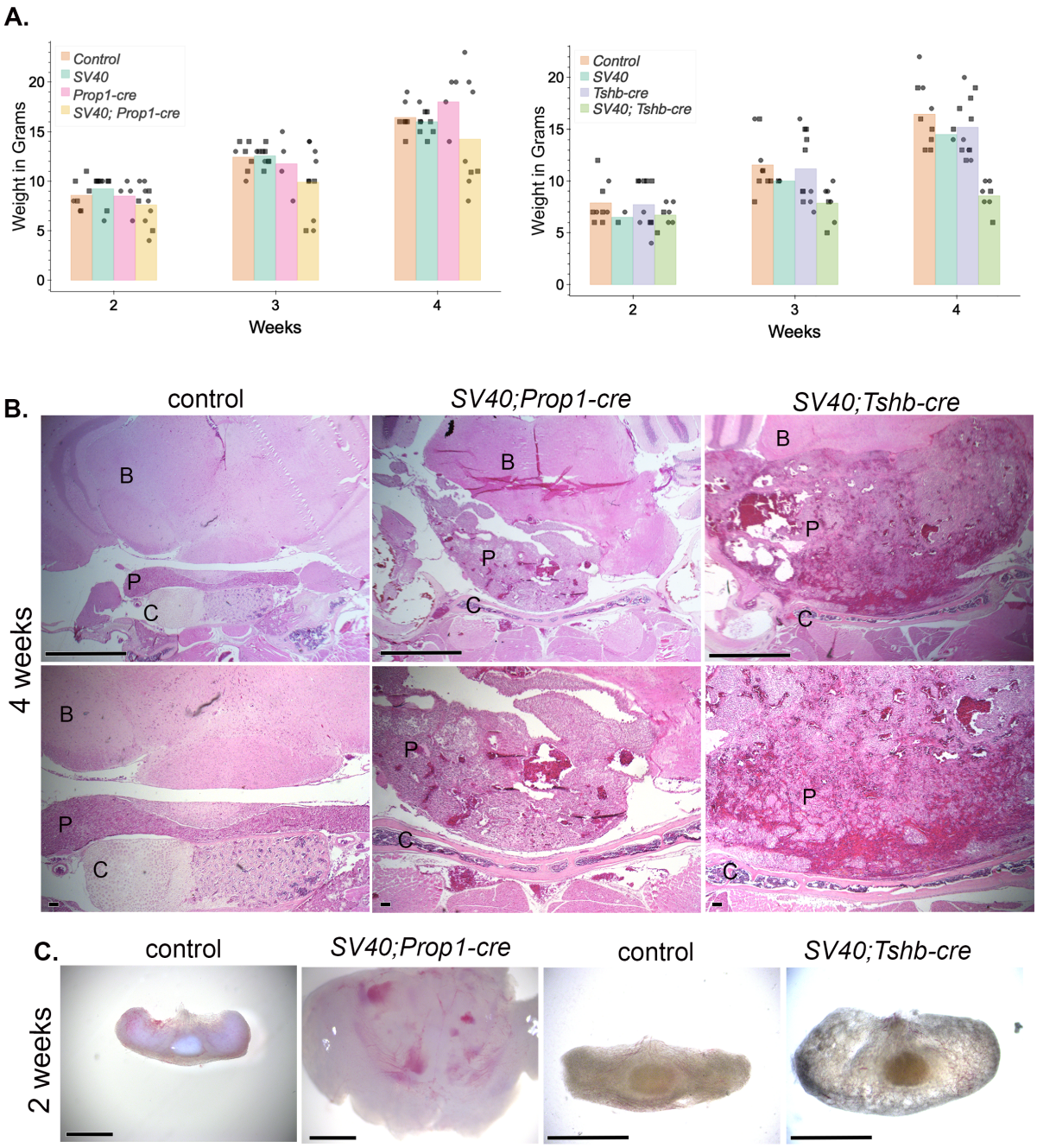

Figure 12: Induction of SV40 TAg expression with *Prop1-cre* and *Tshb-cre* causes dwarfism and large pituitary tumors by four weeks.

(A) Weights of *SV40; Prop1-cre* and *SV40; Tshb-cre* mice and littermates at 2, 3, and 4 weeks. Males and females are indicated with the circle and square symbols, respectively. (B) H&E staining revealed abnormal pituitary histology of 4 wk old *SV40; Prop1-cre* and *SV40; Tshb-cre* mice (N=3/genotype). Top panel magnification is 50X and scale bar is 1000μm. Bottom panel magnification is 100X and scale bar is 100μm. (C) Brightfield images of whole pituitaries from two wk old *SV40; Prop1-cre* and *SV40; Tshb-cre* mice (N=3). *SV40; Prop1-cre* and control pituitary magnification is 32X with 1000μm and *SV40; Tshb-cre* and control pituitary magnification is 50X with a 1000μm scale bar.

weight differences among the genotypes at two weeks, but both male and female *SV40*; *Prop1*-cre mice had immature faces with midfacial hypoplasia, typical of hypopituitarism, and head enlargement not observed with other genotypes. By four weeks most of the *SV40*; *Prop1*-cre mice exhibited dwarfism and all of the *SV40*; *Tshb*-cre did. The dwarf mice were ~30% smaller than their littermates (**Fig. 12A**). Most of the *SV40; Prop1-cre* and *SV40; Tshb-cre* mice had enlarged heads at 4 weeks (data not shown). Males and females were equally affected.

Mice expressing SV40 T antigen in the pituitary gland have large tumors at 4 wks

Mice of both the *SV40; Prop1-cre* and *SV40; Tshb-cre* genotypes had large pituitary masses with abnormal blood accumulation and vascularization at four weeks of age (**Fig. 12B**). At two weeks the pituitaries of *SV40; Prop1-cre* mice were large (n=3) (**Fig. 12C**). The *SV40; Tshb-cre* mice had consistently larger and more vascular pituitaries than their littermate controls at two weeks (N=3). There was some variability in the degree of enlargement and vascularization of *SV40; Tshb-cre* pituitaries at this age, but they were all significantly enlarged relative to littermate controls. No sex differences were noted.

***SV40; Prop1-cre* mice have altered cell specification**

To determine the onset of hyperplasia, we examined *SV40; Prop1-cre* mice at birth. Newborn *SV40; Prop1-cre* mice had hyperplastic pituitaries (**Fig. 13**). Both the intermediate and anterior lobes were enlarged and stained broadly for SV40 T antigen. No SV40 staining was detectable in control littermates. In control pituitaries, immunostaining for the proliferation marker, Ki67, was enriched in the cells in the marginal zone and in cells scattered throughout the anterior lobe. In contrast, nearly every cell in the *SV40; Prop1-cre* pituitaries was positive for Ki67, consistent with the enlarged pituitaries. PECAM immunostaining did not reveal significant changes in vascularization between the controls and the *SV40; Prop1-cre* mutants at this timepoint. PROP1 immunostaining is detectable in the cytoplasm of cells scattered throughout the parenchyma of the anterior lobe of control newborn mice, but very little to no

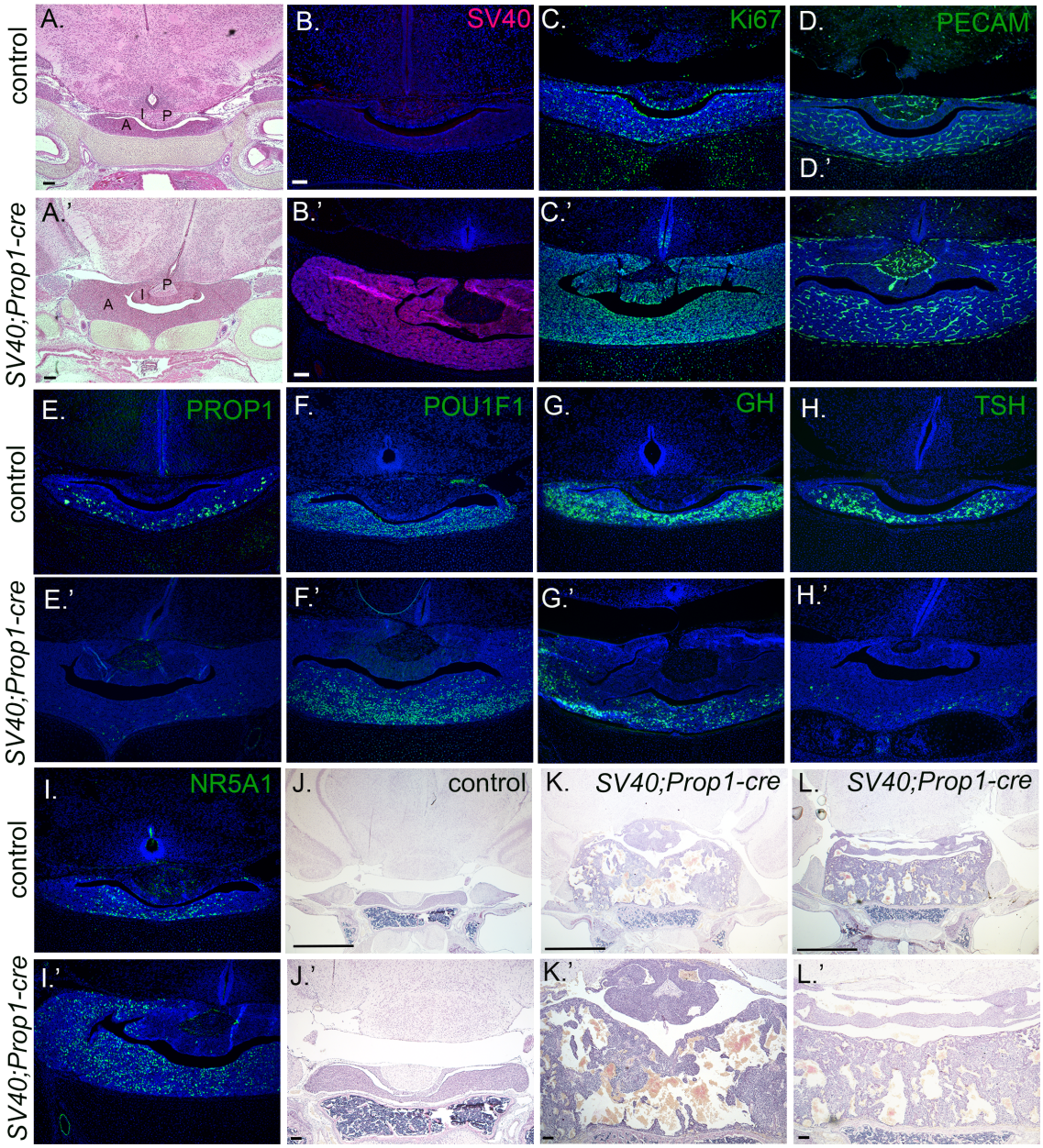

Figure 13: *SV40, Prop1-cre* mice exhibit pituitary hyperplasia and altered cell specification at birth.

Coronal sections of P1 pituitaries from normal littermates (A-I) and *SV40; Prop1*-cre mice (A'-I') were stained with H&E and various antibodies (N=3/genoytype). (A, A') H&E staining at 50X magnification with a 100 μm scale bar. Immunostaining for SV40 (B, B'), Ki67 (C, C'), PROP1 (D, D'), POU1F1 (E, E'), GH (F, F'), TSH (G, G') and NR5A1 (SF1) (I, I'). DAPI staining (blue) of cell nuclei. B-I' Magnification is 100X with 100μm scale bar. Coronal sections of P10 pituitaries from normal littermates (J, J') and *SV40; Prop1-cre* (K, K', L, L') stained with H&E, (N=3/genotype) magnification is 50X with 100μm scale bars (J-L) and magnification is 25X with 1000μm scale bars (J'-L').

PROP1 immunostaining was visible in the *SV40; Prop1-cre* mice. POU1F1 immunostaining was similar in control and *SV40; Prop1-cre* mice. GH immunostaining was significantly reduced in the *SV40; Prop1-cre* mice relative to controls, and TSH immunostaining was nearly undetectable. Normally, NR5A1 staining is enriched in the midline and ventral aspect of the pituitary gland, but NR5A1 immunostaining was markedly increased and laterally expanded in the *SV40; Prop1-cre* anterior pituitary gland. Thus, hyperplasia occurred before birth and affected cell specification in the developing pituitary. Hematoxylin and eosin staining revealed that the hyperplasia of the anterior and intermediate lobes became even more severe by P10.

Onset of hyperplasia in *SV40; Tshb-cre* mice

We examined the pituitaries of *SV40; Tshb-cre* mice and their littermates at birth and P10 (**Fig. 14**). The pituitaries of *SV40; Tshb-cre* mice appeared normal at birth. The size of the organ and histology observed by hematoxylin and eosin staining were indistinguishable. SV40 immunostaining was present in the ventral parenchyma, as expected, because this is where most thyrotropes are found. Immunostaining for POU1F1, GH, TSH, and NR5A1 was indistinguishable between genotypes. At P10 *SV40; Tshb-cre* mice had consistently larger pituitaries with varying abnormalities associated with oncogenesis, including evidence for increased vascularization and large, acellular spaces. Thus, hyperplasia and oncogenesis occurred between P1 and P10.

FACS sorting of genetically marked cells

The IRES-GFP expression cassette in the *Rosa26*$^{LSL\text{-}SV40\text{-}GFP/+}$ line makes it feasible to flow sort cells derived from *cre*-mediated excision of the stop sequence. Wild type mice contain very few auto-fluorescent pituitary cells (**Fig. 15A**). Mice with genetically labeled thyrotropes were generated by crossing *Tshb-cre* mice with the *cre*-reporter strain,

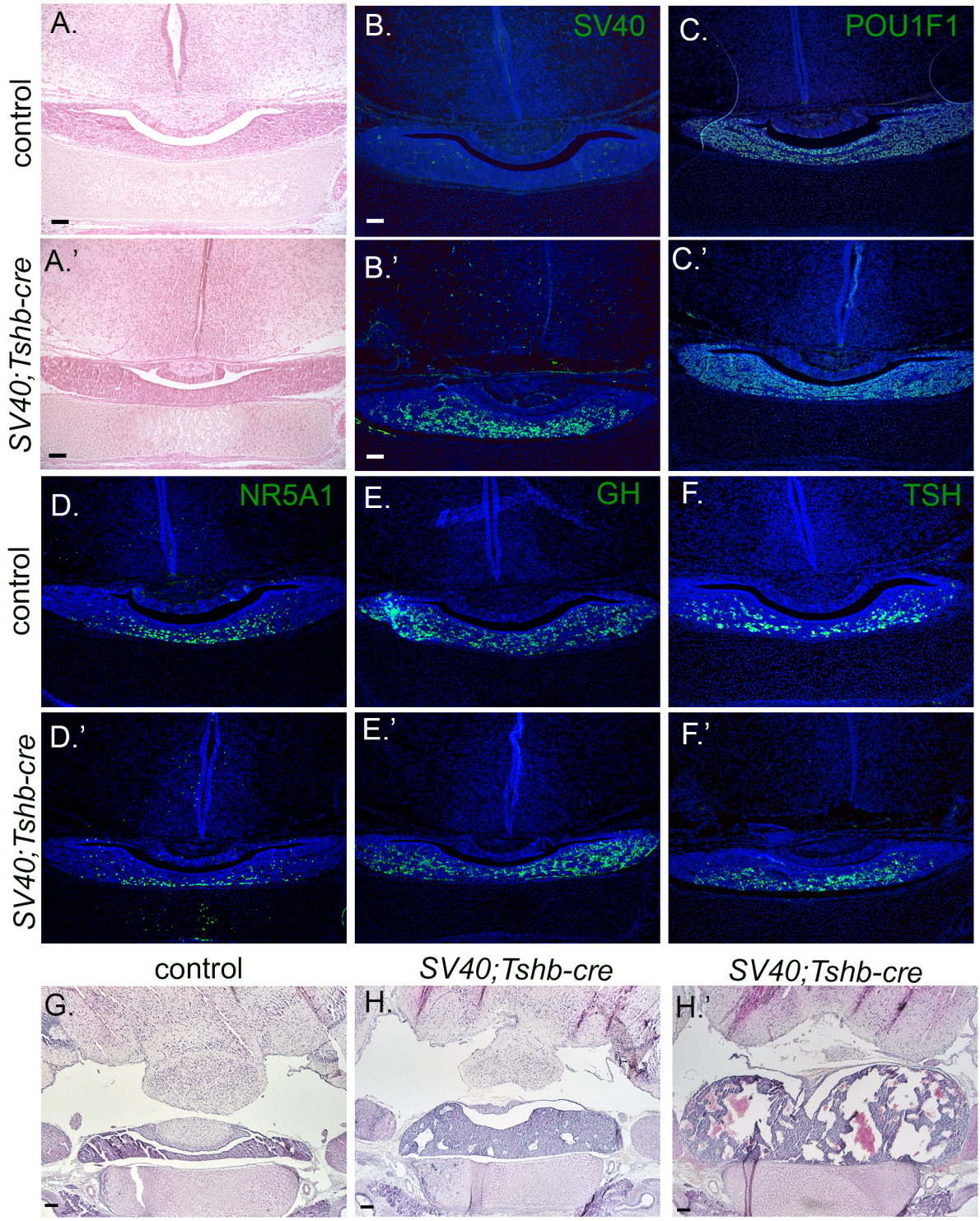

Figure 14: *Tshb-cre* mice have normal pituitary morphology and cell specification at birth and develop tumors by P10.

Coronal sections of P1 pituitaries from normal littermates (A-F) and *SV40; Tshb*-cre mice (A'-F') were stained with H&E and various antibodies (N=3/genoytype). The magnification is 100X with 100μm scale bar. H&E staining (A, A') and immunostaining for SV40 (B, B'), POU1F1 (C, C'), NR5A1 (SF1) (D, D'), GH, (E, E'), and TSH (F, F'). DAPI staining (blue) of cell nuclei B-F'. Coronal sections of P10 pituitaries from normal littermates (G) and *SV40; Tshb-cre* (H, H') stained with H&E, (N=3/genotype) magnification is 50X with 100μm scale bars.

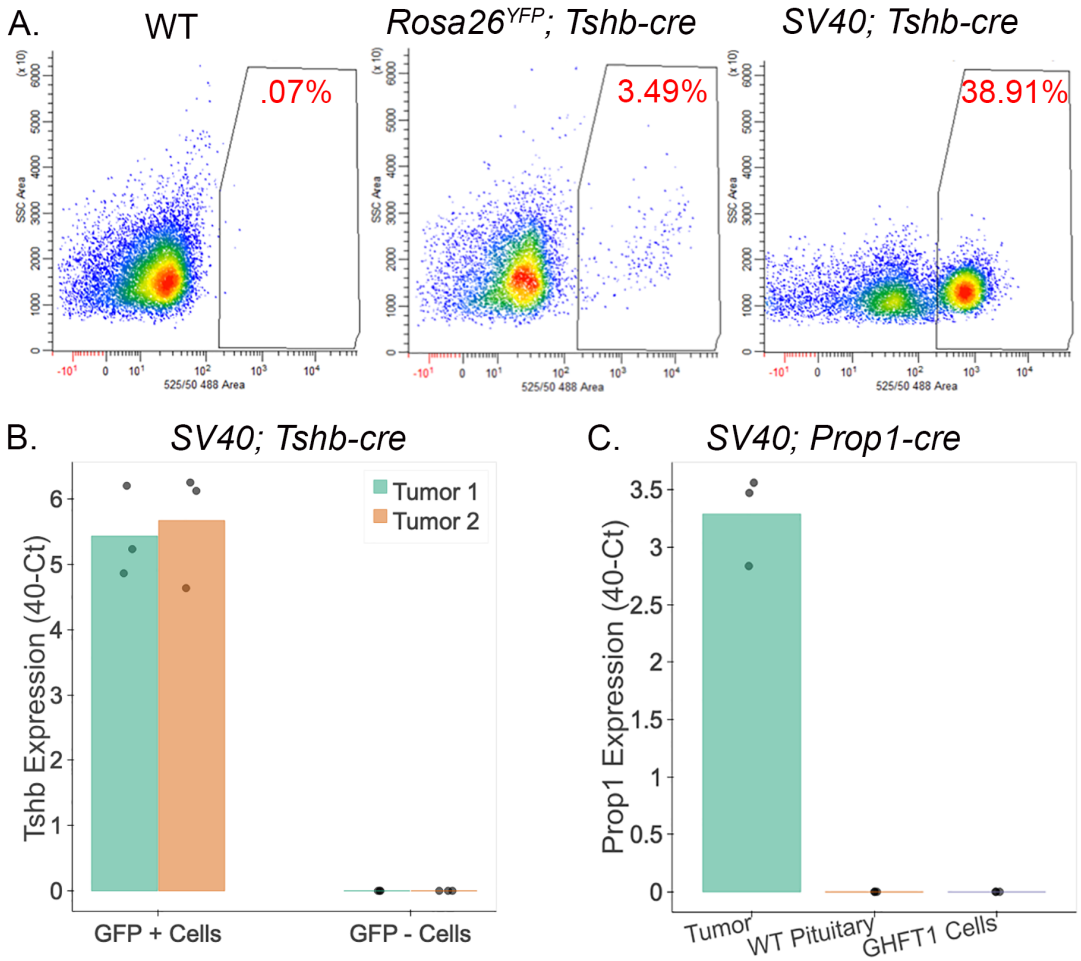

Figure 15: GFP labelled cells from *SV40; Tshb-cre* and *SV40, Prop1-cre* mice have elevated *Tshb* and *Prop1* expression, respectively.

(A) Representative fluorescent-activated cell-sorting of a two-week old wild type mouse, a two-week old *Gt(ROSA)26Sor*$^{tm1(EYFPCos)}$*; Tshb-cre* mouse (*Rosa*^{YFP}*; Tshb-cre)*, and a two-week old *SV40; Tshb*-cre mouse. (B) RNA from GFP-positive and GFP-negative cells sorted from two-week old *SV40; Tshb-cre* animals (N=2) was analyzed for expression of *Tshb* using qRT-PCR, using GAPDH as an internal control. Average GAPDH C_T values were 31 and 35 for GFP-positive and GFP-negative cells, respectively. (C) RNA prepared from cells dispersed from two-week old *SV40; Prop1-cre* mice, two-week old control mice, and GHF-T1 cells was analyzed for expression of *Prop1* by qRT-PCR.

Gt(ROSA)26Sor$^{tm1(EYFP)Cos}$ (*Rosa26*^{YFP}). Pituitaries of two-week old mice of both *Rosa26*^{YFP}*; Tshb-cre* and SV40*; Tshb-cre* mice were dispersed and subjected to FACS to serve as a control for the normal number of genetically labeled thyrotropes. Approximately 3.5% of the *Rosa26*^{YFP}*; Tshb-cre* cells had high levels of fluorescence, similar to the expected value of ~5% [270]. The *SV40; Tshb-cre* pituitaries had a significantly higher number of fluorescent cells, ~ 40%. Two different tumors of *SV40; Tshb-cre* mice were collected at two-weeks of age and subjected to FACS. The GFP-positive and negative cell fractions were analyzed for expression of *Tshb* using qRT-PCR. The GFP-positive cells from each tumor had detectable *Tshb* expression (average C_T value of 34.5), and no *Tshb* expression was detected in the negative fraction (**Fig. 15B**).

Nearly all of the cells from a two-week old *SV40; Prop1-cre* pituitary had strong green fluorescence (data not shown), consistent with the expectation that all hormone-producing cells in the pituitary gland are derived from *Prop1*-expressing cells [131]. *Prop1* expression was detectable in the cells from *SV40; Prop1-cre* pituitaries (average C_T value of 36.7), but not in 2-week-old wild type pituitaries (**Fig. 15C**).

Developing Immortalized Cell Lines

Single pituitary tumors were dissected from a four-week-old *SV40; Prop1-cre* and a *SV40; Tshb-cre* mouse and dispersed separately into single cells in cell culture media (**Fig. 16A**). These heterogeneous cell populations were panned separately for two weeks to reduce fibroblast contamination. After two weeks, the cells from each tumor were collected and plated onto Matrigel. Once the cells reached 50% confluence, the cells were collected and cloned via limited dilution into a 96-well plate. The cells were left for two weeks in the plate, and transferred to 24-well, and 6-well plates respectively as the cells grew confluent. Several clonal cell lines were derived from a tumor from a *SV40; Prop1-cre* mouse and a tumor from a *SV40; Tshb-cre* mouse.

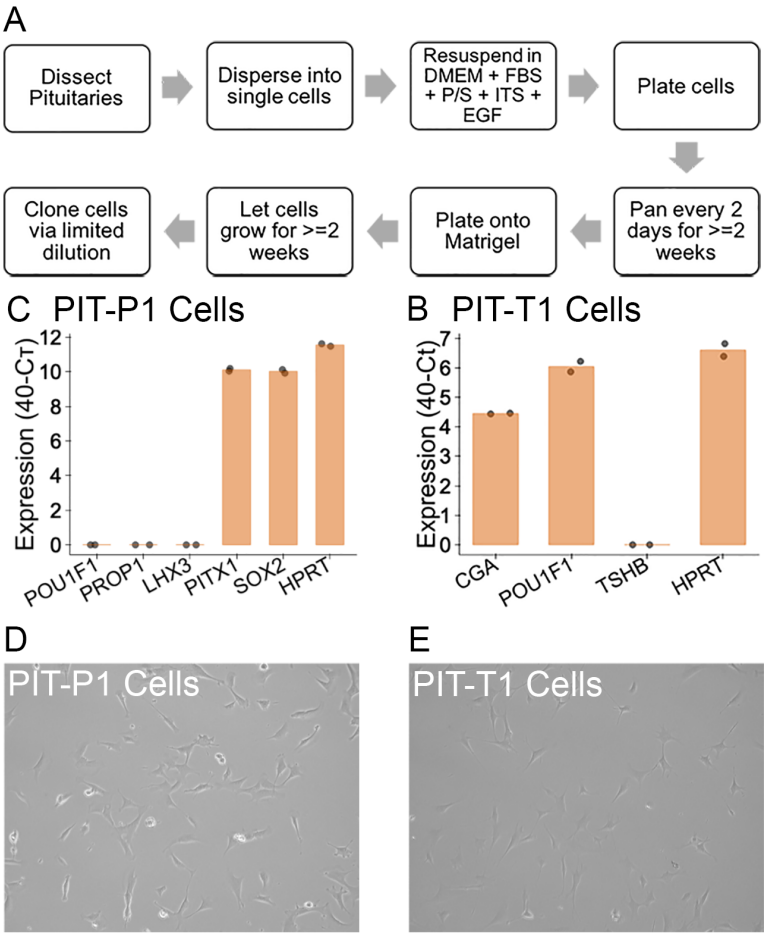

Figure 16: Characterization of immortalized cell lines by gene expression profiling.

(A) Protocol for generating clonal cell lines from SV40-induced tumors. (B) The level of expression of *Cga*, *Pou1f1*, *Tshb*, and *Hprt* was measured by qRT-PCR in RNA prepared from the in the PIT-T1 cell line after freezing, thawing, and passaging five times. (C) The level of expression of *Pou1f1, Prop1, Lhx3, Pitx1, Sox2*, and *Hprt* was measured by qRT-PCR in RNA prepared from the PIT-P1 cell line cell line after freezing, thawing, and passaging five times. (D) Brightfield image of the PIT-P1 cell line. (E) Brightfield image of the PIT-P1 cell line.

We tested the cell lines for expression of several key genes using qRT-PCR, using *Hprt* as an expression control. The precursor cell line (PIT-P1) expressed detectable levels of *Pitx1* and *Sox2* (average C_T values of 29.9, and 30.0, respectively). No expression of *Pou1f1, Prop1,* or *Lhx3* was detected (**Fig. 16B**). The thyrotrope-like cell line (PIT-T1) had detectable expression of *Cga* and *Pou1f1* (average C_T values of 35.5, and 34.0, respectively), but no expression of *Tshb* was detected (**Fig. 16C**). The morphology of these two cell types is subtly different, with the PIT-P1 line having less pronounced projections (**Fig. 16D**) in comparison to the PIT-T1 line (**Fig. 16E**).

Discussion

We have developed a mouse line that conditionally expresses the powerful SV40 T antigen oncogene from the *Rosa26* safe harbor locus. We demonstrate the power of this novel mouse line by mating it to two distinct pituitary-specific cre strains. Both *Tshb-cre* and *Prop1-cre* induced reproducible, high-penetrance, cell-type specific induction of SV40 T antigen expression and tumor formation. We successfully adapted tumors from each of these crosses to cell culture, and they retained expression of some markers specific to thyrotrope cells and pituitary progenitors. This demonstrates the utility of this new line as a tool for immortalizing stable cell lines that represent discrete stages of development.

We observed high penetrance and rapid onset of pituitary hyperplasia and tumors in the *SV40; Prop1-cre* and *SV40; Tshb-cre* mice. Pituitary hyperplasia was evident in newborn *SV40; Prop1-cre* mice, and variable degrees of oncogenesis were evident at P10. The majority of *SV40; Prop1-cre* mice had obvious pituitary tumors by four weeks of age (N=5/8). The onset of hyperplasia was slightly later in *SV40; Tshb-cre* mice. Pituitaries appeared normal at birth,

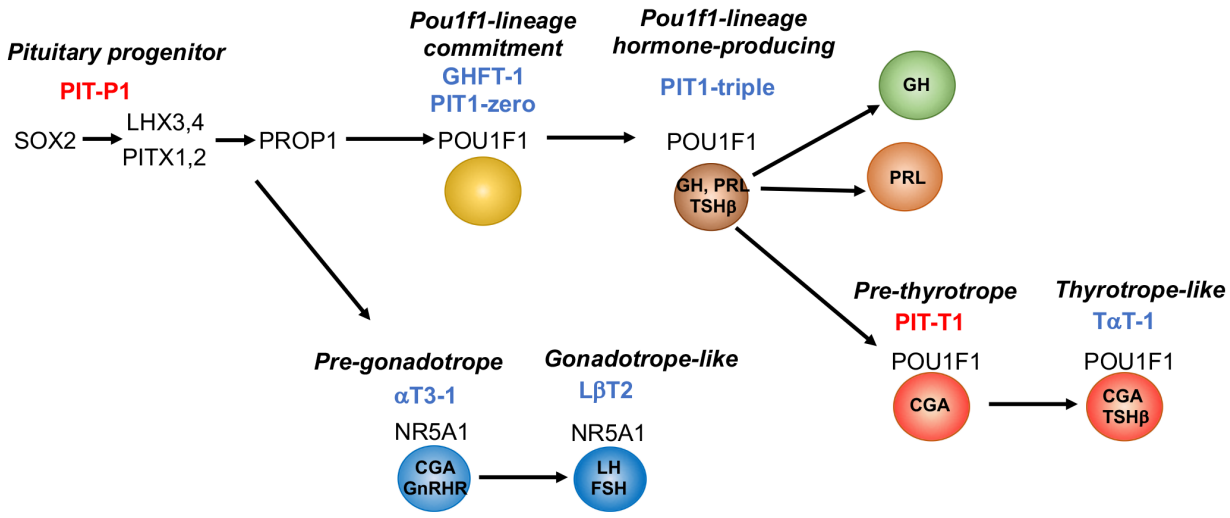

Figure 17: PIT-P1 and PIT-T1 cells represent two new niches within the pituitary differentiation cascade.

Representation of transcription factors regulating pituitary growth and differentiation and the stages represented by commonly used immortalized cell lines. The PIT-P1 cell line represents a *Sox2*- and *Pitx1*-expressing pituitary precursor, whereas PIT-T1 cells represents a pre-thyrotrope expressing *Pou1f1* and *Cga*.

hyperplasia was obvious at 2 weeks, and extensive oncogenesis was obvious in all of the mice at 4 weeks. Founder mice containing fusions of the regulatory elements of *Pou1f1, Cga*, *Lhb*, or *Gh* and the coding region of SV40 were infertile or died before they could be bred [283, 284, 288]. The surviving founders developed tumors at between 4 wk - 5 mo, and the penetrance varied from ~ 6-20%. The binary transgene system we developed circumvents the problems of infertility and sudden death, and it makes it possible to study the path from hyperplasia to oncogenesis in progeny of the same strain. We hypothesize that the high penetrance and rapid latency of oncogenesis we observed in the binary system is the result of two factors: small amounts of cre recombinase are sufficient for elimination of the floxed stop sequence, and the *Rosa26* locus drives consistent and sufficient expression of SV40 to drive hyperplasia and oncogenesis. This contrasts with random integration of SV40 transgenes into the genome, which is subject to position effects that commonly diminish expression.

An added benefit of having inserted the SV40 T antigen into the *Rosa26* locus is the ability to dissect the effects of SV40 expression under different induction conditions. The *SV40; Prop1-cre* mice consistently had earlier hyperplasia and oncogenesis than the *SV40; Tshb-cre* mice. The *Prop1-cre* allele induces cre-mediated expression by e12.5 in undifferentiated progenitor cells, while *Tshb-cre* does not become active until e14.5 in cells that have stopped proliferating and have committed to the thyrotrope lineage [131, 308]. The earlier onset of hyperplasia in *Prop1-cre* mice may be attributable to the activation of oncogene expression prior to cell cycle exit.

SV40 expression prevents cells from leaving the cell cycle. This was made clear by the continued, broad expression of Ki67 in the *SV40; Prop1-cre* mice, and the hypertrophy in the pituitaries of both of the mouse lines. While it is generally believed that cells must exit the cell cycle to differentiate, *SV40; Prop1-cre* mouse pituitaries have significant expression of lineage-specific transcription factors (including POU1F1 and NR5A1) and hormones. This phenotype of persistent proliferation and differentiation is reminiscent of p27 and p57 double knockout mice.

Embryonic pituitaries from p27, p57 knockout mice reveal cycling cells positive for both POMC and TBX19 (TPIT), suggesting that cell cycle exit is not absolutely critical for differentiation [232].

The *SV40; Prop1-cre* mice exhibited evidence of altered cell specification. GH expression was reduced, TSH was lost, and NR5A1 expression was expanded. There is evidence that GATA2 drives both gonadotrope and thyrotrope fate and that competition between POU1F1 and NR5A1 strikes the balance between the two fates. Although the expression of *Pou1f1* was not obviously reduced in newborn mice, we hypothesize that *Pou1f1* expression is reduced or delayed in *SV40; Prop1-cre* mice during gestation, leading to reduced differentiation into GH and TSH-expressing cells, and increased differentiation to the gonadotrope fate.

Existing immortalized pituitary cell lines represent distinct timepoints in development [283]. We were successful in developing stable, clonal cell lines from *SV40; Prop1-cre* mice and *SV40; Tshb-cre* mice that represent pituitary precursors (PIT-P1 cells), and pre-thyrotropes (PIT-T1 cells) respectively. The PIT-P1 cells we report here are the first immortalized, SOX2-positive pituitary precursor cell line. The expression of PITX1 indicates commitment to the pituitary fate, and these cells will be useful for understanding the first steps in that process. The PIT-T1 cells are a pre-thyrotrope-like cell line which is characterized by the expression of POU1F1, and CGA. Although *Tshb* expression was not detected, reduction in SV40 expression might permit these progenitors to differentiate [361]. Nevertheless, they provide an excellent companion cell line for comparison with the more differentiated TαT1 cells, just as comparison of αT3-1 and LβT-2 cells have revealed important genetic changes as gonadotrope differentiation progresses. It is possible that the binary system we developed could give rise to additional cell lines that represent different times in development if tumors were adapted to culture from younger mice. In support of this idea, the Mellon and Liebhaber groups have

generated multiple cell lines with different features from the tumors of different transgene founders carrying the same transgene [283, 288].

These mice represent a significant advance for two reasons: 1) they are a powerful tool for the rapid immortalization of cell lines, and 2) they allow for careful dissection of the effect of SV40 T antigen-mediated immortalization on proper differentiation and organ function during the process of oncogenesis. The binary system is universally applicable because *Rosa26*$^{LSL\text{-}SV40\text{-}GFP/+}$ mice can be mated with any cre strain, including drug inducible cre strains. A strain with universal potential was previously developed that expresses a heat-labile copy of SV40 oncogene driven by the H-2K^{b} promoter, and tissues incubated at 33°C in the presence of IFN-γ are immortalized at high frequency [362]. A binary system with heat-labile SV40 oncogene is an intriguing future direction. Similarly, it is valuable to have a universal system in which the oncogene can be extinguished after immortalization has taken place. Such a system was developed in which flp recombinase can extinguish SV40 T antigen expression [363]. In the meantime, these mice will help to characterize rare cell types being discovered at increasing frequency with single-cell technology. Our ability to generate immortalized cell lines is now only limited by the availability of cre alleles.

Methods

Donor Plasmid Construction

The donor plasmid was constructed using pR26 GFP Dest (gift from Ralf Kuehn, Addgene plasmid # 74283), and SV40 small and Large T in pENTR1A (w611-7, gift from Eric Campeau, Addgene plasmid # 22297). The pR26 GFP Dest plasmid was recombined with the SV40 small and Large T plasmid with a Gateway LR clonase II reaction (ThermoFisher, 11791100). The resulting plasmid was amplified and purified with the Qiagen Maxi Prep

Plasmid (Qiagen, 12163) kit. Endotoxins were removed from the plasmid using the Endotoxin removal Solution (Sigma, E4274-25ML).

Mice and genotyping

All mice were housed in a 12-h light, -12 h dark cycle in ventilated cates with unlimited access to tap water and Purina 5020 chow. All procedures were conducted in accordance with the principles and procedures outlined in the National Institutes of Health Guidelines on the Care and Use of Experimental Animals and approved by our Institutional Animal Care and Use Committee.

The *Rosa26*$^{LSL\text{-}SV40\text{-}GFP/+}$ allele was generated by microinjecting enhanced specificity Cas9 protein (50 ng/ul from Sigma), circular DNA donor plasmid (20 ng/ul, adapted from Addgene), chemically modified sgRosa26-1 (30 ng/ul from Synthego.com) into fertilized eggs obtained by mating (C57BL/6 X SJL)F1 or C57BL/6 female mice with (C57BL/6 X SJL)F1 male mice purchased from the Jackson Laboratory [360]. Pronuclear microinjection was performed as described [364].

Founders were confirmed to have the correct insertion by three separate PCR reactions. The first set was between the first *Rosa26* intron and the splice acceptor of the knock-In allele (forward 5'-GCCTCCTGGCTTCTGAGGACCG-3' and reverse 5'-CCTGGACTACTGCGCCCTACAGA-3'). The second set of primers was designed to detect the presence of the presence of SV40 T antigen (forward 5'-AAAGTGGCATTGCTTTGCTT-3' and reverse 5'-AAATGAGCCTTGGGACTGTG-3'). The third set of primers were designed to distinguish correct insertion into the *Rosa26* locus from random insertion of the donor plasmid. The forward primer was specific for a segment of *Rosa26* genomic DNA not included in the donor plasmid and the reverse primer was specific to the donor plasmid: (Forward 5'-CTGCCCGAGCGGAAACGCCACTGAC-3' and reverse 5'-CCTGGACTACTGCGCCCTACAGA-3'). 16 out of 79 potential founders were positive for all three PCRs. Subsequent genotyping of

mice for the *Rosa26*$^{LSL\text{-}SV40\text{-}GFP/+}$ allele was done using the T antigen specific primer pair described above.

Tg(Prop1-cre)^{432Sac}, referred to here as *Prop1-cre,* were generated at University of Michigan [131]. They were genotyped with the following primers: forward 5'-GGTCTCCCTCCGTTTTTCTC-3' and reverse 5'-CTGCACACAGACAGGAGCAT-3'.

Tg(Tshb-cre)^{Sac}, referred to here as *Tshb-cre,* were generated at University of Michigan [308]. They were genotyped with these primers: forward 5'-GGACATGTTCAGGGATCGCCAGGCG-3' and reverse 5'-GCATAACCAGTGAAACAGCATTGCTG-3'.

Gt(ROSA)26Sor$^{tm1(EYFP)Cos}$, referred to here as *Rosa26*^{YFP}, were generated at Columbia University, and were purchased from Jackson Laboratories, stock number 006148, and were genotyped according to Jackson laboratory recommended primers and conditions [336].

The day of birth was designated postnatal day 1 (P1).

Histology and Immunohistochemistry

Heads from mice younger than two weeks of age were fixed in PFA (5ml formaldehyde in 35ml of PBS) overnight, followed by three washes in PBS. They were put in 10% EDTA for three days, then dehydrated for a minimum of 4 hrs in each step of a gradient of ethanol solutions: 25%, 50%, and 75%. Pituitaries from mice two weeks or older were fixed overnight in PFA, followed by three PBS washes. They were put in 10% EDTA for 3 hours, then dehydrated for a minimum of 1 hr in each step of ethanol solutions described above. Pituitaries and heads were embedded in paraffin with four-hour cycles in a Tissue Tek VIP paraffin tissue processing machine. Sections at 6 um thickness from each at least three different controls and experimental mice and analyzed by hematoxylin and eosin (H&E) and immunohistochemical markers as previously described[337]. Immunostaining for pituitary hormone markers was performed using anti-TSH and anti-GH (1:1000, National Hormone and Peptide Program, UCLA Medical Center, Torrance, CA, USA). Immunostaining for proteins was performed using rabbit

anti-POU1F1 (kindly provided by Dr. Simon Rhodes, University of North Florida, Jacksonville) rabbit anti- Ki67 (1:250, Novocastra, Newcastle, United Kingdom), rabbit anti-NR5A1 (1:100, kindly provided by Dr. Gary Hammer, University of Michigan), guinea pig anti- PROP1 (1:100, kindly provided by Aimee Ryan, Montreal, Quebec), mouse-anti-SV40 (1:1000, kindly provided by Michael J. Imperiale, University of Michigan), and rabbit anti-PECAM (1:100, Thermo Scientific). The following secondary antibodies were used: biotinylated anti-rabbit IgG (1:100, Jackson Immunoresearch) for anti-POU1F1, anti-PECAM, anti-Ki67, anti-NR5A1; anti-human biotin (1:200, ab97223, Abcam) for anti-GH, and biotinylated anti-guinea pig IgG (Jackson Immumoreaserach) for anti-TSH and anti-PROP1. For anti-SV40 the M.O.M.® (Mouse on Mouse) Immunodetection Kit, Basic (Vecetor Laboratories, Burlingame, CBMK-2202) was used.

Antibodies were detected using either the tyramide signal amplification (TSA) (33002 CFF488A Streptavidin HRP, Biotium, Fremont, CA), streptavidin-conjugated Alexa-fluor 488 (1:200, S11223, Invitrogen), streptavidin-conjugated Cy3 (Thermo Fisher 434315). Cell nuclei were stained with DAPI (1:200) for 5 min. Slides were mounted with permount mounting medium containing DABCO. Images were captured with a Leica DMRB fluorescent microscope and a Leica MZ10F dissecting scope.

Cell dispersion and FACS

Pituitaries were removed from mice two weeks or older and placed in PBS. They were transferred to an enzyme mix consisting of collagenase, DNAse, Fungizone, and trypsin in HBSS. The pituitaries were incubated at 37°C for two hours, followed by trituration with a siliconized P1000 tip. The pituitaries were incubated at 37°C for two additional hours, followed by trituration with a siliconized P200 tip. The dispersed cells were collected by a 5 minute, 600 RCF centrifugation, and resuspended in 500µL of PBS and 2µL DAPI. The cells were sorted on a Synergy cell sorter with a 488nm laser. Samples were either taken immediately for RNA or placed in 200uL RNA Later (Invitrogen AM 7020).

RNA Extraction, cDNA Conversion and qPCR

RNA was extracted from flow-sorted cells using the RNAqueous Micro Kit (Invitrogen AM1931), and cDNA was made from the RNA using SuperScript First Strand (Invitrogen, 11904-018). Levels of *Prop1* and *Tshb* transcripts were quantified using the TaqMan Universal PCR Master Mix (Applied Biosystems 4304437), and TaqMan probes Mm00839471_m1 and Mm03990915_g1 for *Prop1* and *Tshb,* respectively (ThermoFisher). The qPCR reaction conditions were two initial hold stages of 50°C for 2 minutes and 95°C for 10 minutes followed by 40 cycles of 95°C for 15 seconds and 60°C for 1 minute. Final expression values were calculated by subtracting the threshold expression value (C_T) from 40.

RNA was extracted from cell lines using the Qiagen RNeasy Micro Kit (74004). qPCR was performed as described above for *Cga* (probe Mm00438189_m1), *Pou1f1* (probe Mm00476852_m1), *Tshb* (probe Mm03990915_g1), *Prop1* (probe Mm00839471_m1), *Lhx3*, (probe Mm01333633_m1), *Pitx1* (probe Mm00440824_m1), *Sox2* (probe Mm03053810_s1), *Hprt* (probe Mm03024075_m1), and *Gapdh* (Thermo Fisher 4308313).

Tissue culture

GHF-T1 cells were provided by Pamela Mellon, University of California San Diego [5].

Tumorous pituitaries were dispersed by mincing, and placing in a mix of HBSS (Gibco, 14175-095) with 10mg/ml collagenase (Gibco, 17104-019) at 37°C for 30 minutes. Cells were collected by centrifugation at 600G for 5 minutes, followed by resuspension in cell culture media. All subsequent cell culture was done in DMEM (Gibco, 11995-065) with 10% Fetal Bovine Serum (Corning 35016CV), 1% Penicillin Streptomycin (Sigma-Aldrich P4333), 10μg/mL hEGF (Gibco, PHG0314), and 1X ITS (Corning MT25800CR).

Panning was done by collecting the media (without trypsin) every two days, collecting the cells by centrifugation, resuspending in fresh media, and plating on a new, non-Matrigel-coated plate. After two weeks of panning, the cells were plated on Matrigel until 50-80%

confluence was achieved. A sample of the heterogenous population of cells was collected for RNA analysis. Clonal cell lines were developed via limited dilution.

We passaged clonal cell lines when they achieved ~80% confluence by washing the cells, trypsinization (Invitrogen 25300054) for three minutes at 37°C, collection with media, centrifugation, resuspension, and plating on Matrigel-covered plates at approximately a 1:10 dilution.

Chapter 4: Conclusion

This work represents advances in both our understanding of pituitary organ formation and in tools that will be useful in the field for years to come. While this work answers questions related to the factors and elements that are responsible for proper thyrotrope function, and how the pituitary responds to oncogenic insult, it raises many more questions. Here I will discuss open questions that are the result of this work and possible next steps that will help to answer them.

Pituitary transcriptome and chromatin analysis

In the second chapter I discussed the analysis of the transcriptome and epigenome of two cell lines that represent pituitary precursor cells committed to the POU1F1 lineage and thyrotropes that express POU1F1 and both subunits of TSH, as well as other thyrotrope signature genes. I performed analyses of gene expression and chromatin states using RNA-seq, ATAC-seq, and CUT&RUN for the major lineage-determining transcription factor POU1F1 and three histone marks (H3K27Ac, H3K4Me1, and H3K27Me3). This study revealed transcription factors that are uniquely expressed in progenitors or thyrotropes as well as putative regulatory elements surrounding these genes that may be responsible for their expression.

I identified nearly one-hundred thousand putative active enhancers across the two cell

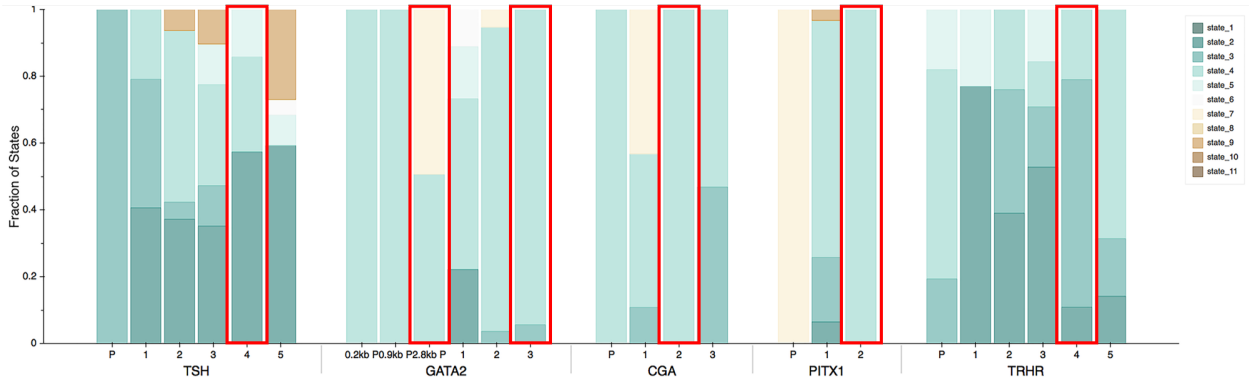

Figure 18: State of each tested element:

The chromatin state for each tested regulatory element discussed in Chapter 2. Elements with activity in TαT1 cells highlighted in red.

types, as defined by the presence of both H3K27Ac and H3K4Me1. We tested twenty of the elements, in context with the gene's promoter proximal region, for activity in TαT1 cells. All twenty elements had predominantly active chromatin marks (they were state seven or lower, Chapter 2, Supplemental Figure 3). Of the twenty elements, seven were predominantly active enhancers (more than 50% of the DNA sequence was state 2 and 3). Only two of the seven predicted enhancer elements had activity in TαT1 cells. Of the twenty elements tested *in vitro*, only seven elements (35%) had activity within TαT1 cells, and the fraction of the element that was labeled as an enhancer in ChromHMM was largely unpredictive of *in vitro* activity (**Fig. 18**). The elements were selected based on ATAC-seq signal, and no ATAC-seq-negative elements were tested. It is therefore possible that seven active elements out of twenty-five represents an enrichment in activity over randomly selected regions in the genome. While likely difficult to perform with the TαT1 cells used here due to their limited transfection efficiency, methods such as STARR-seq, a massively parallel enhancer testing assay, would give greater insight into which chromatin states are predictive of *in vitro* activity in TαT1 cells [365].

Linking the putative enhancers to their respective genes would be highly valuable. Presuming the enhancer is acting upon the nearest gene is often wrong [366-369]. For this reason, circular chromatin confirmation capture (4C) would be valuable to link enhancers to their respective genes, thus helping us find the network of enhancers responsible for proper expression in thyrotropes.

An intriguing avenue of study would be to identify and test other regulatory elements beyond those presented in chapter 2. One such gene to study is ISL1, which is important for developing thyrotropes and gonadotropes. The region surrounding ISL1 is laden with active chromatin marks [281, 282]. Extending the view across the locus reveals many more putative regulatory elements whose activity in the pituitary should be checked (**Fig. 19**). Previous work has uncovered an enhancer 500 kb away from *Isl1* that is derived from an ancient SINE element

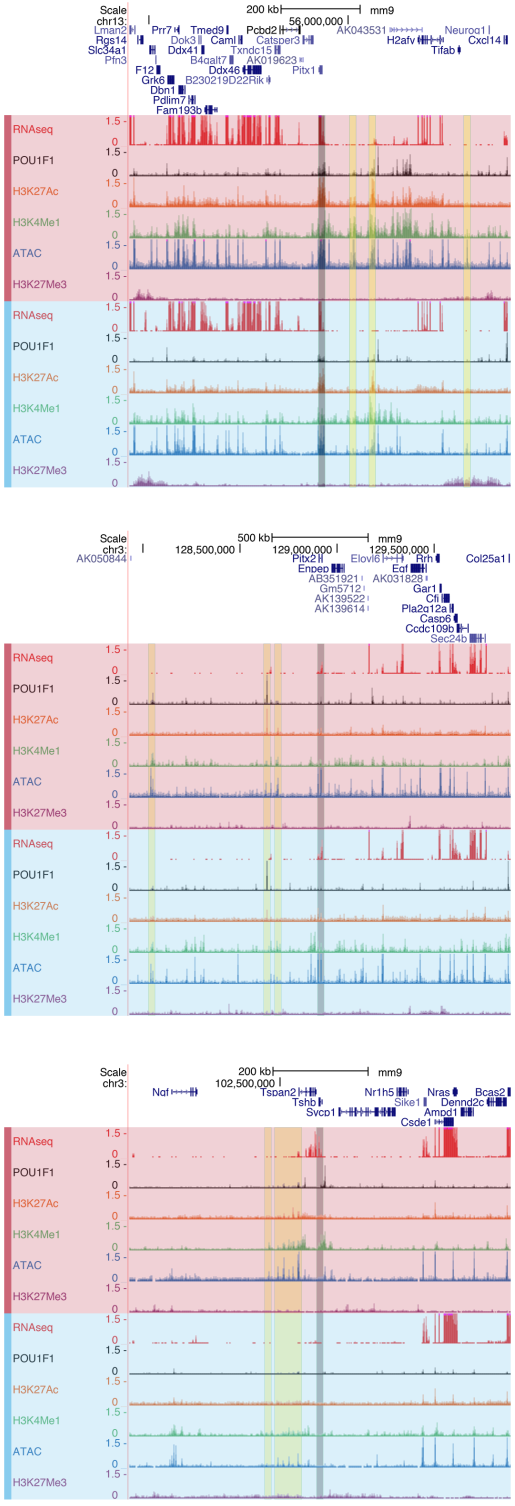

Figure 19: Extended region surrounding key genes:

Extending the view around thyrotrope-signature genes in TαT1 and GHF-T1 cells to show other, more distal regulatory elements that may play a role in regulating these genes. The gene loci are highlighted in black, and the putative regulatory elements are highlighted in yellow.

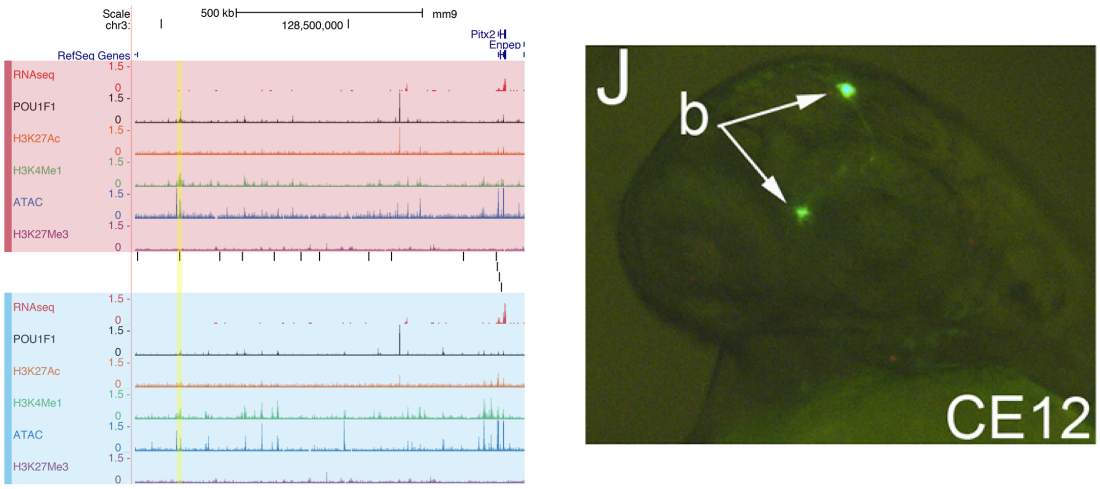

Figure 20: *Pitx2* regulatory element with active chromatin marks in TαT1 and YFP expression in diencephalic neurons:

Yellow bar highlights an ATAC-seq peak found in both TαT1 and GHF-T1 cells that has activity in the diencephalic neurons of zebrafish.

that drove reporter expression in ISL1-positive cell types including the head, spinal cord, the dorsal apical ectodermal ridge, the genital eminence, and in the trigeminal ganglion in mice [370]. No ISL1 element has yet been shown to drive expression in the pituitary. Expanded tracks of other genes such as *Tshb*, *Pitx1*, and *Pitx2* reveal other potential regulatory elements not tested here. The *Pitx1* and *Pitx2* genes are evolutionarily related but not linked in the genome. Both genes neighbor a gene desert filled with putative regulatory elements and POU1F1 binding sites, suggesting regulatory activity. A heroic effort by Elena Semina's lab tested thirteen highly conserved elements within *Pitx2* and the neighboring gene desert [371]. They performed reporter assays in zebrafish, and showed that these elements drove expression in brain, eye, and the craniofacial region. Of the elements tested, only one was in a region marked by active chromatin marks in TαT1 cells (**Fig. 20**). This element (Conserved Element 12) was stated to have activity in the midbrain and diencephalic neurons. This element seems like a strong candidate for further analysis in thyrotropes. An important value of the epigenomic mapping is that it provides a genome-wide catalog of putative regulatory elements for future study.

Some regulatory elements are required for expression *in vivo* but may not readily be identified by transfection. Sometimes this is because the cell line used for analysis does not accurately reflect the differentiation state of the cells that express the gene *in vivo,* i.e. lacks the critical transcription factors that active gene expression via that enhancer element. Likewise, the elements that are sufficient to drive expression in cell lines are often insufficient *in vivo.* We tested a 1.4 kb element ~ 7 kb upstream of *Tshb* in the context of 0.4 kb of the promoter proximal region, for expression in transgenic mice. A construct with Element 4 and promoter proximal sequences was sufficient to drive expression in pituitary thyrotropes in transgenic mice, while previous studies with ~ 6 kb of *Tshb* 5' flanking DNA were not sufficient. Very little expression of the Element 4, *Tshb* promoter construct was detected in TSH-negative cells. The penetrance of transgene expression in TSH immunoreactive cells was not high, however.

There is a large area of open chromatin between the *Tshb* promoter and Element 4. It would be useful to generate transgenic mice with this entire 7 kb region to determine whether this increased the penetrance of expression. All previous studies have focused on this promoter proximal region, demonstrating *in vitro* regulation of *Tshb* by GATA2, POU1F1, PITX1, PITX2, NCOR, NR1D1, and THR [285]. While this promoter proximal region is insufficient to drive expression in thyrotropes *in vivo*, it likely contains transcription factor binding sites that interact with other elements.

GATA2 is an important regulator factor for both thyrotropes and gonadotropes. Very little is known about the regulation of *Gata2* expression in the pituitary gland, other than the fact that it is not dependent on *Isl1*. We tested the sufficiency of the most distal GATA2 regulatory element (Chapter 2, Figure 6, GATA2 Element 3), and the expanded 2.8 kb GATA2 promoter to drive expression in thyrotropes. We developed two constructs, one containing Element 3, in the forward orientation, cloned in front of the 2.8 kb GATA2 promoter and the YFP reporter. The second construct was simply the 2.8 kb GATA2 promoter and the YFP reporter. Both constructs were injected into fertilized eggs to generate transgenic mice. This injection resulted in twenty-five founder mice for each of these constructs. YFP was not detected in any pituitary section of any of the mice we examined. We found this surprising, given the very strong activity of both the promoter proximal element and the distal element in TαT1 cells. However, GATA2 plays a critical role in the development of many organ systems, and transcriptional regulatory elements necessary for expression in other organ systems have been identified that are considerably distant from the gene. Thus, regulation of expression in the pituitary may be complex.

Identifying sets of motifs within regulatory elements may help clarify thyrotrope-specific enhancers, a method successfully used in other tissues [372]. Thus, finding the set of shared motifs across the seven elements we found to have enhancer activity *in vitro* in the thyrotropes may help bring insight into which of the 65,562 enhancers in TαT1 cells we should pursue first.

Including evolutionary conservation and ATAC-seq footprinting will help narrow the list even further [373]. While costlier and more time-intensive, performing CUT&RUN experiments for factors such as GATA2, PITX1, PITX2, NCOR, and NR1D1 would provide higher confidence in the set of enhancers implicated by the suggested motif analyses.

We found that TαT1-specific POU1F1 binding sites that are associated with repressed chromatin in GHF-T1 cells and active chromatin in TαT1 cells have many HTH and bHLH motifs. It is tempting to speculate that POU1F1 interacts with bHLH factors to drive a thyrotrope fate. Consistent with this hypothesis, NEUROD4 and ASCL1 are two of the most highly upregulated genes in TαT1 cells. However, inhibitory bHLH factors are highly expressed in both GHF-T1 and TαT1 cells. It is difficult to bring together the findings that bHLH motifs are heavily enriched at these new POU1F1 binding sites that are associated with open chromatin, TαT1 cells express ASCL1 and NEUROD4 very highly, and that the repressive ID genes are likely to be suppressing bHLH activity in TαT1 cells. It is possible that astrocyte development may give insight into these seemingly paradoxical datasets [325]. ID and HES factors maintain cortical progenitors (consistent with high ID expression seen in the precursor GHF-T1 cells) and are also required for the differentiation of astrocytes. The motif found at these sites does not preclude HES from being the bHLH element that binds these sites. Otherwise, it is possible that ID factors drop in expression briefly allowing for activating bHLH factors to act upon the chromatin landscape before being repressed by reactivation of ID expression, though this seems less likely. Exactly which set of bHLH factors is responsible for these motifs is unclear. However, it is unlikely to be restricted to NEUROD1, NEUROD4, and ASCL1 given the limited effect of their knockout on thyrotrope number in triple knockout mice [291].

An approach to identifying the binding partners for POU1F1 in GHF-T1 and TαT1 cells would be to immunoprecipitate POU1F1 and identify proteins by mass spectrometry. It is likely that this will reveal a short list of high confidence bHLH factors that are important for pituitary

function. Alternatively, we can find more transient POU1F1 partners by leveraging the BioID method, thus promiscuously biotinylating POU1F1 interactors, allowing for efficient pull-down and mass spectrometry [374]. These experiments may also reveal RFX binding partners of POU1F1. Similar to bHLH, HTH motifs were present in the set of TαT1-specific POU1F1 binding sites that are active in TαT1 cells. The best match for the motifs were RFX factors, many of which are upregulated in TαT1 cells, and have proven function in other endocrine cell types, namely the pancreas [318, 375]. Likewise, the bZIP factors could be identified as a POU1F1 binding partner in GHF-T1 cells. Remarkably, bZIP factor expression is also highly enriched in GHF-T1 cells, with CREB5, FOSL2, and MAFF being the three most highly expressed of the bZIP factors.

In chapter 3 I present the development of an additional thyrotrope-like cell line, PIT-T1. This cell line could be leveraged in the future to understand the transition from GHF-T1 cells, which express *Pou1f1* but not thyrotropin, and TαT1 cells, which express *Pou1f1, Tshb* and *Cga.* The PIT-T1 cells express *Pou1f1* and *Cga*, but not *Tshb*. The list of candidate factors for driving thyrotrope fate would be narrowed significantly by performing similar transcriptomic and epigenomic assays on these and other available pituitary cell lines, including the gonadotrope-like αT3-1 and LβT2 line. Doing so would help us eliminate a set of candidates that are not specific to the thyrotrope fate. Having narrowed the list, I would experimentally test the remaining factors by knocking in a GFP reporter into the *Tshb* locus in both of the GHF-T1 and PIT-T1 cell lines. I would then transfect pools of expression vectors containing transcription factors expressed in the TαT1 cells, and sort for GFP expression using FACS. GFP expression would reveal that some combination of the transfected transcription factors can drive expression of *Tshb*. By gradually reducing the pool of factors, this would ultimately reveal the set of factors sufficient for *Tshb* expression. This work is of great clinical importance, as nearly 12% of the population has abnormal levels of circulating *Tshb* [277].

Due to the limited number of thyrotropes in adult mice, this work was done entirely on immortalized cell lines. Since the start of this work, new library preparation methodologies have come about that may allow characterizing the epigenome and transcriptome of individual thyrotropes directly. We used genetic labeling and FACS to enrich for thyrotropes and analyzed the transcriptome using single-cell sequencing (unpublished). This revealed the presence of POU1F1 negative thyrotropes, with the gene expression signatures of *Tshb* expressing cells in the pars tuberalis (pituitary stalk), and two distinct populations of POU1F1 positive thyrotropes. The latter two types represent the expected TSH expressing cells characteristic of the anterior pituitary (pars distalis) and an unexpected cell type with characteristics of gonadotropes and thyrotropes. This may represent an intermediate in differentiation of cell types that express evolutionarily related genes. It is interesting to note that while NR5A1 (the major gonadotrope transcription factor) is not expressed in TαT1 (and lowly expressed in GHF-T1) cells, it is marked in TαT1 (but not GHF-T1) cells with broad stretches of active chromatin marks in these cells, suggesting that its transcription may be possible. Recent methods now also exist for uncovering DNA accessibility and histone marks at a single-cell level [376, 377]. Performing such transcriptomic and epigenomic experiments on purified thyrotropes is a likely fruitful, and certainly compelling future direction.

Generation and utilization of novel pituitary cell lines

The GHF-T1 and TαT1 cell lines are invaluable for uncovering regulatory elements and the factors that bind to them. Such cell lines are all the more indispensable given the diminutive number of thyrotropes and pituitary precursor cells. In order to understand other pituitary (or other rare) cell types, it is important to immortalize more such cell types to allow for these more sophisticated genomic, or other proteomic techniques. For this reason, we developed a mouse

that conditionally expresses the SV40 small and large T-Antigens from the *Rosa26* locus. This allows for the induction and constitutive expression of a powerful oncogene with cell-type specificity. We have performed proof of concept experiments showing that two different pituitary-specific *cre* transgenes can drive highly penetrant, aggressive tumorigenesis. Furthermore, we have shown that we can successfully generate clonal, stable cell lines from these tumors, thus greatly increasing our ability to generate high-quality mouse cell lines quickly.

A major question to be answered with these SV40; pituitary-cre mice is exactly when the tumorigenesis starts and how SV40 expression interferes with differentiation. It is clear that by P1 the *Rosa26*$^{LSL\text{-}SV40\text{-}GFP/+}$*; Prop1-cre* mice (hereafter referred to as *SV40*; *Prop1*-cre) have hyperplasia whereas *Rosa26*$^{LSL\text{-}SV40\text{-}GFP/+}$*; Tshb-cre* mice (hereafter referred to as *SV40*; *Tshb*-cre) appear phenotypically normal. By P10, *SV40; Tshb-cre* mice have clearly become hyperplastic and initiated tumorigenesis. Collecting pituitaries at additional times would be valuable to determine when SV40 expression begins, when Ki67 expression starts increasing, and when hormone expression begins to be affected in *SV40; Prop1-cre* mice. Specifically, we hypothesize that *Prop1-cre* induced expression of SV40 delays activation of POU1F1 expression, leading to an increase in gonadotrope cell specification at the expense of somatotrope and thyrotrope differentiation. If this is the case, then analysis of e14.5-e16.5 embryos would reveal reduced *Pou1f1* expression and elevated expression of *Nr5a1* in mutants relative to normal mice (as the two are antagonistic) [164]. It would be interesting to determine whether expression of *Gata2* or other candidate thyrotrope factors is altered in conjunction with the reduction in thyrotrope differentiation in this model. Similarly, collection of pituitaries between P10 and P21 from *SV40; Tshb-cre* mice might reveal an effect on thyrotrope differentiation and give insight into SV40-mediated pathogenesis. Finally, most of the analysis completed to date has relied on immunohistochemical staining, which is informative for spatial and temporal expression patterns but not particularly quantitative. Augmenting this data with

qRT-PCR for pituitary transcription factors and markers would provide valuable corroboration of quantitative changes in gene expression.

In these two different mouse lines, the expression of key genes is greatly affected. By P1, *Prop1* expression is much lower in the *SV40*; *Prop1*-cre mice than in wild-type mice. In the aforementioned time series, it would be interesting to assess how the expression of *Prop1* is affected by SV40 over time. Another interesting change in expression we witnessed with these mice is the increase in *Nr5a1* expression that seems too great to simply be explained by modest *Pou1f1* expression decrease. An important next step would be to characterize the expression of the other key transcription factors (namely *Tbx19*, and *Gata2*) to determine whether these cells are stalling at a precursor stage. It is possible that expression of the SV40 is resulting in a delay in PROP1 expression, and therefore a delay in POU1F1 expression, thus allowing NR5A1 to "escape" POU1F1 antagonism, and maintain abnormally high expression through P1. Alternatively, if these pituitaries are stuck in a semi-differentiated state, it is possible that the increase in NR5A1 expression is explained by over-proliferation of these NR5A1 cells in relation to the other cell types. A time-series and more immunostaining would help determine which of these may be happening.

In addition to further characterizing the mice, it would be valuable to further characterize the cell lines. One such characterization would be to determine their stability. We have shown that expression of several key genes persists through five passages following a freeze-thaw cycle and five additional passages, but it is critical to continue monitoring after additional passages to ensuring their continued stability. It would also be valuable to check expression of more genes. Furthermore, SV40 has a well-known effect on the ploidy of transformed cell lines. Thus, SNP typing or low-depth whole-genome sequencing would establish the current ploidy of these cell lines. Continued verification of ploidy would be another valuable measure of the stability of these cell lines, and it would be key for achieving reproducibility and rigor.

I would like to perform a similar analysis on both the precursor (PIT-P1) and pre-thyrotrope

(PIT-T1) cell line that I performed on the GHF-T1 and TαT1 cells. Performing RNA-seq on these cell lines would help clarify exactly where in the pituitary lineage these cells lie. Performing ATAC-seq and CUT&RUN experiments for key factors (namely SOX2, PITX1, and an expressed copy of PROP1 in the PIT-P1 line and POU1F1 in the PIT-T1 line) and histone marks would uncover the regulatory elements important in the developing pituitary gland. Regulatory elements in the progenitor pituitary cells have never been interrogated in a genome-wide manner and doing so would give great insight into the differentiation and development process.

Similar to the Yamanaka-like experiments described above, it would be valuable to use both of these cell lines to find transcription factors important for pituitary differentiation. Specifically, one could knock a GFP cassette into any of the key transcription factor genes (*Prop1*, *Pou1f1*, *Gata2*, *Nr5a1*, and *Tbx19*) to find which factors are responsible for differentiation of the precursor cell line (PIT-P1) to a specific fate. The same approach could be taken to find which transcription factors are responsible for sustained, high expression of *Tshb* in PIT-T1 cells. In addition to finding how genes impact *Tshb* expression, one could find signaling molecules required for its expression. One such signaling molecule is thyroid hormone, as some cell lines respond to levels of thyroid hormone in culture conditions, whereas others do not. Using charcoal-stripped serum devoid of thyroid hormone can increase expression of *Tshb* in these sensitive cell lines. Finding the exact cocktail required for *Tshb* expression in the PIT-T1 cells may be helpful in explaining secondary hypothyroidism.

While these two cell lines will certainly answer many outstanding questions, this tool has the capacity to generate a multitude of other cell lines, important to many fields. It would be valuable to expand the set of cre-lineages crossed with these SV40 mice. *Prop1-cre* and *Tshb-cre* have proven to be highly informative and successful, thus we believe that using other cre's developed for studying pituitary function would be equally informative and successful in developing interesting cell lineages. One such cre would be the *Hesx1*-cre. This mouse

construct replaces the coding regions of *Hesx1* with cre, which results in expression of the cre as early as e7.5, in the developing neural plate and forebrain, in addition to Rathke's pouch [378]. *Hesx1-cre* expression is gone by e11.5, but it has effectively marked every cell in the developing Rathke's pouch. Thus, this cre would likely result in an even more severe phenotype than what we saw in the SV40; *Prop1*-cre mice. It is likely to result in broad pan-brain tumorigenesis, embryonic lethality, and perhaps derivation of cell lines that represent an even earlier timepoint, predating even *Pitx1* expression.

This inducible SV40 expression transgenic animal is a tool is limited only by the number of cre mouse lines that are available. With the increasing number of rare cell types discovered with the advent of single-cell sequencing technology, this tool will be invaluable for the cloning and expansion of these rare cell types, important for assays requiring millions of cells. Not only will this be valuable for novel cre's not yet tried, this line is likely to generate new cell lines from the cre's with which it's already been crossed. Deriving lines from tumors that are collected earlier and later will certainly result in the immortalization of different precursor and thyrotrope populations.

While useful, this tool can still be improved. A possible modification would be using a temperature-sensitive SV40 allele. Previous work has shown that knockdown of SV40 expression in immortalized lines has resulted in differentiation of cells [361]. While this is possible with our tool using CRISPR or siRNA technology, the process would be made easier if the oncogene were heat labile, allowing one to simply knock down SV40 function by changing the temperature.

I have been fortunate to work on highly diverse projects in my PhD, from tool development to basic science advancement, to mutation discovery in patients. With the development of this new rapid cell-line generation tool, future work in the pituitary gland requiring millions of cells is now possible. I trust that this work will be important for understanding the diverse networks of regulatory elements in the different cell types in the pituitary, now possible using the cell lines

generated from the tool we have developed, and the chromatin and transcriptome analysis outline we have established.

Bibliography

1. Xue, L., et al., *Global expression profiling reveals genetic programs underlying the developmental divergence between mouse and human embryogenesis.* BMC Genomics, 2013. **14**: p. 568.
2. Kelberman, D., et al., *Genetic regulation of pituitary gland development in human and mouse.* Endocr Rev, 2009. **30**(7): p. 790-829.
3. Rizzoti, K., *Genetic regulation of murine pituitary development.* J Mol Endocrinol, 2015. **54**(2): p. R55-73.
4. Castinetti, F., et al., *Mechanisms in Endocrinology: An Update in the Genetic Aetiologies of Combined Pituitary Hormone Deficiency.* Eur J Endocrinol, 2016.
5. Fang, Q., et al., *Genetics of Combined Pituitary Hormone Deficiency: Roadmap into the Genome Era.* Endocr Rev, 2016. **37**(6): p. 636-675.
6. Lafont, C., et al., *Cellular in vivo imaging reveals coordinated regulation of pituitary microcirculation and GH cell network function.* Proc Natl Acad Sci U S A, 2010. **107**(9): p. 4465-70.
7. Schaeffer, M., et al., *Functional importance of blood flow dynamics and partial oxygen pressure in the anterior pituitary.* Eur J Neurosci, 2010. **32**(12): p. 2087-95.
8. Rinehart, J.F. and M.G. Farquhar, *Electron microscopic studies of the anterior pituitary gland.* J Histochem Cytochem, 1953. **1**(2): p. 93-113.
9. Soji, T., et al., *Folliculo-stellate cells and intercellular communication within the rat anterior pituitary gland.* Microsc Res Tech, 1997. **39**(2): p. 138-49.
10. Matsumoto, A. and S. Ishii, *Atlas of endocrine organs : vertebrates and invertebrates*. 1992, Berlin ; New York: Springer-Verlag. xii, 307 p.
11. Fauquier, T., et al., *Folliculostellate cell network: a route for long-distance communication in the anterior pituitary.* Proc Natl Acad Sci U S A, 2001. **98**(15): p. 8891-6.
12. Mollard, P., et al., *A tridimensional view of pituitary development and function.* Trends Endocrinol Metab, 2012. **23**(6): p. 261-9.
13. Rosso, L. and J.M. Mienville, *Pituicyte modulation of neurohormone output.* Glia, 2009. **57**(3): p. 235-43.
14. Pow, D.V., et al., *Microglia in the neurohypophysis associate with and endocytose terminal portions of neurosecretory neurons.* Neuroscience, 1989. **33**(3): p. 567-78.
15. Fekete, C. and R.M. Lechan, *Central regulation of hypothalamic-pituitary-thyroid axis under physiological and pathophysiological conditions.* Endocr Rev, 2014. **35**(2): p. 159-94.
16. Imam, A., et al., *Role of the pituitary-bone axis in skeletal pathophysiology.* Curr Opin Endocrinol Diabetes Obes, 2009. **16**(6): p. 423-9.
17. Jin, J.M. and W.X. Yang, *Molecular regulation of hypothalamus-pituitary-gonads axis in males.* Gene, 2014. **551**(1): p. 15-25.

18. Keller-Wood, M., *Hypothalamic-Pituitary--Adrenal Axis-Feedback Control.* Compr Physiol, 2015. **5**(3): p. 1161-82.
19. Simon, F.R., et al., *Sexual dimorphic expression of ADH in rat liver: importance of the hypothalamic-pituitary-liver axis.* Am J Physiol Gastrointest Liver Physiol, 2002. **283**(3): p. G646-55.
20. Cohen, L.E., et al., *Defective retinoic acid regulation of the Pit-1 gene enhancer: a novel mechanism of combined pituitary hormone deficiency.* Mol Endocrinol, 1999. **13**(3): p. 476-84.
21. Djakoure, C., et al., *Vitamin A and retinoic acid stimulate within minutes cAMP release and growth hormone secretion in human pituitary cells.* J Clin Endocrinol Metab, 1996. **81**(8): p. 3123-6.
22. Zhu, X., A.S. Gleiberman, and M.G. Rosenfeld, *Molecular physiology of pituitary development: signaling and transcriptional networks.* Physiol Rev, 2007. **87**(3): p. 933-63.
23. Lodge, E.J., et al., *Homeostatic and tumourigenic activity of SOX2+ pituitary stem cells is controlled by the LATS/YAP/TAZ cascade.* Elife, 2019. **8**.
24. Carreno, G., et al., *Hypothalamic sonic hedgehog is required for cell specification and proliferation of LHX3/LHX4 pituitary embryonic precursors.* Development, 2017. **144**(18): p. 3289-3302.
25. Ohuchi, H., et al., *FGF10 acts as a major ligand for FGF receptor 2 IIIb in mouse multi-organ development.* Biochem Biophys Res Commun, 2000. **277**(3): p. 643-9.
26. Davis, S.W. and S.A. Camper, *Noggin regulates Bmp4 activity during pituitary induction.* Dev Biol, 2007. **305**(1): p. 145-60.
27. Ericson, J., et al., *Integrated FGF and BMP signaling controls the progression of progenitor cell differentiation and the emergence of pattern in the embryonic anterior pituitary.* Development, 1998. **125**(6): p. 1005-15.
28. Giacomini, D., et al., *Bone morphogenetic protein-4 control of pituitary pathophysiology.* Front Horm Res, 2006. **35**: p. 22-31.
29. Treier, M., et al., *Hedgehog signaling is required for pituitary gland development.* Development, 2001. **128**(3): p. 377-86.
30. Chambers, T.J., et al., *Wnt signalling in pituitary development and tumorigenesis.* Endocr Relat Cancer, 2013. **20**(3): p. R101-11.
31. Raetzman, L.T., et al., *Developmental regulation of Notch signaling genes in the embryonic pituitary: Prop1 deficiency affects Notch2 expression.* Dev Biol, 2004. **265**(2): p. 329-40.
32. Zhu, X., et al., *Sustained Notch signaling in progenitors is required for sequential emergence of distinct cell lineages during organogenesis.* Genes Dev, 2006. **20**(19): p. 2739-53.
33. Cheung, L., et al., *NOTCH activity differentially affects alternative cell fate acquisition and maintenance.* Elife, 2018. **7**.
34. Rhodes, S.J., et al., *A tissue-specific enhancer confers Pit-1-dependent morphogen inducibility and autoregulation on the pit-1 gene.* Genes Dev, 1993. **7**(6): p. 913-32.
35. Roh, M., et al., *Stage-sensitive blockade of pituitary somatomammotrope development by targeted expression of a dominant negative epidermal growth factor receptor in transgenic mice.* Mol Endocrinol, 2001. **15**(4): p. 600-13.
36. Higham, C.E., G. Johannsson, and S.M. Shalet, *Hypopituitarism.* Lancet, 2016. **388**(10058): p. 2403-2415.
37. Melmed, S., *Pathogenesis of pituitary tumors.* Nat Rev Endocrinol, 2011. **7**(5): p. 257-66.
38. Regal, M., et al., *Prevalence and incidence of hypopituitarism in an adult Caucasian population in northwestern Spain.* Clin Endocrinol (Oxf), 2001. **55**(6): p. 735-40.

39. Gubbay, J., et al., *A gene mapping to the sex-determining region of the mouse Y chromosome is a member of a novel family of embryonically expressed genes.* Nature, 1990. **346**(6281): p. 245-50.
40. Li, M., et al., *Generation of purified neural precursors from embryonic stem cells by lineage selection.* Curr Biol, 1998. **8**(17): p. 971-4.
41. Zappone, M.V., et al., *Sox2 regulatory sequences direct expression of a (beta)-geo transgene to telencephalic neural stem cells and precursors of the mouse embryo, revealing regionalization of gene expression in CNS stem cells.* Development, 2000. **127**(11): p. 2367-82.
42. Avilion, A.A., et al., *Multipotent cell lineages in early mouse development depend on SOX2 function.* Genes Dev, 2003. **17**(1): p. 126-40.
43. Takahashi, K., et al., *Induction of pluripotent stem cells from adult human fibroblasts by defined factors.* Cell, 2007. **131**(5): p. 861-72.
44. Takahashi, K. and S. Yamanaka, *Induction of pluripotent stem cells from mouse embryonic and adult fibroblast cultures by defined factors.* Cell, 2006. **126**(4): p. 663-76.
45. Cha, K.B., et al., *WNT5A signaling affects pituitary gland shape.* Mech Dev, 2004. **121**(2): p. 183-94.
46. Rizzoti, K. and R. Lovell-Badge, *Early development of the pituitary gland: induction and shaping of Rathke's pouch.* Rev Endocr Metab Disord, 2005. **6**(3): p. 161-72.
47. Szeto, D.P., et al., *Role of the Bicoid-related homeodomain factor Pitx1 in specifying hindlimb morphogenesis and pituitary development.* Genes Dev, 1999. **13**(4): p. 484-94.
48. Suh, H., et al., *Pitx2 is required at multiple stages of pituitary organogenesis: pituitary primordium formation and cell specification.* Development, 2002. **129**(2): p. 329-37.
49. Lin, C.R., et al., *Pitx2 regulates lung asymmetry, cardiac positioning and pituitary and tooth morphogenesis.* Nature, 1999. **401**(6750): p. 279-82.
50. Sheng, H.Z., et al., *Multistep control of pituitary organogenesis.* Science, 1997. **278**(5344): p. 1809-12.
51. Kelberman, D., et al., *Mutations within Sox2/SOX2 are associated with abnormalities in the hypothalamo-pituitary-gonadal axis in mice and humans.* J Clin Invest, 2006. **116**(9): p. 2442-55.
52. Jayakody, S.A., et al., *SOX2 regulates the hypothalamic-pituitary axis at multiple levels.* J Clin Invest, 2012. **122**(10): p. 3635-46.
53. Nasonkin, I.O., et al., *Pituitary hypoplasia and respiratory distress syndrome in Prop1 knockout mice.* Hum Mol Genet, 2004. **13**(22): p. 2727-35.
54. Raetzman, L.T., R. Ward, and S.A. Camper, *Lhx4 and Prop1 are required for cell survival and expansion of the pituitary primordia.* Development, 2002. **129**(18): p. 4229-39.
55. Sajedi, E., et al., *Analysis of mouse models carrying the I26T and R160C substitutions in the transcriptional repressor HESX1 as models for septo-optic dysplasia and hypopituitarism.* Dis Model Mech, 2008. **1**(4-5): p. 241-54.
56. Ingraham, H.A., et al., *The nuclear receptor steroidogenic factor 1 acts at multiple levels of the reproductive axis.* Genes Dev, 1994. **8**(19): p. 2302-12.
57. Mortensen, A.H., et al., *Candidate genes for panhypopituitarism identified by gene expression profiling.* Physiol Genomics, 2011. **43**(19): p. 1105-16.
58. Pulichino, A.M., et al., *Tpit determines alternate fates during pituitary cell differentiation.* Genes Dev, 2003. **17**(6): p. 738-47.
59. Fauquier, T., et al., *SOX2-expressing progenitor cells generate all of the major cell types in the adult mouse pituitary gland.* Proc Natl Acad Sci U S A, 2008. **105**(8): p. 2907-12.
60. Andoniadou, C.L., et al., *Sox2(+) stem/progenitor cells in the adult mouse pituitary support organ homeostasis and have tumor-inducing potential.* Cell Stem Cell, 2013. **13**(4): p. 433-45.

61. Rizzoti, K., H. Akiyama, and R. Lovell-Badge, *Mobilized adult pituitary stem cells contribute to endocrine regeneration in response to physiological demand.* Cell Stem Cell, 2013. **13**(4): p. 419-32.
62. Gaston-Massuet, C., et al., *Increased Wingless (Wnt) signaling in pituitary progenitor/stem cells gives rise to pituitary tumors in mice and humans.* Proc Natl Acad Sci U S A, 2011. **108**(28): p. 11482-7.
63. Ragge, N.K., et al., *SOX2 anophthalmia syndrome.* Am J Med Genet A, 2005. **135**(1): p. 1-7; discussion 8.
64. Gage, P.J., H. Suh, and S.A. Camper, *Dosage requirement of Pitx2 for development of multiple organs.* Development, 1999. **126**(20): p. 4643-51.
65. Kitamura, K., et al., *Mouse Pitx2 deficiency leads to anomalies of the ventral body wall, heart, extra- and periocular mesoderm and right pulmonary isomerism.* Development, 1999. **126**(24): p. 5749-58.
66. Lu, M.F., et al., *Function of Rieger syndrome gene in left-right asymmetry and craniofacial development.* Nature, 1999. **401**(6750): p. 276-8.
67. Charles, M.A., et al., *PITX genes are required for cell survival and Lhx3 activation.* Mol Endocrinol, 2005. **19**(7): p. 1893-903.
68. Therrien, M. and J. Drouin, *Pituitary pro-opiomelanocortin gene expression requires synergistic interactions of several regulatory elements.* Mol Cell Biol, 1991. **11**(7): p. 3492-503.
69. Lamonerie, T., et al., *Ptx1, a bicoid-related homeo box transcription factor involved in transcription of the pro-opiomelanocortin gene.* Genes Dev, 1996. **10**(10): p. 1284-95.
70. Szeto, D.P., et al., *P-OTX: a PIT-1-interacting homeodomain factor expressed during anterior pituitary gland development.* Proc Natl Acad Sci U S A, 1996. **93**(15): p. 7706-10.
71. Datson, N.A., et al., *Closing in on the Rieger syndrome gene on 4q25: mapping translocation breakpoints within a 50-kb region.* Am J Hum Genet, 1996. **59**(6): p. 1297-305.
72. Semina, E.V., et al., *Cloning and characterization of a novel bicoid-related homeobox transcription factor gene, RIEG, involved in Rieger syndrome.* Nat Genet, 1996. **14**(4): p. 392-9.
73. Gage, P.J. and S.A. Camper, *Pituitary homeobox 2, a novel member of the bicoid-related family of homeobox genes, is a potential regulator of anterior structure formation.* Hum Mol Genet, 1997. **6**(3): p. 457-64.
74. Lanctot, C., Y. Gauthier, and J. Drouin, *Pituitary homeobox 1 (Ptx1) is differentially expressed during pituitary development.* Endocrinology, 1999. **140**(3): p. 1416-22.
75. Treier, M., et al., *Multistep signaling requirements for pituitary organogenesis in vivo.* Genes Dev, 1998. **12**(11): p. 1691-704.
76. Tremblay, J.J., C. Lanctot, and J. Drouin, *The pan-pituitary activator of transcription, Ptx1 (pituitary homeobox 1), acts in synergy with SF-1 and Pit1 and is an upstream regulator of the Lim-homeodomain gene Lim3/Lhx3.* Mol Endocrinol, 1998. **12**(3): p. 428-41.
77. Charles, M.A., et al., *Pituitary-specific Gata2 knockout: effects on gonadotrope and thyrotrope function.* Mol Endocrinol, 2006. **20**(6): p. 1366-77.
78. Kioussi, C., et al., *Identification of a Wnt/Dvl/beta-Catenin --> Pitx2 pathway mediating cell-type-specific proliferation during development.* Cell, 2002. **111**(5): p. 673-85.
79. Chen, L. and P.J. Gage, *Heterozygous Pitx2 Null Mice Accurately Recapitulate the Ocular Features of Axenfeld-Rieger Syndrome and Congenital Glaucoma.* Invest Ophthalmol Vis Sci, 2016. **57**(11): p. 5023-5030.
80. Alvarado, D.M., et al., *Pitx1 haploinsufficiency causes clubfoot in humans and a clubfoot-like phenotype in mice.* Hum Mol Genet, 2011. **20**(20): p. 3943-52.

81. Gurnett, C.A., et al., *Asymmetric lower-limb malformations in individuals with homeobox PITX1 gene mutation.* Am J Hum Genet, 2008. **83**(5): p. 616-22.
82. Klopocki, E., et al., *Deletions in PITX1 cause a spectrum of lower-limb malformations including mirror-image polydactyly.* Eur J Hum Genet, 2012. **20**(6): p. 705-8.
83. Kragesteen, B.K., et al., *H2AFY promoter deletion causes PITX1 endoactivation and Liebenberg syndrome.* J Med Genet, 2019. **56**(4): p. 246-251.
84. Spielmann, M., et al., *Homeotic arm-to-leg transformation associated with genomic rearrangements at the PITX1 locus.* Am J Hum Genet, 2012. **91**(4): p. 629-35.
85. Sadeghi-Nejad, A. and B. Senior, *Autosomal dominant transmission of isolated growth hormone deficiency in iris-dental dysplasia (Rieger's syndrome).* J Pediatr, 1974. **85**(5): p. 644-8.
86. Xu, Y., et al., *LH-2: a LIM/homeodomain gene expressed in developing lymphocytes and neural cells.* Proc Natl Acad Sci U S A, 1993. **90**(1): p. 227-31.
87. Taira, M., et al., *The LIM domain-containing homeo box gene Xlim-1 is expressed specifically in the organizer region of Xenopus gastrula embryos.* Genes Dev, 1992. **6**(3): p. 356-66.
88. Singh, G., et al., *Identification of 10 murine homeobox genes.* Proc Natl Acad Sci U S A, 1991. **88**(23): p. 10706-10.
89. Porter, F.D., et al., *Lhx2, a LIM homeobox gene, is required for eye, forebrain, and definitive erythrocyte development.* Development, 1997. **124**(15): p. 2935-44.
90. Li, H., et al., *Gsh-4 encodes a LIM-type homeodomain, is expressed in the developing central nervous system and is required for early postnatal survival.* EMBO J, 1994. **13**(12): p. 2876-85.
91. Zhao, Y., et al., *A role of the LIM-homeobox gene Lhx2 in the regulation of pituitary development.* Dev Biol, 2010. **337**(2): p. 313-23.
92. Sheng, H.Z., et al., *Specification of pituitary cell lineages by the LIM homeobox gene Lhx3.* Science, 1996. **272**(5264): p. 1004-7.
93. Ellsworth, B.S., D.L. Butts, and S.A. Camper, *Mechanisms underlying pituitary hypoplasia and failed cell specification in Lhx3-deficient mice.* Dev Biol, 2008. **313**(1): p. 118-29.
94. Perez, C., et al., *Screening of LHX2 in patients presenting growth retardation with posterior pituitary and ocular abnormalities.* Eur J Endocrinol, 2012. **167**(1): p. 85-91.
95. Gergics, P., M.L. Brinkmeier, and S.A. Camper, *Lhx4 deficiency: increased cyclin-dependent kinase inhibitor expression and pituitary hypoplasia.* Mol Endocrinol, 2015. **29**(4): p. 597-612.
96. Netchine, I., et al., *Mutations in LHX3 result in a new syndrome revealed by combined pituitary hormone deficiency.* Nat Genet, 2000. **25**(2): p. 182-6.
97. Bhangoo, A.P., et al., *Clinical case seminar: a novel LHX3 mutation presenting as combined pituitary hormonal deficiency.* J Clin Endocrinol Metab, 2006. **91**(3): p. 747-53.
98. Pfaeffle, R.W., et al., *Four novel mutations of the LHX3 gene cause combined pituitary hormone deficiencies with or without limited neck rotation.* J Clin Endocrinol Metab, 2007. **92**(5): p. 1909-19.
99. Rajab, A., et al., *Novel mutations in LHX3 are associated with hypopituitarism and sensorineural hearing loss.* Hum Mol Genet, 2008. **17**(14): p. 2150-9.
100. Kristrom, B., et al., *A novel mutation in the LIM homeobox 3 gene is responsible for combined pituitary hormone deficiency, hearing impairment, and vertebral malformations.* J Clin Endocrinol Metab, 2009. **94**(4): p. 1154-61.
101. Bechtold-Dalla Pozza, S., et al., *A recessive mutation resulting in a disabling amino acid substitution (T194R) in the LHX3 homeodomain causes combined pituitary hormone deficiency.* Horm Res Paediatr, 2012. **77**(1): p. 41-51.

102. Bonfig, W., H. Krude, and H. Schmidt, *A novel mutation of LHX3 is associated with combined pituitary hormone deficiency including ACTH deficiency, sensorineural hearing loss, and short neck-a case report and review of the literature.* Eur J Pediatr, 2011. **170**(8): p. 1017-21.
103. Sobrier, M.L., et al., *Symptomatic heterozygotes and prenatal diagnoses in a nonconsanguineous family with syndromic combined pituitary hormone deficiency resulting from two novel LHX3 mutations.* J Clin Endocrinol Metab, 2012. **97**(3): p. E503-9.
104. Gregory, L.C., et al., *Novel Lethal Form of Congenital Hypopituitarism Associated With the First Recessive LHX4 Mutation.* J Clin Endocrinol Metab, 2015. **100**(6): p. 2158-64.
105. Ramzan, K., et al., *Two novel LHX3 mutations in patients with combined pituitary hormone deficiency including cervical rigidity and sensorineural hearing loss.* BMC Endocr Disord, 2017. **17**(1): p. 17.
106. Jullien, N., et al., *Heterozygous LHX3 mutations may lead to a mild phenotype of combined pituitary hormone deficiency.* Eur J Hum Genet, 2019. **27**(2): p. 216-225.
107. Riepe, F.G., et al., *Longitudinal imaging reveals pituitary enlargement preceding hypoplasia in two brothers with combined pituitary hormone deficiency attributable to PROP1 mutation.* J Clin Endocrinol Metab, 2001. **86**(9): p. 4353-7.
108. Tajima, T., et al., *A novel missense mutation (P366T) of the LHX4 gene causes severe combined pituitary hormone deficiency with pituitary hypoplasia, ectopic posterior lobe and a poorly developed sella turcica.* Endocr J, 2007. **54**(4): p. 637-41.
109. Pfaeffle, R.W., et al., *Three novel missense mutations within the LHX4 gene are associated with variable pituitary hormone deficiencies.* J Clin Endocrinol Metab, 2008. **93**(3): p. 1062-71.
110. Dateki, S., et al., *Mutation and gene copy number analyses of six pituitary transcription factor genes in 71 patients with combined pituitary hormone deficiency: identification of a single patient with LHX4 deletion.* J Clin Endocrinol Metab, 2010. **95**(8): p. 4043-7.
111. Tajima, T., et al., *A novel mutation (V101A) of the LHX4 gene in a Japanese patient with combined pituitary hormone deficiency.* Exp Clin Endocrinol Diabetes, 2010. **118**(7): p. 405-9.
112. Filges, I., et al., *Panhypopituitarism presenting as life-threatening heart failure caused by an inherited microdeletion in 1q25 including LHX4.* Pediatrics, 2012. **129**(2): p. e529-34.
113. Rochette, C., et al., *Identifying the Deleterious Effect of Rare LHX4 Allelic Variants, a Challenging Issue.* PLoS One, 2015. **10**(5): p. e0126648.
114. Thomas, P.Q. and P.D. Rathjen, *HES-1, a novel homeobox gene expressed by murine embryonic stem cells, identifies a new class of homeobox genes.* Nucleic Acids Res, 1992. **20**(21): p. 5840.
115. Thomas, P.Q., et al., *Sequence, genomic organization, and expression of the novel homeobox gene Hesx1.* J Biol Chem, 1995. **270**(8): p. 3869-75.
116. Hermesz, E., S. Mackem, and K.A. Mahon, *Rpx: a novel anterior-restricted homeobox gene progressively activated in the prechordal plate, anterior neural plate and Rathke's pouch of the mouse embryo.* Development, 1996. **122**(1): p. 41-52.
117. Gage, P.J., et al., *The Ames dwarf gene, df, is required early in pituitary ontogeny for the extinction of Rpx transcription and initiation of lineage-specific cell proliferation.* Mol Endocrinol, 1996. **10**(12): p. 1570-81.
118. Dasen, J.S., et al., *Temporal regulation of a paired-like homeodomain repressor/TLE corepressor complex and a related activator is required for pituitary organogenesis.* Genes Dev, 2001. **15**(23): p. 3193-207.
119. Dattani, M.T., et al., *Mutations in the homeobox gene HESX1/Hesx1 associated with septo-optic dysplasia in human and mouse.* Nat Genet, 1998. **19**(2): p. 125-33.

120. Olson, L.E., et al., *Homeodomain-mediated beta-catenin-dependent switching events dictate cell-lineage determination.* Cell, 2006. **125**(3): p. 593-605.
121. Chou, S.J., et al., *Conserved regulatory elements establish the dynamic expression of Rpx/Hesxl in early vertebrate development.* Dev Biol, 2006. **292**(2): p. 533-45.
122. Thomas, P.Q., et al., *Heterozygous HESX1 mutations associated with isolated congenital pituitary hypoplasia and septo-optic dysplasia.* Hum Mol Genet, 2001. **10**(1): p. 39-45.
123. Sornson, M.W., et al., *Pituitary lineage determination by the Prophet of Pit-1 homeodomain factor defective in Ames dwarfism.* Nature, 1996. **384**(6607): p. 327-33.
124. Schaible, R. and J.W. Gowen, *A new dwarf mouse.* Genetics, 1961. **46**: p. 896.
125. Bartke, A., *The response of two types of dwarf mice to growth hormone, thyrotropin, and thyroxine.* Gen Comp Endocrinol, 1965. **5**(4): p. 418-26.
126. Cheng, T.C., et al., *Etiology of growth hormone deficiency in little, Ames, and Snell dwarf mice.* Endocrinology, 1983. **113**(5): p. 1669-78.
127. Gage, P.J., et al., *Ames dwarf mice exhibit somatotrope commitment but lack growth hormone-releasing factor response.* Endocrinology, 1995. **136**(3): p. 1161-7.
128. Andersen, B., et al., *The Ames dwarf gene is required for Pit-1 gene activation.* Dev Biol, 1995. **172**(2): p. 495-503.
129. Buckwalter, M.S., R.W. Katz, and S.A. Camper, *Localization of the panhypopituitary dwarf mutation (df) on mouse chromosome 11 in an intersubspecific backcross.* Genomics, 1991. **10**(3): p. 515-26.
130. Perez Millan, M.I., et al., *PROP1 triggers epithelial-mesenchymal transition-like process in pituitary stem cells.* Elife, 2016. **5**.
131. Davis, S.W., et al., *All Hormone-Producing Cell Types of the Pituitary Intermediate and Anterior Lobes Derive From Prop1-Expressing Progenitors.* Endocrinology, 2016. **157**(4): p. 1385-96.
132. Ward, R.D., et al., *Role of PROP1 in pituitary gland growth.* Mol Endocrinol, 2005. **19**(3): p. 698-710.
133. Himes, A.D. and L.T. Raetzman, *Premature differentiation and aberrant movement of pituitary cells lacking both Hes1 and Prop1.* Dev Biol, 2009. **325**(1): p. 151-61.
134. Ward, R.D., et al., *Comparative genomics reveals functional transcriptional control sequences in the Prop1 gene.* Mamm Genome, 2007. **18**(6-7): p. 521-37.
135. Wu, W., et al., *Mutations in PROP1 cause familial combined pituitary hormone deficiency.* Nat Genet, 1998. **18**(2): p. 147-9.
136. Cogan, J.D., et al., *The PROP1 2-base pair deletion is a common cause of combined pituitary hormone deficiency.* J Clin Endocrinol Metab, 1998. **83**(9): p. 3346-9.
137. Deladoey, J., et al., *"Hot spot" in the PROP1 gene responsible for combined pituitary hormone deficiency.* J Clin Endocrinol Metab, 1999. **84**(5): p. 1645-50.
138. Lemos, M.C., et al., *PROP1 gene analysis in Portuguese patients with combined pituitary hormone deficiency.* Clin Endocrinol (Oxf), 2006. **65**(4): p. 479-85.
139. Navardauskaite, R., et al., *High prevalence of PROP1 defects in Lithuania: phenotypic findings in an ethnically homogenous cohort of patients with multiple pituitary hormone deficiency.* J Clin Endocrinol Metab, 2014. **99**(1): p. 299-306.
140. Lebl, J., et al., *Auxological and endocrine phenotype in a population-based cohort of patients with PROP1 gene defects.* Eur J Endocrinol, 2005. **153**(3): p. 389-96.
141. Dusatkova, P., et al., *Genesis of two most prevalent PROP1 gene variants causing combined pituitary hormone deficiency in 21 populations.* Eur J Hum Genet, 2016. **24**(3): p. 415-20.
142. Bodner, M., et al., *The pituitary-specific transcription factor GHF-1 is a homeobox-containing protein.* Cell, 1988. **55**(3): p. 505-18.

143. Ingraham, H.A., et al., *A tissue-specific transcription factor containing a homeodomain specifies a pituitary phenotype.* Cell, 1988. **55**(3): p. 519-29.
144. Nelson, C., et al., *Discrete cis-active genomic sequences dictate the pituitary cell type-specific expression of rat prolactin and growth hormone genes.* Nature, 1986. **322**(6079): p. 557-62.
145. Bodner, M. and M. Karin, *A pituitary-specific trans-acting factor can stimulate transcription from the growth hormone promoter in extracts of nonexpressing cells.* Cell, 1987. **50**(2): p. 267-75.
146. McCormick, A., et al., *Extinction of growth hormone expression in somatic cell hybrids involves repression of the specific trans-activator GHF-1.* Cell, 1988. **55**(2): p. 379-89.
147. Theill, L.E., et al., *Dissection of functional domains of the pituitary-specific transcription factor GHF-1.* Nature, 1989. **342**(6252): p. 945-8.
148. Snell, G.D., *Dwarf, a New Mendelian Recessive Character of the House Mouse.* Proc Natl Acad Sci U S A, 1929. **15**(9): p. 733-4.
149. Smith, P.E. and E.C. MacDowell, *An hereditary anterior-pituitary deficiency in the mouse.* The Anatomical Record, 1930. **46**: p. 249-257.
150. Carsner, R.L. and E.G. Reynolds, *Primary site of gene action in anterior pituitary dwarf mice.* Science, 1960. **131**: p. 829.
151. Camper, S.A., et al., *The Pit-1 transcription factor gene is a candidate for the murine Snell dwarf mutation.* Genomics, 1990. **8**(3): p. 586-90.
152. Li, S., et al., *Dwarf locus mutants lacking three pituitary cell types result from mutations in the POU-domain gene pit-1.* Nature, 1990. **347**(6293): p. 528-33.
153. Eicher, E.M. and W.G. Beamer, *New mouse dw allele: genetic location and effects on lifespan and growth hormone levels.* J Hered, 1980. **71**(3): p. 187-90.
154. Tatsumi, K., et al., *Cretinism with combined hormone deficiency caused by a mutation in the PIT1 gene.* Nat Genet, 1992. **1**(1): p. 56-8.
155. Radovick, S., et al., *A mutation in the POU-homeodomain of Pit-1 responsible for combined pituitary hormone deficiency.* Science, 1992. **257**(5073): p. 1115-8.
156. Ohta, K., et al., *Mutations in the Pit-1 gene in children with combined pituitary hormone deficiency.* Biochem Biophys Res Commun, 1992. **189**(2): p. 851-5.
157. Okamoto, N., et al., *Monoallelic expression of normal mRNA in the PIT1 mutation heterozygotes with normal phenotype and biallelic expression in the abnormal phenotype.* Hum Mol Genet, 1994. **3**(9): p. 1565-8.
158. Enwright, J.F., 3rd, et al., *A PIT-1 homeodomain mutant blocks the intranuclear recruitment of the CCAAT/enhancer binding protein alpha required for prolactin gene transcription.* Mol Endocrinol, 2003. **17**(2): p. 209-22.
159. Skowronska-Krawczyk, D., et al., *Required enhancer-matrin-3 network interactions for a homeodomain transcription program.* Nature, 2014. **514**(7521): p. 257-61.
160. Sobrier, M.L., et al., *Functional characterization of a human POU1F1 mutation associated with isolated growth hormone deficiency: a novel etiology for IGHD.* Hum Mol Genet, 2016. **25**(3): p. 472-83.
161. Fofanova, O.V., et al., *Rarity of PIT1 involvement in children from Russia with combined pituitary hormone deficiency.* Am J Med Genet, 1998. **77**(5): p. 360-5.
162. DiMattia, G.E., et al., *The Pit-1 gene is regulated by distinct early and late pituitary-specific enhancers.* Dev Biol, 1997. **182**(1): p. 180-90.
163. Gordon, D.F., et al., *Pit-1 and GATA-2 interact and functionally cooperate to activate the thyrotropin beta-subunit promoter.* J Biol Chem, 1997. **272**(39): p. 24339-47.
164. Dasen, J.S., et al., *Reciprocal interactions of Pit1 and GATA2 mediate signaling gradient-induced determination of pituitary cell types.* Cell, 1999. **97**(5): p. 587-98.
165. Wang, J., et al., *Opposing LSD1 complexes function in developmental gene activation and repression programmes.* Nature, 2007. **446**(7138): p. 882-7.

166. Rice, D.A., et al., *A shared promoter element regulates the expression of three steroidogenic enzymes.* Mol Endocrinol, 1991. **5**(10): p. 1552-61.
167. Morohashi, K., et al., *A common trans-acting factor, Ad4-binding protein, to the promoters of steroidogenic P-450s.* J Biol Chem, 1992. **267**(25): p. 17913-9.
168. Honda, S., K. Morohashi, and T. Omura, *Novel cAMP regulatory elements in the promoter region of bovine P-450(11 beta) gene.* J Biochem, 1990. **108**(6): p. 1042-9.
169. Lala, D.S., D.A. Rice, and K.L. Parker, *Steroidogenic factor I, a key regulator of steroidogenic enzyme expression, is the mouse homolog of fushi tarazu-factor I.* Mol Endocrinol, 1992. **6**(8): p. 1249-58.
170. Honda, S., et al., *Ad4BP regulating steroidogenic P-450 gene is a member of steroid hormone receptor superfamily.* J Biol Chem, 1993. **268**(10): p. 7494-502.
171. Ikeda, Y., et al., *Developmental expression of mouse steroidogenic factor-1, an essential regulator of the steroid hydroxylases.* Mol Endocrinol, 1994. **8**(5): p. 654-62.
172. Shima, Y., et al., *Ventromedial hypothalamic nucleus-specific enhancer of Ad4BP/SF-1 gene.* Mol Endocrinol, 2005. **19**(11): p. 2812-23.
173. Horn, F., et al., *Tissue-specific gene expression in the pituitary: the glycoprotein hormone alpha-subunit gene is regulated by a gonadotrope-specific protein.* Mol Cell Biol, 1992. **12**(5): p. 2143-53.
174. Barnhart, K.M. and P.L. Mellon, *The orphan nuclear receptor, steroidogenic factor-1, regulates the glycoprotein hormone alpha-subunit gene in pituitary gonadotropes.* Mol Endocrinol, 1994. **8**(7): p. 878-85.
175. Halvorson, L.M., U.B. Kaiser, and W.W. Chin, *Stimulation of luteinizing hormone beta gene promoter activity by the orphan nuclear receptor, steroidogenic factor-1.* J Biol Chem, 1996. **271**(12): p. 6645-50.
176. Keri, R.A., et al., *The proximal promoter of the bovine luteinizing hormone beta-subunit gene confers gonadotrope-specific expression and regulation by gonadotropin-releasing hormone, testosterone, and 17 beta-estradiol in transgenic mice.* Mol Endocrinol, 1994. **8**(12): p. 1807-16.
177. Keri, R.A. and J.H. Nilson, *A steroidogenic factor-1 binding site is required for activity of the luteinizing hormone beta subunit promoter in gonadotropes of transgenic mice.* J Biol Chem, 1996. **271**(18): p. 10782-5.
178. Duval, D.L., S.E. Nelson, and C.M. Clay, *A binding site for steroidogenic factor-1 is part of a complex enhancer that mediates expression of the murine gonadotropin-releasing hormone receptor gene.* Biol Reprod, 1997. **56**(1): p. 160-8.
179. Tremblay, J.J., et al., *Ptx1 regulates SF-1 activity by an interaction that mimics the role of the ligand-binding domain.* EMBO J, 1999. **18**(12): p. 3431-41.
180. Lee, S.L., et al., *Luteinizing hormone deficiency and female infertility in mice lacking the transcription factor NGFI-A (Egr-1).* Science, 1996. **273**(5279): p. 1219-21.
181. Tremblay, J.J. and J. Drouin, *Egr-1 is a downstream effector of GnRH and synergizes by direct interaction with Ptx1 and SF-1 to enhance luteinizing hormone beta gene transcription.* Mol Cell Biol, 1999. **19**(4): p. 2567-76.
182. Topilko, P., et al., *Multiple pituitary and ovarian defects in Krox-24 (NGFI-A, Egr-1)-targeted mice.* Mol Endocrinol, 1998. **12**(1): p. 107-22.
183. Jacobs, S.B., et al., *Nuclear factor Y and steroidogenic factor 1 physically and functionally interact to contribute to cell-specific expression of the mouse Follicle-stimulating hormone-beta gene.* Mol Endocrinol, 2003. **17**(8): p. 1470-83.
184. Luo, X., Y. Ikeda, and K.L. Parker, *A cell-specific nuclear receptor is essential for adrenal and gonadal development and sexual differentiation.* Cell, 1994. **77**(4): p. 481-90.
185. Ikeda, Y., et al., *The nuclear receptor steroidogenic factor 1 is essential for the formation of the ventromedial hypothalamic nucleus.* Mol Endocrinol, 1995. **9**(4): p. 478-86.

186. Kaiser, U.B., L.M. Halvorson, and M.T. Chen, *Sp1, steroidogenic factor 1 (SF-1), and early growth response protein 1 (egr-1) binding sites form a tripartite gonadotropin-releasing hormone response element in the rat luteinizing hormone-beta gene promoter: an integral role for SF-1.* Mol Endocrinol, 2000. **14**(8): p. 1235-45.
187. Melamed, P., et al., *Gonadotropin-releasing hormone activation of c-jun, but not early growth response factor-1, stimulates transcription of a luteinizing hormone beta-subunit gene.* Endocrinology, 2006. **147**(7): p. 3598-605.
188. Salisbury, T.B., et al., *GnRH-regulated expression of Jun and JUN target genes in gonadotropes requires a functional interaction between TCF/LEF family members and beta-catenin.* Mol Endocrinol, 2009. **23**(3): p. 402-11.
189. Zhao, L., et al., *Steroidogenic factor 1 (SF1) is essential for pituitary gonadotrope function.* Development, 2001. **128**(2): p. 147-54.
190. Cushman, L.J., et al., *Cre-mediated recombination in the pituitary gland.* Genesis, 2000. **28**(3-4): p. 167-74.
191. Achermann, J.C., et al., *A mutation in the gene encoding steroidogenic factor-1 causes XY sex reversal and adrenal failure in humans.* Nat Genet, 1999. **22**(2): p. 125-6.
192. Achermann, J.C., et al., *Gonadal determination and adrenal development are regulated by the orphan nuclear receptor steroidogenic factor-1, in a dose-dependent manner.* J Clin Endocrinol Metab, 2002. **87**(4): p. 1829-33.
193. Correa, R.V., et al., *A microdeletion in the ligand binding domain of human steroidogenic factor 1 causes XY sex reversal without adrenal insufficiency.* J Clin Endocrinol Metab, 2004. **89**(4): p. 1767-72.
194. Mallet, D., et al., *Gonadal dysgenesis without adrenal insufficiency in a 46, XY patient heterozygous for the nonsense C16X mutation: a case of SF1 haploinsufficiency.* J Clin Endocrinol Metab, 2004. **89**(10): p. 4829-32.
195. Lin, L., et al., *Heterozygous missense mutations in steroidogenic factor 1 (SF1/Ad4BP, NR5A1) are associated with 46,XY disorders of sex development with normal adrenal function.* J Clin Endocrinol Metab, 2007. **92**(3): p. 991-9.
196. Swartz, J.M., et al., *A 46,XX Ovotesticular Disorder of Sex Development Likely Caused by a Steroidogenic Factor-1 (NR5A1) Variant.* Horm Res Paediatr, 2017. **87**(3): p. 191-195.
197. Hasegawa, T., et al., *Testicular dysgenesis without adrenal insufficiency in a 46,XY patient with a heterozygous inactive mutation of steroidogenic factor-1.* J Clin Endocrinol Metab, 2004. **89**(12): p. 5930-5.
198. Swartz, J.M., et al., *Two Unrelated Undervirilized 46,XY Males with Inherited NR5A1 Variants Identified by Whole-Exome Sequencing.* Horm Res Paediatr, 2017. **87**(4): p. 264-270.
199. Biason-Lauber, A. and E.J. Schoenle, *Apparently normal ovarian differentiation in a prepubertal girl with transcriptionally inactive steroidogenic factor 1 (NR5A1/SF-1) and adrenocortical insufficiency.* Am J Hum Genet, 2000. **67**(6): p. 1563-8.
200. Guran, T., et al., *Rare Causes of Primary Adrenal Insufficiency: Genetic and Clinical Characterization of a Large Nationwide Cohort.* J Clin Endocrinol Metab, 2016. **101**(1): p. 284-92.
201. Lourenco, D., et al., *Mutations in NR5A1 associated with ovarian insufficiency.* N Engl J Med, 2009. **360**(12): p. 1200-10.
202. Bashamboo, A., et al., *Human male infertility associated with mutations in NR5A1 encoding steroidogenic factor 1.* Am J Hum Genet, 2010. **87**(4): p. 505-12.
203. Bashamboo, A., et al., *A recurrent p.Arg92Trp variant in steroidogenic factor-1 (NR5A1) can act as a molecular switch in human sex development.* Hum Mol Genet, 2016. **25**(23): p. 5286.

204. Baetens, D., et al., *NR5A1 is a novel disease gene for 46,XX testicular and ovotesticular disorders of sex development.* Genet Med, 2017. **19**(4): p. 367-376.
205. Igarashi, M., et al., *Identical NR5A1 Missense Mutations in Two Unrelated 46,XX Individuals with Testicular Tissues.* Hum Mutat, 2017. **38**(1): p. 39-42.
206. Sekido, R. and R. Lovell-Badge, *Sex determination involves synergistic action of SRY and SF1 on a specific Sox9 enhancer.* Nature, 2008. **453**(7197): p. 930-4.
207. Shima, Y., et al., *Pituitary homeobox 2 regulates adrenal4 binding protein/steroidogenic factor-1 gene transcription in the pituitary gonadotrope through interaction with the intronic enhancer.* Mol Endocrinol, 2008. **22**(7): p. 1633-46.
208. Stallings, N.R., et al., *Development of a transgenic green fluorescent protein lineage marker for steroidogenic factor 1.* Endocr Res, 2002. **28**(4): p. 497-504.
209. Karpova, T., et al., *A FTZ-F1-containing yeast artificial chromosome recapitulates expression of steroidogenic factor 1 in vivo.* Mol Endocrinol, 2005. **19**(10): p. 2549-63.
210. Therrien, M. and J. Drouin, *Cell-specific helix-loop-helix factor required for pituitary expression of the pro-opiomelanocortin gene.* Mol Cell Biol, 1993. **13**(4): p. 2342-53.
211. Poulin, G., B. Turgeon, and J. Drouin, *NeuroD1/beta2 contributes to cell-specific transcription of the proopiomelanocortin gene.* Mol Cell Biol, 1997. **17**(11): p. 6673-82.
212. Poulin, G., et al., *Specific protein-protein interaction between basic helix-loop-helix transcription factors and homeoproteins of the Pitx family.* Mol Cell Biol, 2000. **20**(13): p. 4826-37.
213. Lamolet, B., et al., *A pituitary cell-restricted T box factor, Tpit, activates POMC transcription in cooperation with Pitx homeoproteins.* Cell, 2001. **104**(6): p. 849-59.
214. Pulichino, A.M., et al., *Human and mouse TPIT gene mutations cause early onset pituitary ACTH deficiency.* Genes Dev, 2003. **17**(6): p. 711-6.
215. Metherell, L.A., et al., *TPIT mutations are associated with early-onset, but not late-onset isolated ACTH deficiency.* Eur J Endocrinol, 2004. **151**(4): p. 463-5.
216. Vallette-Kasic, S., et al., *Congenital isolated adrenocorticotropin deficiency: an underestimated cause of neonatal death, explained by TPIT gene mutations.* J Clin Endocrinol Metab, 2005. **90**(3): p. 1323-31.
217. Couture, C., et al., *Phenotypic homogeneity and genotypic variability in a large series of congenital isolated ACTH-deficiency patients with TPIT gene mutations.* J Clin Endocrinol Metab, 2012. **97**(3): p. E486-95.
218. Jostes, B., C. Walther, and P. Gruss, *The murine paired box gene, Pax7, is expressed specifically during the development of the nervous and muscular system.* Mech Dev, 1990. **33**(1): p. 27-37.
219. Mansouri, A. and P. Gruss, *Pax3 and Pax7 are expressed in commissural neurons and restrict ventral neuronal identity in the spinal cord.* Mech Dev, 1998. **78**(1-2): p. 171-8.
220. Seale, P., et al., *Pax7 is required for the specification of myogenic satellite cells.* Cell, 2000. **102**(6): p. 777-86.
221. Oustanina, S., G. Hause, and T. Braun, *Pax7 directs postnatal renewal and propagation of myogenic satellite cells but not their specification.* EMBO J, 2004. **23**(16): p. 3430-9.
222. Relaix, F., et al., *A Pax3/Pax7-dependent population of skeletal muscle progenitor cells.* Nature, 2005. **435**(7044): p. 948-53.
223. Kassar-Duchossoy, L., et al., *Pax3/Pax7 mark a novel population of primitive myogenic cells during development.* Genes Dev, 2005. **19**(12): p. 1426-31.
224. Relaix, F., et al., *Pax3 and Pax7 have distinct and overlapping functions in adult muscle progenitor cells.* J Cell Biol, 2006. **172**(1): p. 91-102.
225. Mansouri, A., et al., *Dysgenesis of cephalic neural crest derivatives in Pax7-/- mutant mice.* Development, 1996. **122**(3): p. 831-8.

226. Guner, B., et al., *Graded hedgehog and fibroblast growth factor signaling independently regulate pituitary cell fates and help establish the pars distalis and pars intermedia of the zebrafish adenohypophysis.* Endocrinology, 2008. **149**(9): p. 4435-51.
227. Hosoyama, T., et al., *A Postnatal Pax7 Progenitor Gives Rise to Pituitary Adenomas.* Genes Cancer, 2010. **1**(4): p. 388-402.
228. Goldberg, L.B., P.K. Aujla, and L.T. Raetzman, *Persistent expression of activated Notch inhibits corticotrope and melanotrope differentiation and results in dysfunction of the HPA axis.* Dev Biol, 2011. **358**(1): p. 23-32.
229. Budry, L., et al., *The selector gene Pax7 dictates alternate pituitary cell fates through its pioneer action on chromatin remodeling.* Genes Dev, 2012. **26**(20): p. 2299-310.
230. Mayran, A., et al., *Pioneer factor Pax7 deploys a stable enhancer repertoire for specification of cell fate.* Nat Genet, 2018. **50**(2): p. 259-269.
231. Barr, F.G., et al., *In vivo amplification of the PAX3-FKHR and PAX7-FKHR fusion genes in alveolar rhabdomyosarcoma.* Hum Mol Genet, 1996. **5**(1): p. 15-21.
232. Bilodeau, S., A. Roussel-Gervais, and J. Drouin, *Distinct developmental roles of cell cycle inhibitors p57Kip2 and p27Kip1 distinguish pituitary progenitor cell cycle exit from cell cycle reentry of differentiated cells.* Mol Cell Biol, 2009. **29**(7): p. 1895-908.
233. Davis, S.W., A.H. Mortensen, and S.A. Camper, *Birthdating studies reshape models for pituitary gland cell specification.* Dev Biol, 2011. **352**(2): p. 215-27.
234. von Möllendorff, W. and W. Bargmann, *Handbuch der mikroskopischen Anatomie des Menschen: Hypofyse. Blutgefäss- und Lymphgefässapparat; Innersekretorische Drüsen.* 1940.
235. Phifer, R.F., A.R. Midgley, and S.S. Spicer, *Immunohistologic and histologic evidence that follicle-stimulating hormone and luteinizing hormone are present in the same cell type in the human pars distalis.* J Clin Endocrinol Metab, 1973. **36**(1): p. 125-41.
236. Robyn, C., et al., *Immunohistochemical study of the human pituitary with anti-luteinizing hormone, anti-follicle stimulating hormone and anti-thyrotrophin sera.* Acta Endocrinol (Copenh), 1973. **72**(4): p. 625-42.
237. Horvath, E., R.V. Lloyd, and K. Kovacs, *Propylthiouracyl-induced hypothyroidism results in reversible transdifferentiation of somatotrophs into thyroidectomy cells. A morphologic study of the rat pituitary including immunoelectron microscopy.* Lab Invest, 1990. **63**(4): p. 511-20.
238. Frawley, L.S., F.R. Boockfor, and J.P. Hoeffler, *Identification by plaque assays of a pituitary cell type that secretes both growth hormone and prolactin.* Endocrinology, 1985. **116**(2): p. 734-7.
239. Borrelli, E., et al., *Transgenic mice with inducible dwarfism.* Nature, 1989. **339**(6225): p. 538-41.
240. Wen, S., et al., *Embryonic gonadotropin-releasing hormone signaling is necessary for maturation of the male reproductive axis.* Proc Natl Acad Sci U S A, 2010. **107**(37): p. 16372-7.
241. Qiao, S., et al., *Molecular Plasticity of Male and Female Murine Gonadotropes Revealed by mRNA Sequencing.* Endocrinology, 2016. **157**(3): p. 1082-93.
242. Peel, M.T., Y. Ho, and S.A. Liebhaber, *Transcriptome Analyses of Female Somatotropes and Lactotropes Reveal Novel Regulators of Cell Identity in the Pituitary.* Endocrinology, 2018. **159**(12): p. 3965-3980.
243. Buenrostro, J.D., et al., *Transposition of native chromatin for fast and sensitive epigenomic profiling of open chromatin, DNA-binding proteins and nucleosome position.* Nat Methods, 2013. **10**(12): p. 1213-8.
244. Langlais, D., et al., *The Stat3/GR interaction code: predictive value of direct/indirect DNA recruitment for transcription outcome.* Mol Cell, 2012. **47**(1): p. 38-49.

245. Baek, S. and M.H. Sung, *Genome-Scale Analysis of Cell-Specific Regulatory Codes Using Nuclear Enzymes.* Methods Mol Biol, 2016. **1418**: p. 225-40.
246. Barski, A., et al., *High-resolution profiling of histone methylations in the human genome.* Cell, 2007. **129**(4): p. 823-37.
247. Creyghton, M.P., et al., *Histone H3K27ac separates active from poised enhancers and predicts developmental state.* Proc Natl Acad Sci U S A, 2010. **107**(50): p. 21931-6.
248. Young, M.D., et al., *ChIP-seq analysis reveals distinct H3K27me3 profiles that correlate with transcriptional activity.* Nucleic Acids Res, 2011. **39**(17): p. 7415-27.
249. Jones, B.K., et al., *The human growth hormone gene is regulated by a multicomponent locus control region.* Mol Cell Biol, 1995. **15**(12): p. 7010-21.
250. Ho, Y., et al., *The juxtaposition of a promoter with a locus control region transcriptional domain activates gene expression.* EMBO Rep, 2008. **9**(9): p. 891-8.
251. Ho, Y., et al., *Distinct chromatin configurations regulate the initiation and the maintenance of hGH gene expression.* Mol Cell Biol, 2013. **33**(9): p. 1723-34.
252. Tsai, Y.C., N.E. Cooke, and S.A. Liebhaber, *Long-range looping of a locus control region drives tissue-specific chromatin packing within a multigene cluster.* Nucleic Acids Res, 2016. **44**(10): p. 4651-64.
253. Ho, Y., N.E. Cooke, and S.A. Liebhaber, *An autoregulatory pathway establishes the definitive chromatin conformation at the pit-1 locus.* Mol Cell Biol, 2015. **35**(9): p. 1523-32.
254. Sarro, R., et al., *Disrupting the three-dimensional regulatory topology of the Pitx1 locus results in overtly normal development.* Development, 2018. **145**(7).
255. Navin, N., et al., *Tumour evolution inferred by single-cell sequencing.* Nature, 2011. **472**(7341): p. 90-4.
256. Shapiro, E., T. Biezuner, and S. Linnarsson, *Single-cell sequencing-based technologies will revolutionize whole-organism science.* Nat Rev Genet, 2013. **14**(9): p. 618-30.
257. Ziegenhain, C., et al., *Comparative Analysis of Single-Cell RNA Sequencing Methods.* Mol Cell, 2017. **65**(4): p. 631-643 e4.
258. Zheng, G.X., et al., *Massively parallel digital transcriptional profiling of single cells.* Nat Commun, 2017. **8**: p. 14049.
259. Trapnell, C., et al., *The dynamics and regulators of cell fate decisions are revealed by pseudotemporal ordering of single cells.* Nat Biotechnol, 2014. **32**(4): p. 381-386.
260. Cheung, L.Y.M., et al., *Single-Cell RNA Sequencing Reveals Novel Markers of Male Pituitary Stem Cells and Hormone-Producing Cell Types.* Endocrinology, 2018. **159**(12): p. 3910-3924.
261. Ruf-Zamojski, F., et al., *Regulatory Architecture of the LbetaT2 Gonadotrope Cell Underlying the Response to Gonadotropin-Releasing Hormone.* Front Endocrinol (Lausanne), 2018. **9**: p. 34.
262. Camper, S.A., et al., *Implementing transgenic and embryonic stem cell technology to study gene expression, cell-cell interactions and gene function.* Biol Reprod, 1995. **52**(2): p. 246-57.
263. Cong, L., et al., *Multiplex genome engineering using CRISPR/Cas systems.* Science, 2013. **339**(6121): p. 819-23.
264. Sato, T., et al., *Single Lgr5 stem cells build crypt-villus structures in vitro without a mesenchymal niche.* Nature, 2009. **459**(7244): p. 262-5.
265. Nakano, T., et al., *Self-formation of optic cups and storable stratified neural retina from human ESCs.* Cell Stem Cell, 2012. **10**(6): p. 771-785.
266. Xia, Y., et al., *Directed differentiation of human pluripotent cells to ureteric bud kidney progenitor-like cells.* Nat Cell Biol, 2013. **15**(12): p. 1507-15.
267. Suga, H., et al., *Self-formation of functional adenohypophysis in three-dimensional culture.* Nature, 2011. **480**(7375): p. 57-62.

268. Ozone, C., et al., *Functional anterior pituitary generated in self-organizing culture of human embryonic stem cells.* Nat Commun, 2016. **7**: p. 10351.
269. Chen, J., et al., *The adult pituitary contains a cell population displaying stem/progenitor cell and early embryonic characteristics.* Endocrinology, 2005. **146**(9): p. 3985-98.
270. Kulig, E., et al., *Remodeling of Hyperplastic Pituitaries in Hypothyroid us-Subunit Knockout Mice After Thyroxine and 1713-Estradiol Treatment: Role of Apoptosis.* Endocr Pathol, 1998. **9**(3): p. 261-274.
271. Gordon, D.F., et al., *MED220/thyroid receptor-associated protein 220 functions as a transcriptional coactivator with Pit-1 and GATA-2 on the thyrotropin-beta promoter in thyrotropes.* Mol Endocrinol, 2006. **20**(5): p. 1073-89.
272. Jarvis, J.P., et al., *Patterns of ancestry, signatures of natural selection, and genetic association with stature in Western African pygmies.* PLoS Genet, 2012. **8**(4): p. e1002641.
273. Turchin, M.C., et al., *Evidence of widespread selection on standing variation in Europe at height-associated SNPs.* Nat Genet, 2012. **44**(9): p. 1015-9.
274. Ye, Z., et al., *Common variants at 10p12.31, 10q21.1 and 13q12.13 are associated with sporadic pituitary adenoma.* Nat Genet, 2015. **47**(7): p. 793-7.
275. Edwards, S.L., et al., *Beyond GWASs: illuminating the dark road from association to function.* Am J Hum Genet, 2013. **93**(5): p. 779-97.
276. Mayran, A., et al., *Pioneer and nonpioneer factor cooperation drives lineage specific chromatin opening.* Nat Commun, 2019. **10**(1): p. 3807.
277. Canaris, G.J., et al., *The Colorado thyroid disease prevalence study.* Arch Intern Med, 2000. **160**(4): p. 526-34.
278. Persani, L., B. Cangiano, and M. Bonomi, *The diagnosis and management of central hypothyroidism in 2018.* Endocr Connect, 2019. **8**(2): p. R44-R54.
279. Hashimoto, K., et al., *cAMP response element-binding protein-binding protein mediates thyrotropin-releasing hormone signaling on thyrotropin subunit genes.* J Biol Chem, 2000. **275**(43): p. 33365-72.
280. Wood, W.M., et al., *An upstream regulator of the glycoprotein hormone alpha-subunit gene mediates pituitary cell type activation and repression by different mechanisms.* J Biol Chem, 1999. **274**(22): p. 15526-32.
281. Brinkmeier, M.L., et al., *Rathke's cleft-like cysts arise from Isl1 deletion in murine pituitary progenitors.* J Clin Invest, 2020.
282. Castinetti, F., et al., *ISL1 Is Necessary for Maximal Thyrotrope Response to Hypothyroidism.* Mol Endocrinol, 2015. **29**(10): p. 1510-21.
283. Alarid, E.T., et al., *Immortalization of pituitary cells at discrete stages of development by directed oncogenesis in transgenic mice.* Development, 1996. **122**(10): p. 3319-29.
284. Lew, D., et al., *GHF-1-promoter-targeted immortalization of a somatotropic progenitor cell results in dwarfism in transgenic mice.* Genes Dev, 1993. **7**(4): p. 683-93.
285. Aninye, I.O., et al., *Circadian regulation of Tshb gene expression by Rev-Erbalpha (NR1D1) and nuclear corepressor 1 (NCOR1).* J Biol Chem, 2014. **289**(24): p. 17070-7.
286. Janssen, J.S., et al., *A rexinoid antagonist increases the hypothalamic-pituitary-thyroid set point in mice and thyrotrope cells.* Mol Cell Endocrinol, 2011. **339**(1-2): p. 1-6.
287. Nakajima, Y., et al., *NR4A1 (Nur77) mediates thyrotropin-releasing hormone-induced stimulation of transcription of the thyrotropin beta gene: analysis of TRH knockout mice.* PLoS One, 2012. **7**(7): p. e40437.
288. Sizova, D., et al., *Research resource: T-antigen transformation of pituitary cells captures three novel cell lines in the Pit-1 lineage.* Mol Endocrinol, 2010. **24**(11): p. 2232-40.
289. Ashburner, M., et al., *Gene ontology: tool for the unification of biology. The Gene Ontology Consortium.* Nat Genet, 2000. **25**(1): p. 25-9.

290. The Gene Ontology, C., *The Gene Ontology Resource: 20 years and still GOing strong.* Nucleic Acids Res, 2019. **47**(D1): p. D330-D338.
291. Ando, M., et al., *The proneural bHLH genes Mash1, Math3 and NeuroD are required for pituitary development.* J Mol Endocrinol, 2018. **61**(3): p. 127-138.
292. Zhang, F., et al., *Enhancer-bound LDB1 regulates a corticotrope promoter-pausing repression program.* Proc Natl Acad Sci U S A, 2015. **112**(5): p. 1380-5.
293. Skene, P.J. and S. Henikoff, *An efficient targeted nuclease strategy for high-resolution mapping of DNA binding sites.* Elife, 2017. **6**.
294. Boyer, L.A., et al., *Polycomb complexes repress developmental regulators in murine embryonic stem cells.* Nature, 2006. **441**(7091): p. 349-53.
295. Bracken, A.P., et al., *Genome-wide mapping of Polycomb target genes unravels their roles in cell fate transitions.* Genes Dev, 2006. **20**(9): p. 1123-36.
296. Lee, T.I., et al., *Control of developmental regulators by Polycomb in human embryonic stem cells.* Cell, 2006. **125**(2): p. 301-13.
297. Brown, N.S., et al., *Thyroid hormone resistance and increased metabolic rate in the RXR-gamma-deficient mouse.* J Clin Invest, 2000. **106**(1): p. 73-9.
298. Ernst, J. and M. Kellis, *ChromHMM: automating chromatin-state discovery and characterization.* Nat Methods, 2012. **9**(3): p. 215-6.
299. Chen, R.P., et al., *Autoregulation of pit-1 gene expression mediated by two cis-active promoter elements.* Nature, 1990. **346**(6284): p. 583-6.
300. Kress, W., et al., *Saethre-Chotzen syndrome caused by TWIST 1 gene mutations: functional differentiation from Muenke coronal synostosis syndrome.* Eur J Hum Genet, 2006. **14**(1): p. 39-48.
301. Parker, S.C., et al., *Chromatin stretch enhancer states drive cell-specific gene regulation and harbor human disease risk variants.* Proc Natl Acad Sci U S A, 2013. **110**(44): p. 17921-6.
302. Varshney, A., et al., *Cell Specificity of Human Regulatory Annotations and Their Genetic Effects on Gene Expression.* Genetics, 2019. **211**(2): p. 549-562.
303. Iotchkova, V., et al., *GARFIELD classifies disease-relevant genomic features through integration of functional annotations with association signals.* Nat Genet, 2019. **51**(2): p. 343-353.
304. Nagel, M., et al., *Item-level analyses reveal genetic heterogeneity in neuroticism.* Nat Commun, 2018. **9**(1): p. 905.
305. Minegishi, N., et al., *Alternative promoters regulate transcription of the mouse GATA-2 gene.* J Biol Chem, 1998. **273**(6): p. 3625-34.
306. Brinkmeier, M.L., et al., *Cell-specific expression of the mouse glycoprotein hormone alpha-subunit gene requires multiple interacting DNA elements in transgenic mice and cultured cells.* Mol Endocrinol, 1998. **12**(5): p. 622-33.
307. Daly, A.Z. and S.A. Camper, *Pituitary Development and Organogenesis: Transcription Factors in Development and Disease*, in *Developmental Neuroendocrinology*, S. Wray and S. Blackshaw, Editors. 2020, Springer International Publishing: Cham. p. 129-177.
308. Castinetti, F., et al., *PITX2 AND PITX1 regulate thyrotroph function and response to hypothyroidism.* Mol Endocrinol, 2011. **25**(11): p. 1950-60.
309. Kragesteen, B.K., et al., *Dynamic 3D chromatin architecture contributes to enhancer specificity and limb morphogenesis.* Nat Genet, 2018. **50**(10): p. 1463-1473.
310. Khetchoumian, K., et al., *Pituitary cell translation and secretory capacities are enhanced cell autonomously by the transcription factor Creb3l2.* Nat Commun, 2019. **10**(1): p. 3960.
311. Gergics, P., et al., *Gene Expression in Mouse Thyrotrope Adenoma: Transcription Elongation Factor Stimulates Proliferation.* Endocrinology, 2016. **157**(9): p. 3631-46.

312. Fletcher, P.A., A. Sherman, and S.S. Stojilkovic, *Common and diverse elements of ion channels and receptors underlying electrical activity in endocrine pituitary cells.* Mol Cell Endocrinol, 2018. **463**: p. 23-36.
313. Mollard, P., et al., *Thyrotropin-releasing hormone activates a [Ca2+]i-dependent K+ current in GH3 pituitary cells via Ins(1,4,5)P3-sensitive and Ins(1,4,5)P3-insensitive mechanisms.* Biochem J, 1990. **268**(2): p. 345-52.
314. Tomic, M., et al., *Calcium signaling properties of a thyrotroph cell line, mouse TalphaT1 cells.* Cell Calcium, 2015. **58**(6): p. 598-605.
315. Tommiska, J., et al., *Two missense mutations in KCNQ1 cause pituitary hormone deficiency and maternally inherited gingival fibromatosis.* Nat Commun, 2017. **8**(1): p. 1289.
316. Cheung, L.Y.M. and S.A. Camper, *PROP1-Dependent Retinoic Acid Signaling Regulates Developmental Pituitary Morphogenesis and Hormone Expression.* Endocrinology, 2020. **161**(2).
317. Daly, A.M., AH; Bando, H; Camper, SA, *Pituitary tumors and immortalized cell lines generated by cre-inducible expression of SV40 T antigen*
318. Ait-Lounis, A., et al., *Novel function of the ciliogenic transcription factor RFX3 in development of the endocrine pancreas.* Diabetes, 2007. **56**(4): p. 950-9.
319. Elkon, R., et al., *RFX transcription factors are essential for hearing in mice.* Nat Commun, 2015. **6**: p. 8549.
320. Brinkmeier, M.L., et al., *Discovery of transcriptional regulators and signaling pathways in the developing pituitary gland by bioinformatic and genomic approaches.* Genomics, 2009. **93**(5): p. 449-60.
321. Herzog, W., et al., *Genetic analysis of adenohypophysis formation in zebrafish.* Mol Endocrinol, 2004. **18**(5): p. 1185-95.
322. Pogoda, H.M., et al., *The proneural gene ascl1a is required for endocrine differentiation and cell survival in the zebrafish adenohypophysis.* Development, 2006. **133**(6): p. 1079-89.
323. Vierbuchen, T., et al., *Direct conversion of fibroblasts to functional neurons by defined factors.* Nature, 2010. **463**(7284): p. 1035-41.
324. Wapinski, O.L., et al., *Hierarchical mechanisms for direct reprogramming of fibroblasts to neurons.* Cell, 2013. **155**(3): p. 621-35.
325. Ross, S.E., M.E. Greenberg, and C.D. Stiles, *Basic helix-loop-helix factors in cortical development.* Neuron, 2003. **39**(1): p. 13-25.
326. Staff, M.C. *Hypothyroidism (underactive thyroid)*. 2020 [cited 2020; Available from: https://www.mayoclinic.org/diseases-conditions/hypothyroidism/symptoms-causes/syc-20350284.
327. Cornwell, M., et al., *VIPER: Visualization Pipeline for RNA-seq, a Snakemake workflow for efficient and complete RNA-seq analysis.* BMC Bioinformatics, 2018. **19**(1): p. 135.
328. Hartley, S.W. and J.C. Mullikin, *QoRTs: a comprehensive toolset for quality control and data processing of RNA-Seq experiments.* BMC Bioinformatics, 2015. **16**: p. 224.
329. Lee, C., S. Patil, and M.A. Sartor, *RNA-Enrich: a cut-off free functional enrichment testing method for RNA-seq with improved detection power.* Bioinformatics, 2016. **32**(7): p. 1100-2.
330. Buenrostro, J.D., et al., *ATAC-seq: A Method for Assaying Chromatin Accessibility Genome-Wide.* Curr Protoc Mol Biol, 2015. **109**: p. 21 29 1-21 29 9.
331. Rai, V., et al., *Single-cell ATAC-Seq in human pancreatic islets and deep learning upscaling of rare cells reveals cell-specific type 2 diabetes regulatory signatures.* Mol Metab, 2020. **32**: p. 109-121.

332. Prince, K.L., et al., *Developmental analysis and influence of genetic background on the Lhx3 W227ter mouse model of combined pituitary hormone deficiency disease.* Endocrinology, 2013. **154**(2): p. 738-48.
333. Quinlan, A.R. and I.M. Hall, *BEDTools: a flexible suite of utilities for comparing genomic features.* Bioinformatics, 2010. **26**(6): p. 841-2.
334. Orchard, P., et al., *Genome-wide chromatin accessibility and transcriptome profiling show minimal epigenome changes and coordinated transcriptional dysregulation of hedgehog signaling in Danforth's short tail mice.* Hum Mol Genet, 2019. **28**(5): p. 736-750.
335. Buniello, A., et al., *The NHGRI-EBI GWAS Catalog of published genome-wide association studies, targeted arrays and summary statistics 2019.* Nucleic Acids Res, 2019. **47**(D1): p. D1005-D1012.
336. Srinivas, S., et al., *Cre reporter strains produced by targeted insertion of EYFP and ECFP into the ROSA26 locus.* BMC Dev Biol, 2001. **1**: p. 4.
337. Mortensen, A.H., et al., *Deletion of OTX2 in neural ectoderm delays anterior pituitary development.* Hum Mol Genet, 2015. **24**(4): p. 939-53.
338. Zhu, Z., et al., *Common tools for pituitary adenomas research: cell lines and primary cells.* Pituitary, 2020. **23**(2): p. 182-188.
339. Ahuja, D., M.T. Saenz-Robles, and J.M. Pipas, *SV40 large T antigen targets multiple cellular pathways to elicit cellular transformation.* Oncogene, 2005. **24**(52): p. 7729-45.
340. Manfredi, J.J. and C. Prives, *The transforming activity of simian virus 40 large tumor antigen.* Biochim Biophys Acta, 1994. **1198**(1): p. 65-83.
341. Mellon, P.L., et al., *Immortalization of hypothalamic GnRH neurons by genetically targeted tumorigenesis.* Neuron, 1990. **5**(1): p. 1-10.
342. Windle, J.J., R.I. Weiner, and P.L. Mellon, *Cell lines of the pituitary gonadotrope lineage derived by targeted oncogenesis in transgenic mice.* Mol Endocrinol, 1990. **4**(4): p. 597-603.
343. Bilezikjian, L.M., et al., *Regulation and actions of Smad7 in the modulation of activin, inhibin, and transforming growth factor-beta signaling in anterior pituitary cells.* Endocrinology, 2001. **142**(3): p. 1065-72.
344. Fowkes, R.C., J. Burch, and J.M. Burrin, *Stimulation of extracellular signal-regulated kinase by pituitary adenylate cyclase-activating polypeptide in alpha T3-1 gonadotrophs.* J Endocrinol, 2001. **171**(3): p. R5-10.
345. McGillivray, S.M., et al., *Mouse GnRH receptor gene expression is mediated by the LHX3 homeodomain protein.* Endocrinology, 2005. **146**(5): p. 2180-5.
346. Navratil, A.M., et al., *Constitutive localization of the gonadotropin-releasing hormone (GnRH) receptor to low density membrane microdomains is necessary for GnRH signaling to ERK.* J Biol Chem, 2003. **278**(34): p. 31593-602.
347. Xie, H., et al., *Chromatin status and transcription factor binding to gonadotropin promoters in gonadotrope cell lines.* Reprod Biol Endocrinol, 2017. **15**(1): p. 86.
348. Breen, K.M., et al., *Runt-related transcription factors impair activin induction of the follicle-stimulating hormone {beta}-subunit gene.* Endocrinology, 2010. **151**(6): p. 2669-80.
349. Cherrington, B.D., et al., *NeuroD1 and Mash1 temporally regulate GnRH receptor gene expression in immortalized mouse gonadotrope cells.* Mol Cell Endocrinol, 2008. **295**(1-2): p. 106-14.
350. Lawson, M.A., et al., *Pulse sensitivity of the luteinizing hormone beta promoter is determined by a negative feedback loop Involving early growth response-1 and Ngfi-A binding protein 1 and 2.* Mol Endocrinol, 2007. **21**(5): p. 1175-91.
351. Sasson, R., et al., *Glucocorticoids induce human glycoprotein hormone alpha-subunit gene expression in the gonadotrope.* Endocrinology, 2008. **149**(7): p. 3643-55.

352. Thackray, V.G. and P.L. Mellon, *Synergistic induction of follicle-stimulating hormone beta-subunit gene expression by gonadal steroid hormone receptors and Smad proteins.* Endocrinology, 2008. **149**(3): p. 1091-102.
353. Day, R.N., et al., *Imaging the localized protein interactions between Pit-1 and the CCAAT/enhancer binding protein alpha in the living pituitary cell nucleus.* Mol Endocrinol, 2003. **17**(3): p. 333-45.
354. Hoffmann, H.M., et al., *Transcriptional interaction between cFOS and the homeodomain-binding transcription factor VAX1 on the GnRH promoter controls Gnrh1 expression levels in a GnRH neuron maturation specific manner.* Mol Cell Endocrinol, 2018. **461**: p. 143-154.
355. Longo, K.M., Y. Sun, and A.C. Gore, *Insulin-like growth factor-I effects on gonadotropin-releasing hormone biosynthesis in GT1-7 cells.* Endocrinology, 1998. **139**(3): p. 1125-32.
356. Nelson, S.B., et al., *Neuron-specific expression of the rat gonadotropin-releasing hormone gene is conferred by interactions of a defined promoter element with the enhancer in GT1-7 cells.* Mol Endocrinol, 2000. **14**(9): p. 1509-22.
357. Davis, S.W., et al., *Molecular mechanisms of pituitary organogenesis: In search of novel regulatory genes.* Mol Cell Endocrinol, 2010. **323**(1): p. 4-19.
358. Zimmer, B., et al., *Derivation of Diverse Hormone-Releasing Pituitary Cells from Human Pluripotent Stem Cells.* Stem Cell Reports, 2016. **6**(6): p. 858-872.
359. Mellon, P.L., J.J. Windle, and R.I. Weiner, *Immortalization of neuroendocrine cells by targeted oncogenesis.* Recent Prog Horm Res, 1991. **47**: p. 69-93; discussion 93-6.
360. Chu, V.T., et al., *Efficient generation of Rosa26 knock-in mice using CRISPR/Cas9 in C57BL/6 zygotes.* BMC Biotechnol, 2016. **16**: p. 4.
361. Chou, J.Y., *Differentiated mammalian cell lines immortalized by temperature-sensitive tumor viruses.* Mol Endocrinol, 1989. **3**(10): p. 1511-4.
362. Jat, P.S., et al., *Direct derivation of conditionally immortal cell lines from an H-2Kb-tsA58 transgenic mouse.* Proc Natl Acad Sci U S A, 1991. **88**(12): p. 5096-100.
363. Hu, X., et al., *CRISPR/Cas9-mediated reversibly immortalized mouse bone marrow stromal stem cells (BMSCs) retain multipotent features of mesenchymal stem cells (MSCs).* Oncotarget, 2017. **8**(67): p. 111847-111865.
364. Pease, S., T.L. Saunders, and International Society for Transgenic Technologies., *Advanced protocols for animal transgenesis : an ISTT manual*. Springer protocols. 2011, Heidelberg ; New York ;: Springer. xv, 669 p.
365. Arnold, C.D., et al., *Genome-wide quantitative enhancer activity maps identified by STARR-seq*. Science, 2013. **339**(6123): p. 1074-7.
366. Chepelev, I., et al., *Characterization of genome-wide enhancer-promoter interactions reveals co-expression of interacting genes and modes of higher order chromatin organization.* Cell Res, 2012. **22**(3): p. 490-503.
367. Gallo, S.M., et al., *REDfly v3.0: toward a comprehensive database of transcriptional regulatory elements in Drosophila.* Nucleic Acids Res, 2011. **39**(Database issue): p. D118-23.
368. Li, G., et al., *Extensive promoter-centered chromatin interactions provide a topological basis for transcription regulation.* Cell, 2012. **148**(1-2): p. 84-98.
369. Sanyal, A., et al., *The long-range interaction landscape of gene promoters.* Nature, 2012. **489**(7414): p. 109-13.
370. Bejerano, G., et al., *A distal enhancer and an ultraconserved exon are derived from a novel retroposon.* Nature, 2006. **441**(7089): p. 87-90.
371. Volkmann, B.A., et al., *Potential novel mechanism for Axenfeld-Rieger syndrome: deletion of a distant region containing regulatory elements of PITX2.* Invest Ophthalmol Vis Sci, 2011. **52**(3): p. 1450-9.

372. Yao, Y., et al., *Cis-regulatory architecture of a brain signaling center predates the origin of chordates.* Nat Genet, 2016. **48**(5): p. 575-80.
373. Hosoya, T., et al., *Global dynamics of stage-specific transcription factor binding during thymocyte development.* Sci Rep, 2018. **8**(1): p. 5605.
374. Roux, K.J., et al., *A promiscuous biotin ligase fusion protein identifies proximal and interacting proteins in mammalian cells.* J Cell Biol, 2012. **196**(6): p. 801-10.
375. Varshney, A., et al., *Genetic regulatory signatures underlying islet gene expression and type 2 diabetes.* Proc Natl Acad Sci U S A, 2017. **114**(9): p. 2301-2306.
376. Buenrostro, J.D., et al., *Single-cell chromatin accessibility reveals principles of regulatory variation.* Nature, 2015. **523**(7561): p. 486-90.
377. Kaya-Okur, H.S., et al., *CUT&Tag for efficient epigenomic profiling of small samples and single cells.* Nat Commun, 2019. **10**(1): p. 1930.
378. Andoniadou, C.L., et al., *Lack of the murine homeobox gene Hesx1 leads to a posterior transformation of the anterior forebrain.* Development, 2007. **134**(8): p. 1499-508.